SEDIMENTOLOGY the journal of the International Association of Sedimentologists IAS

Sedimentology (2024) doi: 10.1111/sed.13234

Towards a new generation of fluvial facies models for the interpretation of ancient deposits, based on inter-annual peak discharge variance of modern rivers

CHRISTOPHER R. FIELDING*, JAN ALEXANDER† and ADAM ARGIRO*
*Department of Earth Sciences, University of Connecticut, Beach Hall, 354 Mansfield Road (Unit 1045), Storrs, CT 06269, USA (E-mail: christopher.fielding@uconn.edu)
†School of Environmental Sciences, University of East Anglia, Norwich Research Park, Norwich NR4 7TJ, UK

Associate Editor – Theresa Schwartz

ABSTRACT

Fluvial facies models based on river planform are flawed and not fully fit for purpose. An alternative approach to classifying fluvial deposits is based on river discharge characteristics. A recent paper showed that the co-efficient of variance of annual peak discharge (CVQ_p) correlates well with the characteristics of preserved alluvium for a suite of modern rivers. Here, the database of rivers is expanded and augmented, and the utility of this statistic confirmed. For modern rivers, plotting the running-value of CVQ_p for a set interval (for example, 30 years) over a longer discharge record shows that the statistic varies both spatially and temporally. The CVQ_p can rise abruptly at a given location in response to a single flow event if that event is significantly larger than is common in that river. Such abrupt changes in CVQ_p are superimposed on longer-term patterns of more gradual change stimulated by environmental factors or anthropogenic effects such as dam construction. If the period of calculation for CVQ_p is relatively short, 'anomalous' events appear more frequently. Sequential studies of modern rivers indicate that such anomalous events have a high probability of being preserved in the alluvial record of the river, and suggest that, over the timeframes of channel filling and abandonment, they may constitute the dominant (characteristic) portion of the record in high CVQ_p systems. Since flow events with strongly peaked hydrographs (flashy discharges) are more common in high CVQ_p systems and leave a record dominated by upper flow regime stratification styles, it follows that the alluvial record of high CVQ_p rivers will be dominated by upper flow regime stratification. In contrast, in lower CVQ_p systems the occurrence of an event that changes the running CVQ_p value significantly may form a distinct event deposit, and the temporarily changed CVQ_p is unrepresentative for the duration of the channel's life. The dominance of upper flow regime stratification, together with decreased preservation of identifiable macroform structure, increased lateral lithological heterogeneity, and in many cases increased preservation of *in situ* tree fossils in channel deposits of higher CVQ_p rivers, forms the basis for a series of new facies models for low, moderate, high and very high/ultra-high CVQ_p alluvial systems and deposits. The new models can be applied to ancient successions either in combination with traditional, planform-based models, or not. These models provide information about ancient palaeoenvironmental conditions,

and changes in such conditions over time at various scales via stratigraphic investigations.

Keywords Alluvial, discharge variability, fluvial facies models, planform, preservation potential.

INTRODUCTION

Historically, the basis for fluvial facies models, which are used to summarize the one-dimensional, two-dimensional and three-dimensional arrangement of sedimentary deposits in rivers, has been river planform (e.g. Miall, 2010). Many researchers have nonetheless pointed out that there are multiple weaknesses in this approach (Bridge, 1985, 1993a,b; Brierley, 1996; Bristow, 1996; Ethridge, 2011). Among these flaws are that planform is both spatially and temporally variable, even at different flow stages of the same river at the same locality (e.g. Thorne *et al.*, 1993, fig. 2), that multiple planforms can coexist along reaches of some rivers (e.g. Bridge, 2003, fig. 5.5) and that some rivers display characteristics transitional between recognized planform styles (e.g. Holbrook & Allen, 2021). Furthermore, Lyster *et al.* (2022a,b) have shown that predicting river planform from hydraulic parameters is fraught with difficulty. Despite these well-documented issues, geologists persist in using planform as the primary basis for categorizing and classifying alluvium, although some attempts have been made to employ a 'constructivist' approach by recognizing component architectural elements of alluvial deposits and assembling models from arrays of such 'building blocks' (e.g. Allen, 1983; Friend, 1983; Miall, 1985; Brierley, 1996).

Many factors influence the nature of river beds, and more still influence the character of resulting channel deposits. The planform of a river is a consequence of both internal (autogenic) and external (allogenic) controls, and although it might locally influence sediment accumulation patterns, it is itself controlled by factors that also independently control the river sediment character and depositional patterns. The hydrology of a river is, in contrast, mostly externally controlled, such that it may be more profitable to seek to understand alluvial deposits by understanding hydrology rather than planform.

Fielding *et al.* (2018) proposed using a statistic of discharge variability, the coefficient of variance of peak, inter-annual discharge (CVQ_p, defined as the standard deviation of the annual peak flood discharge divided by the mean annual peak flood discharge over the length of record) as a measure of flow variability in rivers. Those authors found a strong correlation between this parameter and preserved alluvial sediment character in a set of modern rivers for which both long gauging records and data on subsurface alluvial stratigraphy were available. The rivers examined in that study spanned a broad range of geographical context, planform and river size, and the CVQ_p in these rivers ranged from 0.18 to 1.01. Preserved alluvial character was found to be largely independent of planform, but it covaried strongly with CVQ_p. In particular, the prevalence of mesoform (dune-scale) cross-bedding as opposed to structures indicative of more powerful flows, the preservation of macroform features (channel scale), the lateral variability in lithology (including the preservation of pedogenically-modified mud), and the preservation of large woody debris and *in situ* tree stumps within channel deposits was found to correlate strongly with low, moderate, high and very high CVQ_p classes (Table 1).

This covariance allowed the recognition of CVQ_p classes of alluvial deposits in the rock record, thereby enabling a less ambiguous classification of ancient alluvium and providing insights into ancient palaeoenvironmental conditions (and their changes) from alluvial successions. The new framework has gained some traction, being used by researchers either explicitly (e.g. Hess & Fielding, 2020; Manna *et al.*, 2021; Schöpfer *et al.*, 2022; Dillinger *et al.*, 2024) or implicitly (e.g. Zellman *et al.*, 2020; Schwartz *et al.*, 2021; Arévalo *et al.*, 2022; Barefoot *et al.*, 2022; Sharma *et al.*, 2024) to classify and interpret several ancient alluvial successions.

Hansford *et al.* (2020) "define hydroclimate types that combine the Koppen-Geiger climate types with precipitation variability". Those authors used a variety of indices to show variations in flood magnitude, hydrograph shape and inter-annual variability in discharge for a suite of modern rivers. Using these statistics, they divided fluvial systems into four distinct groups: rivers with low hydrological variability, rivers

Table 1. Characteristics of the channel deposits of low, moderate, high and very high/ultra-high CVQ_p rivers. Class boundaries are somewhat arbitrary but informed by information presented in Table 2. Sedimentary structures common to all classes are not included (ripple cross-lamination, climbing ripple cross-lamination and soft-sediment deformation structures). Such structures are nonetheless likely to be more abundantly preserved in the channel deposits of lower and moderate CVQ_p rivers because of the less 'flashy' discharge patterns and gradual channel migration patterns prevalent in such rivers. Internal lithological heterogeneity is highly variable among all classes.

	Low CVQ_p (<0.5)	Moderate CVQ_p (0.5–0.8)	High CVQ_p (0.8–1.5)	Very High (1.5–2.0) and Ultra-High (>2.0) CVQ_p
Cross-sectional geometry	'Boat-shaped' cross-sections with clear channel forms	'Boat-shaped' cross-sections with channel forms	Variable, some lacking obvious channel forms	Tabular bodies lacking obvious channel forms
Within-channel sedimentary structures (ripple cross-lamination and soft-sediment deformation structures may occur in any of the classes)	Dune-derived cross-bedding dominant	Dune-derived cross-bedding, flat and low-angle stratification all common	Dune-derived cross-bedding subordinate, flat/low-angle stratification and antidunal bedding more common, some massive beds	Dune-derived cross-bedding only locally preserved, dominant flat/low-angle stratification, antidunal bedding (± chute and pool, cyclic steps), common massive beds
Within channel macroform structure	Well-developed and well-preserved	Partially-preserved	Limited preservation	Poorly-preserved or absent
Channel deposit internal lithological heterogeneity	Variable, generally limited lateral and vertical lithological changes	Variable, generally limited lateral and vertical lithological changes	Common lateral and vertical facies changes among mud, sand and gravel-grade units, some pedogenic modification	Common lateral and vertical facies changes among mud, sand and gravel-grade units, facies often show primary reddening and pedogenic modification
Characteristic plant and animal fossils	Root traces penetrate down into channel deposits from vegetation including trees on top of riverbanks and more stable bars (islands). The vegetation has limited impact on the architecture of sediments in the main part of channels	Some trees and shrubs may be established on lower bars and lower banks	Channel bed and bar top vegetation common including trees, influences sediment architecture and may be preserved in deposits. Trace fossils of burrowing animals present throughout channel fills	Vegetation is often more abundant in the channels than on the adjacent banks. In extreme arid conditions, vegetation and woody debris are rare. Trace fossils of burrowing animals common throughout channel fills

with seasonally variable hydrology, variable discharge rivers controlled by single storms (in an annual cycle) and extreme/erratic hydrology rivers. The Hansford *et al.* (2020) classes, though defined using different statistical factors and not tested against river deposit characteristics, are similar to the CVQ_p classes defined by Fielding *et al.* (2018). Certainly, rivers that are controlled by infrequent, large runoff events, and those characterized by intermittent/erratic runoff events (the third and fourth groups of Hansford *et al.*, 2020, listed above) are also those most likely to correspond to high and very high values of CVQ_p. Therefore, the question arises as to why the CVQ_p correlates so well with alluvial deposit characteristics, and whether other statistical factors of discharge variance might provide as good or better correlation. What evidently determines the properties of the alluvial record is not the seasonality or unevenness of discharge in a river on an annual cycle, nor the magnitude of peak discharge, but the relative prominence of extreme discharge events of varying magnitude, and the severity and length of droughts, particularly those that last over multiple years.

The dataset of Fielding *et al.* (2018) comprises only 16 rivers, some with multiple locations used to show down-river variability in the CVQ_p. To more fully evaluate the concept, more rivers should be included in the analysis, spanning a fuller range of latitude, climatic zone, drainage basin and river size, planform shape, and other variables. Furthermore, an exploration of the controls on the CVQ_p is warranted, along with an evaluation of sensitivities to major flow events. The data in Table 1 of Fielding *et al.* (2018) suggest that CVQ_p varies longitudinally along any one river, so an exploration of scale and causes of such variation is justified. Finally, running values of fixed-interval CVQ_p for a given gauging station may show major changes over time, and the causes of such changes are worthy of investigation. The CVQ_p is only one of many statistical measures of hydrological character, and although it is used here as the means to subdivide rivers and facies types, it should not be considered in isolation when studying individual rivers.

Other variables that can be estimated or calculated from ancient alluvium are useful in interpreting their formative conditions (see review by Long, 2021). Among them are various measures of flow properties such as flow velocity, flow depth, bankfull discharge and Froude number. Geomorphic parameters such as bed slope and roughness, and drainage basin area can also be calculated, making certain assumptions about natural conditions. Other researchers have more recently proposed using the coefficient of variation of preserved cross-set thickness to infer disequilibrium conditions between bedforms and formative flows in rivers, thereby attaining a metric of discharge variability (Leary & Ganti, 2020; Das *et al.*, 2022; Lyster *et al.*, 2022a,b; McLeod *et al.*, 2023), but Colombera *et al.* (2024) found that variability in cross-bed thickness may be a poor predictor of discharge variability.

In this paper, a more substantial database than presented by Fielding *et al.* (2018) is provided from which to consolidate and strengthen the concept of discharge variability-based facies models. The controls on the CVQ_p, both spatially and temporally for individual sites, are explored and a single drainage basin (the Platte River in central USA) is used as a case study to investigate both temporal and spatial changes in CVQ_p, and their impacts on the sedimentary record. This incorporates information from several classic fluvial facies publications. The central hypothesis that CVQ_p robustly correlates with preserved alluvial stratigraphy, in part independent of climatic mode (for example, monsoonal) is explored, and facies models for alluvial systems based on this variable are proposed.

DATA AND METHODS

Discharge data are increasingly available, either from the organizations responsible for the gauges or via national or international databases. The data sets are very large, recorded in different ways, and the peak flood data are of variable quality. Few rivers have been gauged for more than a few decades and none for longer than about 140 years. A lot of studies of fluvial sediments, however, record facies that may have been deposited tens to hundreds of years before they were studied. Many classic facies models were published tens of years ago, and consequently they may relate to runoff patterns and vegetation distributions that are different from those observed today. Relatively few studies of fluvial channel facies include geochronological data. When comparing discharge data with sediment facies characteristics, the age of the facies should be estimated and the appropriateness of discharge data records considered.

There are inherent issues with peak discharge data. Some databases include annual peak discharge datasets, and where these are based on reliable data records this makes calculating CVQ_p straightforward, but often river annual peak discharge series may be flawed. There are three reasons for this: (i) at peak flow, gauges might fail or gauge range be exceeded such that the peak value is not recorded at all or only estimated; (ii) many datasets use daily data and record daily mean data and both of those may significantly under-estimate true peak discharge particularly in flashy events; and (iii) some published annual series of peak flood discharges are based on data averaged over more than a single day and this underestimates peak discharge yet further. Thus, it is best to carefully investigate the nature of the original gauge data record, identifying data gaps and any other issues that lead to inaccurate estimates of peak values before calculating CVQ_p and other statistics. It is also important to find what controls there are on the river system (for example, large dams and major extraction points) and to consider the peak discharge series either before and/or after construction to avoid generating a CVQ_p that is controlled in major part by the initiation of the control. When comparing sedimentary facies records to discharge data, ideally the CVQ_p is calculated from data recorded near to the study site and for the period when the facies were deposited (i.e. if the facies were deposited before construction of a major dam, or major change in land use in the catchment, the CVQ_p used to relate to the facies patterns should be for the period before that change).

Some organizations give direct public access to vast amounts of data in a format that is easy to process. A lot of such data are available via The Global Runoff Data Centre. Some organizations restrict access to data or give access to data with less resolution or background information about reliability of peak data. A full list of data sources used herein is given below.

As stated previously, knowledge and understanding of rivers is very strongly biased by a predominance of studies of rivers in temperate countries. Add to this that most of the 'classic' studies of fluvial facies were undertaken in temperate northern areas gives a bias to the data included in this and other studies (Miall, 1978; Bridge, 2003). Obtaining suitable data for CVQ_p comparisons from some geographic settings is problematic either because of unreliable or non-existent river gauges or non-availability of data. The lack of reliable data is particularly acute in very arid areas. In ephemeral channels where water may flow for a few days once in many years, the CVQ_p will be very high. For example, if CVQ_p is calculated for a 30-year period of data for a stream that normally has a dry bed but records three separate flow events of 100 $m^3\ s^{-1}$ in different years the CVQ_p will be 3, whereas if the same size event happens only once in those 30 years, the value rises above 5.

The length of discharge data needed to generate a reliable CVQ_p varies with the character of discharge variability. In an unchanging system, the longer the gauging record the better. However, CVQ_p calculated over long periods will mask runoff pattern changes that may cause changes in facies patterns. A compromise is to use a record that is about 30+ years long. This then can give CVQ_p values that relate better to the discharge characteristics at the time the sediments studied in any particular example were deposited. The variation in CVQ_p over time is discussed further below.

CONTROLS ON THE INTER-ANNUAL PEAK DISCHARGE VARIANCE (CVQ_P)

The newly augmented database (Table 2) lists CVQ_p and alluvial record summary characteristics of 43 rivers. Most of the rivers presented in Table 2 are those for which sedimentological studies have been published, and wherever possible are based on subsurface geophysical imagery and drilling or trenching data. A major proportion of these rivers have been used to formulate published alluvial facies models. The data used to calculate CVQ_p are from the nearest gauging station to the sedimentological study sites. The variance in this database ranges from 0.08 to 3.45 (Table 2). CVQ_p for arid settings may be considerably higher but streams in such settings rarely have reliable gauging records for more than a few years. In some cases, CVQ_p is cited as a range where good data, available from multiple gauging stations, have been used to calculate the statistic. This provides an immediate indication that CVQ_p varies along the course of an individual river, and in some cases substantially (for example, Niobrara; Table 2). An example of CVQ_p changing through the Platte River basin in response to contributions from tributaries is given below. Also, CVQ_p may change over time in response to a variety of stimuli, both natural and anthropogenical.

Table 2. A database of 40 rivers for which both a long gauging record and an understanding of sedimentology and subsurface stratigraphy is available, extended and augmented from Table 1 of Fielding *et al.* (2018), listed in order of increasing CVQ_p. Values of CVQ_p cited in the Table are for the full period of record where data were of acceptable quality, and this coincides with the stated length of record. For rivers in the USA, the State listed is that where the gauging station(s) used are located. Some entries include data for both pre-regulation and post-regulation intervals, and they illustrate the varying response of rivers to regulation effects. Köppen climate zone given is the dominant classification across the drainage basin, acknowledging that many rivers cross multiple climatic zones.

River (and Location)	CVQ_p (and record length in years)	Area of catchment above gauging station in km^2	Geography – Climate zone Landscape type	Facies characteristics	Arborescent flora (*in situ* or transported) on banks or in channel	Plan form at facies study site	References
Amazon (Brazil)	0.08 (51) 0.13 (36)	4 680 000 2 854 286	Köppen Aw, Alluvial plain	Sand and mud, structures dominated by dune-derived cross-bedding at various scales, channel-scale features clearly identifiable (GPR)	Riparian vegetation including trees, some large, woody debris in channel	Spatially variable	Galeazzi *et al.* (2018), Tamura *et al.* (2019), Almeida *et al.* (2024)
Paraná do Careiro (Brazil)	0.15 (37)	2 583 079	Köppen Aw, Alluvial plain	Sand and mud, structures dominated by dune-derived cross-bedding at various scales, channel-scale features clearly identifiable (GPR)	Riparian tree vegetation, some large, woody debris	Spatially variable	Galeazzi *et al.* (2018), Tamura *et al.* (2019), Almeida *et al.* (2024)
Fraser (Northwest Territories, Canada)	0.19 (48) 0.21 (62)	114 000 32 400	Köppen Dfc, Mountainous to coastal plain	Gravel to sand downstream, gravel sheets and bar margin slipface deposits (some dune-derived cross-beds) including chute and channel fills, macroform structure clear (GPR)	Riparian trees on banks and on some bars	Wandering	Wooldridge & Hickin (2005), Rice *et al.* (2009), Rennie & Church (2010)
Mackenzie (Northwest Territories, Canada)	0.19 (70)	1 301 435	Köppen Dsc/Dfc, Mountainous to coastal plain (taiga)	Mainly silt and clay, basal rippled sands, little other information (no GPR)	Riparian tree vegetation on levées	Anabranching	Hill *et al.* (2001), Vesakoski *et al.* (2017)
Mekong (Laos and Vietnam)	0.19 (33)	545 000	Koppen Aw, Am, Alluvial and coastal plain	Vf–m sand, abundant mud, structures include dune-derived cross-bedding, flat and low-angle stratification, structureless sand, no information on macroform features (no GPR)	Variable riparian and channel bed tree vegetation, large woody debris	Spatially variable	Carling (2009), Gugliotta *et al.* (2018), Ishii *et al.* (2021)

Table 2. (continued)

River (and Location)	CVQ_p (and record length in years)	Area of catchment above gauging station in km^2	Geography – Climate zone Landscape type	Facies characteristics	Arborescent flora (*in situ* or transported) on banks or in channel	Plan form at facies study site	References
Ob' (Siberia)	0.18 (59) 0.26 (73)	2 160 000 486 000	Köppen Dfc, Lowland plain and taiga	Sand, silt and clay No data available on facies	Riparian vegetation in overbank domains	Spatially variable	Bobrovitskaya *et al.* (1997), Meade *et al.* (2000), Yang *et al.* (2004)
Jamuna (Bangladesh)	0.20 (56)	636 130	Köppen Aw, Lowland plain	Dominantly f–m sand, structures dominated by dune-derived cross-bedding at various scales, channel-scale features clearly identifiable (GPR)	Riparian vegetation includes trees on some mid-channel bars	Spatially variable (anabranching or braiding)	Bristow (1987, 1993), Ashworth *et al.* (2000), Best *et al.* (2003)
Ganges (Bangladesh)	0.21 (6) 0.24 (24) Limited gauging data, from Shan *et al.* (2020)		Köppen Cwa, Alluvial plain	Dominantly vf–f sand and mud, structures include dune-derived cross-bedding at various scales, flat and low-angle stratification, structureless sand, channel-scale features clearly identifiable (trenches, etc.)	Local riparian tree vegetation and large, woody debris	Braiding	Shan *et al.* (2020)
Mississippi (Central USA)	0.22 (103) 0.22 (71)	2 415 941 2 964 241	Köppen Cfa (Dfa), Lowland plain	Sand, silt and clay, structures dominated by dune-derived cross-bedding at various scales, channel-scale features clearly identifiable (trenches, etc.)	Riparian vegetation including trees on abandoned bars and in abandoned channels	Mainly meandering	Fisk (1944), Jordan & Pryor (1992), Harbor (1998), Nittrouer et al. (2008, 2012), Nittouer *et al.* (2011)
Paraná (Argentina)	0.24 (117)	1 950 000	Köppen Cfa, Alluvial plain	Vf–vc sand and mud, structures dominated by dune-derived cross-bedding at various scales, some flat and low-angle stratification, channel-scale features clearly identifiable (GPR)	Local riparian tree vegetation and large, woody debris	Low sinuosity	Parsons *et al.* (2005), Sambrook Smith *et al.* (2009), Reesink *et al.* (2014)
Kicking Horse (British Columbia, Canada)	0.24 (58)	1850	Köppen Dfc, Alluvial valley	Gravel and sand, structures dominated by dune-derived cross-bedding at various scales, channel-scale features clearly identifiable (GPR)	Minimal riparian vegetation of any kind, some large woody debris	Braiding	Cyples *et al.* (2020)

Table 2. (continued)

River (and Location)	CVQ_p (and record length in years)	Area of catchment above gauging station in km^2	Geography – Climate zone Landscape type	Facies characteristics	Arborescent flora (*in situ* or transported) on banks or in channel	Plan form at facies study site	References
Madison (Montana, USA)	0.31 (96)	1127	Köppen Dfb, Alluvial valley	Gravel and sand, structures dominated by dune-derived cross-bedding at various scales, flat stratification and imbrication, channel-scale features clearly identifiable (GPR)	Local riparian tree vegetation and large, woody debris	Meandering	Gawthorpe *et al.* (1993), Alexander *et al.* (1994)
Squamish (British Columbia, Canada)	0.33 (58)	2330	Köppen Dfc, Alluvial valley and plain	Gravel and sand, structures include dune-derived cross-bedding and flat/low-angle stratification, channel-scale features identifiable (GPR)	Large woody debris (log jams) common	Wandering	Wooldridge & Hickin (2005), Bauch & Hickin (2010)
Wisconsin (Wisconsin, USA)	0.39 (102)	26 936	Köppen Dfb, Alluvial plain	Dominantly f–c sand with minor small gravel and mud, structures include dune-derived cross-bedding, flat and low-angle stratification, channel-scale features clearly identifiable (GPR)	Variable riparian vegetation including trees, abundant large, woody debris	Braiding	Mumpy *et al.* (2007)
Calamus (Nebraska, USA)	0.40 (7) 0.42 (8) Gauge data too limited to be reliable, groundwater input	1796 2574	Köppen Dfa, Alluvial plain established on previous aeolian dune field	Vf–vc sand, minor mud and organic debris, peat, structures dominated by dune-derived cross-bedding, channel-scale features clearly identifiable (GPR)	Riparian vegetation (shrubs, small trees, reeds etc.), bars have reed growth	Braiding	Bridge & Gabel (1992), Gabel (1993), Bridge *et al.* (1998)
South Esk (Scotland, UK)	0.42 (30)	130	Köppen Cfb, Mountainous	Basal gravel, dominantly f–c sand, minor mud and organic debris, peat, structures dominated by dune-derived cross-bedding, channel-scale features clearly identifiable (GPR)	None (cleared for grazing)	Meandering on a narrow alluvial plain within a previously glaciated U-shaped valley	Bridge & Jarvis (1982), Bridge *et al.* (1995)
Kuparuk (Alaska, USA)	0.43 (52)	8651	Köppen Dfc, Alluvial plain	Gravel and sand, dune-derived cross-bedding on various scales, flat/low-angle stratification, channel-scale features abundantly preserved (no GPR)	Little if any riparian vegetation	Braiding	Tye (2004)

Table 2. (continued)

River (and Location)	CVQ_p (and record length in years)	Area of catchment above gauging station in km^2	Geography – Climate zone Landscape type	Facies characteristics	Arborescent flora (*in situ* or transported) on banks or in channel	Plan form at facies study site	References
Zambezi (Southeast Africa)	0.44 (69)	334 000	Köppen Cwa, Aw, Alluvial plain	Little available information	Variable riparian vegetation and large woody debris	Spatially variable	Moore *et al.* (2022)
Sagavanirktok (Alaska, USA)	0.44 (40)	4791	Köppen Dfc, Alluvial plain	Gravel and sand, dune-derived cross-bedding on various scales, flat/low-angle stratification, channel-scale features abundantly preserved (GPR)	Little if any riparian vegetation	Braiding	Lunt *et al.* (2004), Lunt & Bridge (2004), Tye (2004)
Wabash (Illinois/ Indiana, USA)	0.45 (140) 0.52 (86, pre-regulation) 0.33 (54, post-regulation)	74 164	Köppen Cfa, Alluvial plain	Mainly f–vc sand, minor gravel and mud, structures dominated by dune-derived cross-bedding (trenches, etc.)	Common riparian tree vegetation, large woody debris evident	Meandering	Jackson II (1975, 1976a,b), Zinger *et al.* (2011)
South Saskatchewan (Saskatchewan, Canada)	0.53 (20, pre-regulation) 0.72 (29, post-regulation) Some uncertainty because of winter ice affecting record	141 000	Köppen Dfb, Alluvial plain	Mainly f–c sand, structures include dune-derived cross-bedding, low-angle and undulatory stratification, channel-scale features visible but muted (GPR)	Minor riparian tree vegetation	Braiding	Cant (1978a,b), Cant & Walker (1978), Sambrook Smith *et al.* (2006, 2010), Parker *et al.* (2013)
Red (Arkansas, USA)	0.59 (105)	124 319	Köppen Cfa, Alluvial plain	Mud, sand and gravel, structures include dune-derived cross-bedding, flat and low-angle stratification, 'convex-upward stratification'	Riparian and channel-bed tree vegetation and large woody debris noted	Spatially variable	Schwartz (1978a,b)
Niobrara (Nebraska, USA)	0.61 (34) 0.32 (46, regulated)	2419 3781	Köppen Dfb, Alluvial plain	Dominantly m sand, minor silt, clay, organic debris, structures comprise dune-derived cross-bedding at various scales, flat, low-angle and undulatory stratification, channel-scale features clearly identifiable (GPR)	Riparian tree vegetation common, buried transported tree trunks noted in alluvium	Braiding	Ethridge *et al.* (1999), Bristow *et al.* (1999), Skelly *et al.* (2003)

Table 2. (continued)

River (and Location)	CVQ_p (and record length in years)	Area of catchment above gauging station in km^2	Geography – Climate zone Landscape type	Facies characteristics	Arborescent flora (*in situ* or transported) on banks or in channel	Plan form at facies study site	References
Congaree (South Carolina, USA)	0.75 (36, pre-regulation) 0.66 (130, all data)	20 331 20 331	Köppen Cfa, Coastal alluvial plain	M–c sand with minor gravel and mud, structures apparently dominated by dune-derived cross-bedding (trenches, etc.)	Minor riparian tree vegetation	Meandering	Levey (1978), Levey *et al.* (1980)
Eel (California, USA)	0.75 (30) 0.86 (100)	1368 751	Köppen Csb, Valley and alluvial plain	Gravel, sand and mud, flat and low-angle stratification common, limited data (no GPR)	Riparian tree vegetation and large woody debris common	Wandering	Brown III & Ritter (1971), Sloan *et al.* (2001)
Platte (Nebraska, USA)	0.65 (112) 0.82 (106)	153 586 145 816	Köppen Dfa, Alluvial plain	Dominantly m sand, minor gravel and mud, structures comprise dune-derived cross-bedding, flat and low-angle stratification, and abundant scour surfaces, channel-scale features identifiable but muted (GPR)	Riparian tree vegetation, including on bars, and large, woody debris common	Braiding and Anabranching	Smith (1970, 1971a,b), Miall (1977), Blodgett & Stanley (1980), Crowley (1983), Joeckel & Henebry (2008), Horn *et al.* (2012a, b), Joeckel *et al.* (2015)
Powder (Montana, USA)	0.75 (94)	20 795	Koppen BSk, Alluvial plain	Dominantly m–c sand, lesser gravel and mud, structures include dune-derived cross-bedding, flat and low-angle stratification, convex-upward antidunal stratification, channel-scale features preserved (trenches, etc.)	Riparian tree vegetation and large woody debris noted	Meandering	Moody & Meade (2014), Ghinassi & Moody (2021), Maitan *et al.* (2024)
Amite (Louisiana, USA)	0.80 (63)	2290	Köppen Cfa, Alluvial plain	Dominantly gravel and c sand, structures dominated by dune-derived cross-bedding and flat and low-angle stratification, channel-scale features identifiable (trenches, etc.)	Riparian and channel bed tree vegetation, large woody debris common	Meandering	McGowen & Garner (1970)

Table 2. (continued)

River (and Location)	CVQ_p (and record length in years)	Area of catchment above gauging station in km^2	Geography – Climate zone Landscape type	Facies characteristics	Arborescent flora (*in situ* or transported) on banks or in channel	Plan form at facies study site	References
Bijou Creek (Colorado, USA)	0.84 (11) Gauge data too limited to be reliable	3582	Köppen Bsk, Alluvial plain	Dominantly f–c sand, structures dominated by flat and low-angle stratification (including antidunes), massive/faintly stratified and convolute sand beds, channel-scale features not preserved (trenches, etc.)	Riparian and channel bed tree vegetation, large woody debris common	Wandering	McKee *et al.* (1967)
Lower Burdekin (Queensland, Australia)	0.90 (61)	129 876	Köppen Aw, Alluvial and coastal plain	Bedload c–vc sand and gravel, suspended load c sand to clay, structures comprise flat and low-angle stratification, gravelly antidunes, dune-derived cross-bedding, scour surfaces (GPR)	Riparian and channel bed tree vegetation abundant, large woody debris and *in situ* stumps abundant	Low sinuosity	Alexander *et al.* (1999), Amos *et al.* (2004), Fielding *et al.* (2005, 2011)
Elkhorn (Nebraska, USA)	0.93 (104)	17 871	Köppen Dfa, Alluvial plain	Dominantly f–c sand, minor gravel and mud, structures include dune-derived cross-bedding, flat and low-angle stratification, channel-scale structures unknown (no GPR)	Scattered riparian tree vegetation, common large woody debris	Spatially variable	Personal observations
Upper Burdekin (Queensland, Australia)	1.0 (90) Influenced by some groundwater input	36 390	Köppen Bsh, Alluvial plain	Bedload c–vc sand and gravel, suspended load c sand to clay, structures comprise flat and low-angle stratification, gravelly antidunes, cross-bedded scour fills, minor dune-derived cross-bedding, channel-scale features rarely preserved (GPR)	Riparian and channel bed tree vegetation abundant, large woody debris and *in situ* stumps abundant	Spatially variable	Fielding & Alexander (1996), Alexander & Fielding (1997), Fielding *et al.* (1997, 1999, 2011)
Fitzroy (Queensland, Australia)	1.01 (51)	135 860	Köppen Cfa, Bsh, Alluvial plain	Gravel, sand and mud, structures comprise flat and low-angle stratification, minor dune-derived cross-bedding, channel-scale structures unknown (no GPR)	Riparian and channel bed tree vegetation, large woody debris, abundant	Anabranching and meandering	Croke *et al.* (2011)
Orange (Southwest Africa)	1.05 (77)	364 560	Köppen BWh, Alluvial plain	Dominantly gravelly sand, few details of bedforms, channel-scale features identifiable in palaeo-channel deposits	Riparian tree vegetation and large woody debris common	Spatially variable, study reach anabranching	Jacob *et al.* (1999), Tooth & McCarthy (2004)

Table 2. (continued)

River (and Location)	CVQ_p (and record length in years)	Area of catchment above gauging station in km^2	Geography – Climate zone Landscape type	Facies characteristics	Arborescent flora (*in situ* or transported) on banks or in channel	Plan form at facies study site	References
Loup (Nebraska, USA)	1.07 (83) 0.86 (63)	37 088 39 368	Köppen Dfa, Alluvial plain	Dominantly f–m sand, structures include dune-derived cross-bedding, flat and low-angle stratification, multiple scour surfaces, channel-scale features recognizable but muted (GPR)	Riparian tree vegetation, large woody debris and buried tree trunks common	Braiding	Fielding *et al.* (2018), Mason *et al.* (2020)
Colorado (Texas, USA)	1.17 (71) 0.94 (8, pre-regulation) Strongly regulated after 1940	75 027	Köppen Cfa, Alluvial plain	Dominantly gravel and c sand, structures dominated by dune-derived cross-bedding and flat and low-angle stratification, channel-scale features identifiable (trenches, etc.)	Riparian tree vegetation and large woody debris common	Meandering	McGowen & Garner (1970)
Nueces (Texas, USA)	1.20 (107)	39 956	Köppen Cfa, Alluvial plain	Dominantly gravel, minor sand and mud, structures include gravel sheets, flat and low-angle stratification, gravel antidunes, dune-derived cross-bedding (no GPR)	Riparian and channel bed tree vegetation abundant, large woody debris common	Wandering	Gustavson (1978)
Luni (Northwest India)	1.95 (31) (Estimated from peak data in Kale *et al.* 2000)	32 010	Köppen BWh, Ephemeral stream in desert	Dominantly f–m sand with common mud partings and local gravel, abundant dune-derived cross-bedding, flat and low-angle stratification, antidune bedding, channel-scale features unclear (trenches, etc.)	Bushes in channel bed	Low sinuosity	Kale *et al.* (2000), Carling & Leclair (2019)
Cooper Creek (Central Australia)	2.06 (48)	232 846	Köppen BWh, ('Channel Country'), Alluvial plain	Dominantly clay to f sand and m–c sand-sized mud aggregates, structures include flat and low-angle stratification, dune-derived cross-bedding, channel-scale features unclear (no GPR)	Abundant riparian and channel bed tree vegetation, large woody debris	Anabranching	Nanson *et al.* (1986), Gibling *et al.* (1998), Maroulis (2000)
Big Thompson (Colorado, USA)	2.09 (101) 3.45 (51)	790 355	Köppen Dfc/Dfb, Bedrock-floored canyon/alluvial plain	Gravel and sand, structures dominated by clast imbrication and upper flow regime stratification (cutbanks, etc.)	Isolated vegetation on transient bar tops	Low sinuosity	NOAA (1976), Kimbrough & Holmes Jr. (2015)

Table 2. (continued)

River (and Location)	CVQ_p (and record length in years)	Area of catchment above gauging station in km^2	Geography – Climate zone Landscape type	Facies characteristics	Arborescent flora (*in situ* or transported) on banks or in channel	Plan form at facies study site	References
Hugh (Northern Territory, Australia)	2.45 (49)	3324	Köppen BWh, (tributary of Finke River), Alluvial plain	Sand and mud, no information on structures or macroforms available	Abundant riparian and channel bed tree vegetation, large woody debris	Wandering	
Wadi Yanqul (Oman)	2.80 (15) Gauge data too limited to be reliable	472	Köppen BWh, Ephemeral stream in desert NB: Arid streams may have much higher variance but lack long-term gauging records	Dominantly sand, minor mud and gravel, structures include flat and low-angle stratification, dune-derived cross-bedding, some channel-scale features identifiable (GPR, cutbanks, etc.)	Scattered trees in channel	Low sinuosity/ braided	Fryberger *et al.* (2016), Kocurek *et al.* (2020)
Roaring/Fall (Colorado, USA)	3.45 (51) (Gauge located below confluence with Big Thompson River)	355	Köppen Dfc, Bedrock-floored canyon/alluvial valley	Confluence alluvial fan dominated by coarse gravel and sand, structures dominated by clast imbrication and upper flow regime stratification, up to 14 m thick deposit formed in 1982 flash flood (cutbanks, etc.)	Little if any vegetation in channels	Low sinuosity/ meandering	Jarrett & Costa (1986), Blair (1987)
Jökulsá á Fjöllum (Iceland)	0.27 (24) Modelled impact of imposing flow ×10–1.72 ×50–3.63 ×100–4.16 (see Table 3)	2023	Köppen ET, Glacier-fed river subject to outburst floods ('jökulhlaups')	Gravel and sand, structures include abundant flat and low-angle stratification, scour fills, possible cross-bedding (GPR)	Little if any riparian vegetation	Low sinuosity/ braided	Cassidy *et al.* (2004), Alho *et al.* (2005)

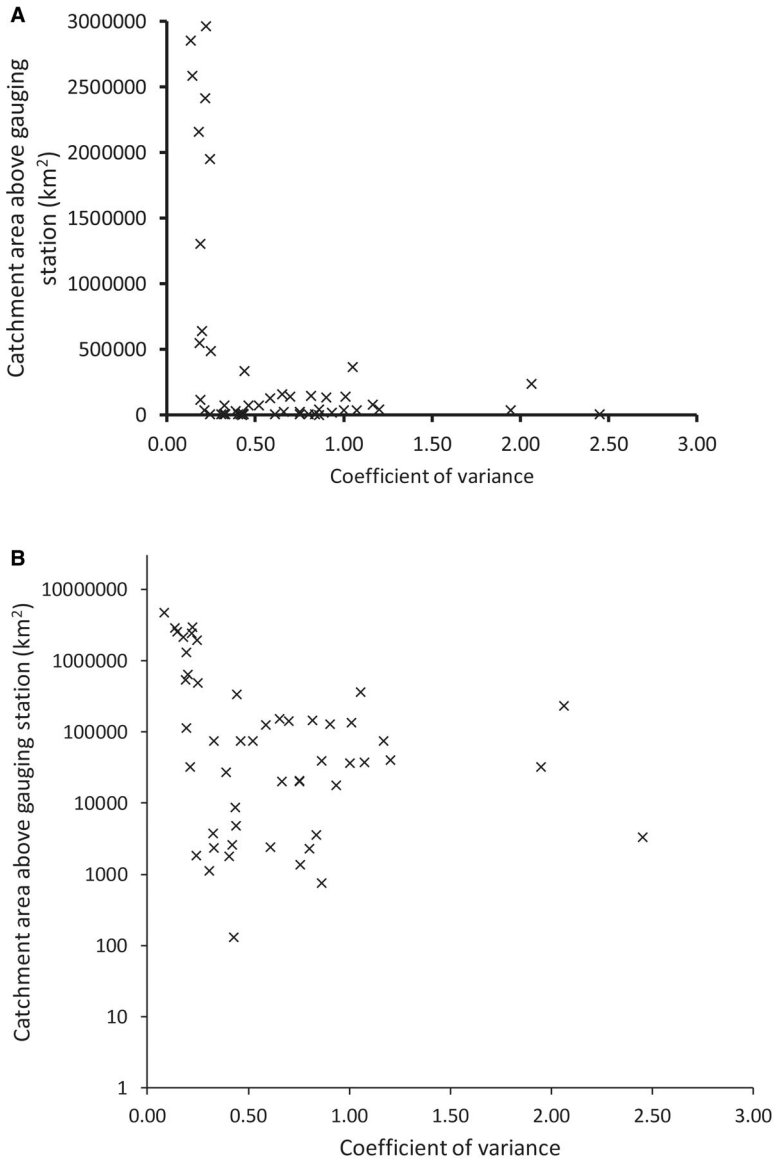

Fig. 1. Plot of CVQ_p versus drainage area above the gauging station where CVQ_p was calculated (shown on a logarithmic scale), for a globally distributed suite of rivers (including all those listed in Table 2): (A) using a linear scale; and (B) using a logarithmic scale for drainage area.

To provide insight into the role of drainage area on CVQ_p, the area of drainage basin above the gauging station(s) used is listed (Column 3 of Table 2). Figure 1 shows CVQ_p plotted against catchment area above the gauging site; this suggests that there is a complex non-linear relationship between the two variables, and the understanding of this can be improved by plotting CVQ_p against mean annual peak discharge (Fig. 2) which shows a weak negative correlation. Rivers with smaller mean annual peak discharge exhibit a much broader range in CVQ_p (see also Table 2). This is as expected for several reasons: (i) weather events causing major floods may affect the entirety of one small river catchment but only part of a big catchment; (ii) flood waves may be attenuated as they move down river systems, making their duration longer compared to their peak magnitude, and CVQ_p is a statistic of peak magnitude variance; and (iii) in any one event the peak discharge from different tributaries may reach a point on the trunk stream at different times, such that the size of a major event may not appear relatively as big lower in a drainage system. Because the main stem (trunk) channel(s) of continent-scale rivers receive water from many tributaries, anomalous effects of individual tributaries will be subdued in a manner comparable to that documented for downstream 'shredding' of

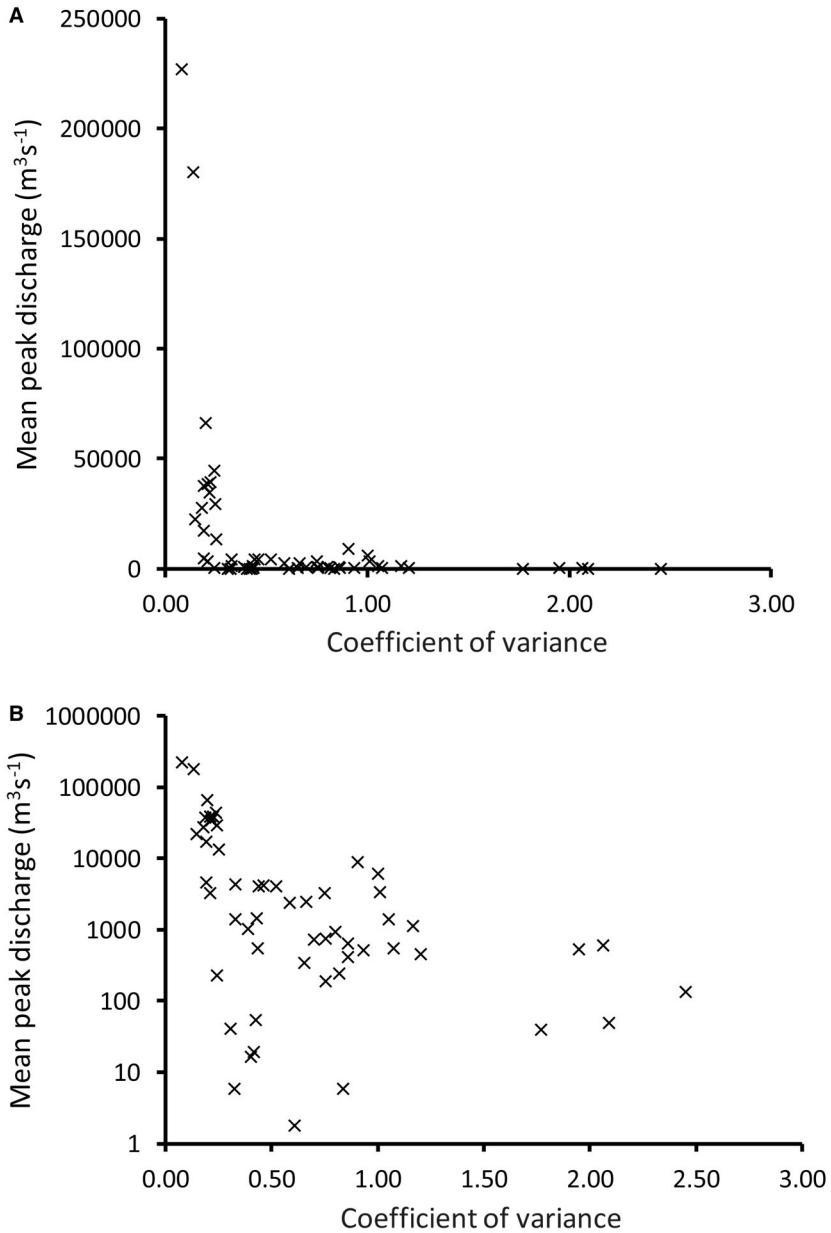

Fig. 2. Plot of CVQ_p versus peak discharge for a globally distributed suite of rivers (including all those listed in Table 2): (A) using a linear scale, and (B) using a logarithmic scale for peak discharge.

environmental signals in sedimentary records (Jerolmack & Paola, 2010; Romans *et al.*, 2016). That large, continental scale rivers will show low values of CVQ_p is therefore predictable.

Rivers with high and very high/ultra-high CVQ_p are concentrated in areas with arid, semi-arid or at least subhumid climate, at a variety of latitudes. The few examples of good gauging data available for arid areas give very high CVQ_p. In contrast, there is less relationship between rivers with low values of CVQ_p and climatic context, with examples in a variety of latitudinal belts (Table 2). Some large rivers with low CVQ_p are affected by monsoonal precipitation patterns (for example, Jamuna, Ganges), while others are in non-monsoonal, warm temperate (for example, Mississippi) or in cool to cold temperate climate zones (Mackenzie, Ob'). Groundwater-fed rivers tend to have low CVQ_p and can occur in any climatic setting. Plotting CVQ_p against river location (at the gauging station) in degrees of latitude north or south of the Equator indicates some coherent relationships. Rivers in the Equatorial belt tend to have low CVQ_p values, which rise towards the subtropical zone (20–30° north and south) where climate is typically subhumid to

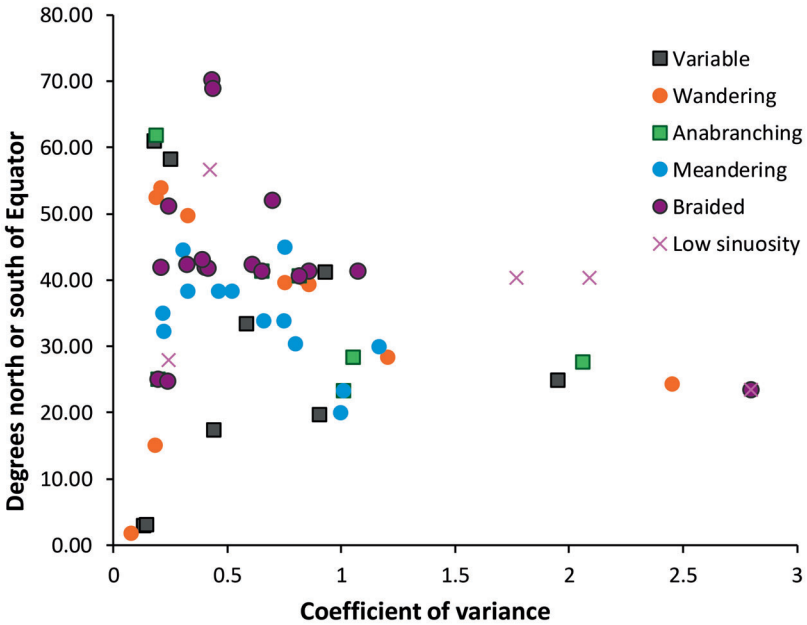

Fig. 3. Plot of CVQ_p versus degrees of latitude north or south of the Equator for the rivers included in Table 2, with data points colour-coded by river planform. The cluster of braided rivers at about 40 degrees partly reflects the concentration of effort on sand bed braided rivers in Nebraska, central USA. See text for further discussion.

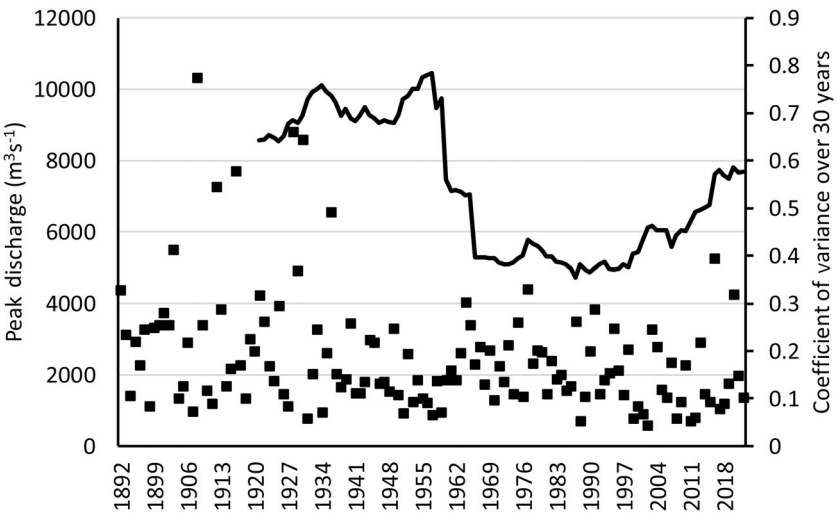

Fig. 4. Plot of CVQ_p versus time for the Congaree River in South Carolina, USA, with 30 year moving values. To calculate the 30 year moving CVQ_p for a given year, the peak discharge for that year and the preceding 29 years are used – thus the line on the graph is generated by a moving data window for calculation of CVQ_p.

semiarid and strongly seasonal. Rivers in the database with the highest CVQ_p values (Fig. 3) are located about the Intertropical Convergence Zone. Rivers in mid-latitudes and high-latitudes show a progressive decrease in CVQ_p values (Fig. 3). There is no correlation between CVQ_p and river planform (Fig. 3).

Examination of long gauge records (of the order of 100 years or more) shows that CVQ_p has changed in modern rivers over time, in some cases abruptly due to a single flow event, in some rapidly because of damming or land use change, and in others more gradually in response to some external forcing. Discharge data from the Congaree River of South Carolina, USA, illustrates moderately rapid change (Fig. 4). The 30-year moving CVQ_p value declines steeply over the period 1950 to 1970, a time when numerous dams were constructed on the river. This illustrates how regulation related to dam construction may have a profound impact on rivers. Natural variability can only be reliably assessed by examining pre-regulation records. Since 2000, there has been a gradual

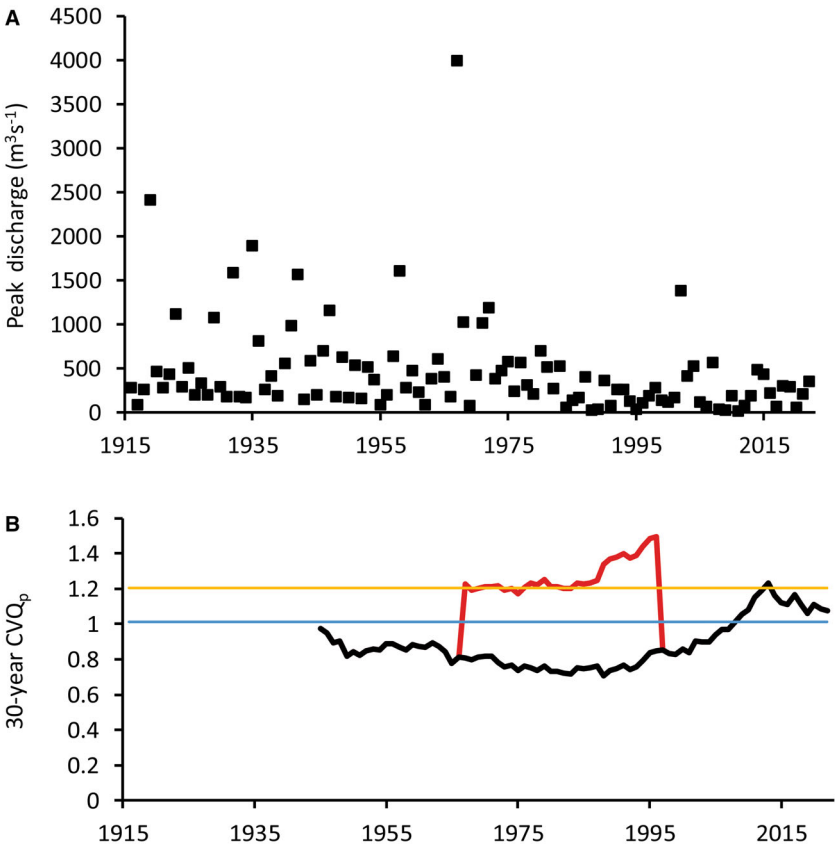

Fig. 5. Discharge and CVQ_p for the Nueces River at Three Rivers, Texas, to illustrate the effect of an anomalous flow event, in 1967. (A) Annual peak discharge series, in $m^3\ s^{-1}$. (B) Plots of the overall and 30 year moving values of CVQ_p versus time. Orange line – CVQ_p for all data (1.2), blue line – CVQ_p for all data excluding 1967 (1.0), red line – CVQ_p 30 year moving value for all data, black line – CVQ_p 30 year moving value for all data excluding 1967.

rise in CVQ_p in the Congaree River (Fig. 4) which could be a consequence of climate change, land use change and/or degradation of storage in the dams.

The impact of a single, anomalously high flow event on CVQ_p is illustrated by data from the Nueces River of Texas, USA (Fig. 5). In Fig. 5A, the anomalous nature of the 1967 event is evident from a plot of average annual peak discharge, and the effects of that event on both the CVQ_p calculated over the total record (over 100 years) and the 30-year moving CVQ_p are shown in Fig. 5B. This shows how major, anomalously large flow events will have a significant effect on the statistic. It is likely that such anomalously large events have sedimentological significance (see below).

THE RELATIONSHIP BETWEEN CVQ_P AND ALLUVIAL SEDIMENT CHARACTER

The expanded database (Table 2) confirms and strengthens the already robust relationship between CVQ_p and characteristics of preserved alluvium posited by Fielding *et al.* (2018). As CVQ_p increases, the proportion of dune-scale cross-bedding preserved in river-channel deposits decreases and the proportion of sedimentary structures generated in the upper flow regime, such as planar stratification, cross-bedded scour fills and antidunal bedding, increases. Concomitantly, the degree of preservation of recognizable macroform features decreases, and in-channel lateral variability in lithology increases. This all reflects the increasingly peaked (or 'flashy') nature of discharge in high CVQ_p systems, in which the bed is rarely able to attain or retain equilibrium with flow conditions during rapidly falling stage such that bedforms representative of peak or early falling stage are less likely to be reworked and more likely to be preserved. Furthermore, because many rivers that have high CVQ_p are in arid, semiarid or subhumid areas, it is also common for such systems to host river bed trees, because the river bed in these systems is both dry for extended periods (thereby allowing opportunistic woody

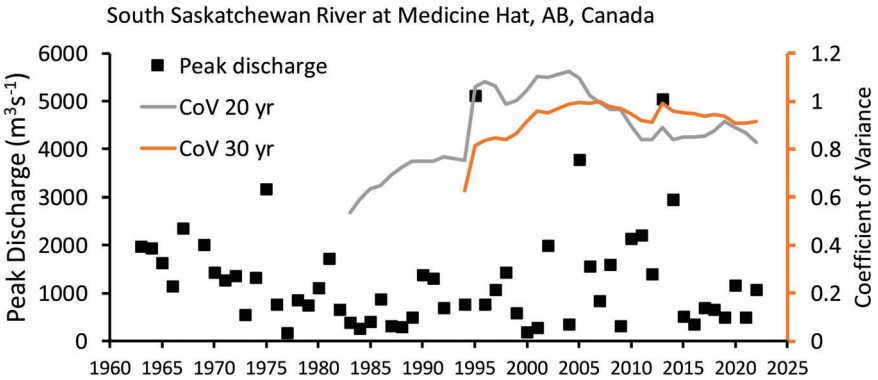

Fig. 6. Annual peak discharge series, and 20 and 30 year moving values of CVQ_p for the South Saskatchewan River at Medicine Hat, Alberta, showing the 2005 event investigated by Sambrook Smith *et al.* (2010) and its minimal effect on CVQ_p. The Medicine Hat gauge data are used here in preference to those from the closer Saskatoon gauge because the data series is longer-lived with fewer time gaps. The CVQ_p running values rise significantly after the river became heavily regulated in the 1990s.

vegetation to become established) and constitutes the only reliable, year-round source of moisture at a depth roots can reach. Thus, the presence of both *in situ* tree stumps and of large woody debris is enhanced in many high CVQ_p systems.

The changing nature of preserved alluvium with increasing CVQ_p is not just a function of flow conditions but also one of the manner in which sediment is accumulated differently in rivers with varying flow regime. For example, Sambrook Smith *et al.* (2010) found, through repeat Ground-Penetrating Radar (GPR) surveys, that a major flow event in 2005 on the South Saskatchewan River in western Canada (CVQ_p = 0.72; Fig. 6), made little if any recognizable difference to the accumulated sediment in the river. This implies that for rivers with low to moderate CVQ_p, such as the South Saskatchewan, the preserved record is one of repeated small incremental additions of beds over long timeframes. In contrast, Fielding *et al.* (1999) found that a single major flow event on the upper Burdekin River in Queensland, Australia (CVQ_p = 0.92–1.22) in 1997 entailed up to 6 m of bed erosion and redeposition. McKee *et al.* (1967) also documented deposition of up to 4 m of alluvium during the catastrophic flood of June 1965 on Bijou Creek, Colorado, USA (CVQ_p = 0.92). This limited dataset suggests that the nature of sediment accumulation may vary with CVQ_p, with high CVQ_p systems more prone to wholesale reworking and partial to complete channel filling from single events. Given this pattern, and the increased presence of stratification styles indicative of upper flow regime conditions, it is logical that high CVQ_p rivers will preserve a greater proportion of such deposits in their sedimentary record. The extreme of this is in arid settings where the only fluvial deposition occurs in infrequent runoff events (e.g. Fryberger *et al.*, 2016; Kocurek *et al.*, 2020). In such settings the CVQ_p is likely to be well over 2.

Alexander *et al.* (2020) examined sequential remotely sensed imagery of the lower Burdekin River (CVQ_p = 1.00) and compared patterns of river bed change (inferring from that sediment accumulation) with discharge data between 1977 and 2018 in order to assess how runoff events with different hydrograph size and shape correlated to significant sediment accumulation or erosion on the river bed (Fig. 7A). These authors found that flow events with peak discharge greater than 14 000 $m^3\ s^{-1}$ (Type A; Fig. 7A) had considerable impact on the bed. Events with peaks 10 000 to 14 000 $m^3\ s^{-1}$ and a gradual discharge decline (Type B; Fig. 7A) produced modest changes, whereas events with 10 000 to 14 000 $m^3\ s^{-1}$ peak and rapid discharge fall (along with lesser runoff events, Type C; Fig. 7A) produced little if any change on the bed. The largest and most prolonged runoff event in the interval of study was in January/February 1991, which according to Alexander *et al.* (2020) 'reset' the channel bed significantly. It is conceivable that the sediment seen 4 to 10 m below the river bed in GPR data acquired in 1999 (fig. 6 of Fielding *et al.*, 2011), which preserves trough cross-beds

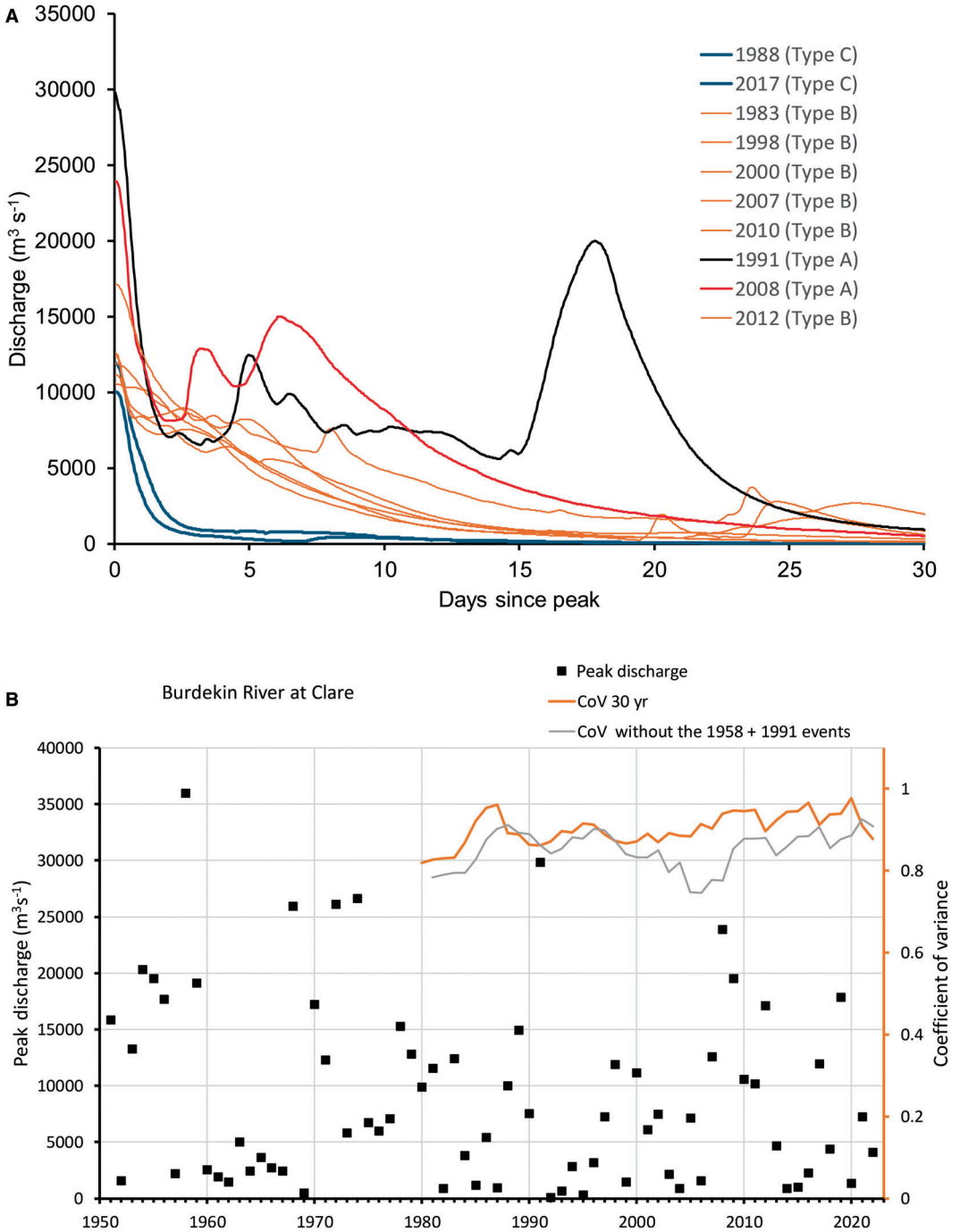

Fig. 7. (A) Falling stage hydrographs of several recent major flow events on the lower Burdekin River, and their correlation to bed change as determined by examination of serial remotely sensed imagery (from Alexander *et al.*, 2020). Type A events with peak discharge greater than 14 000 m^3 s^{-1} had considerable impact on the bed. Type B events with peaks 10 000 to 14 000 m^3 s^{-1} and a gradual discharge decline produced modest changes, whereas Type C events with 10 000 to 14 000 m^3 s^{-1} peak and rapid discharge fall (along with lesser runoff events) produced little if any change on the bed. (B) Annual peak discharge series for Clare gauging station on the lower Burdekin River. Note that of the events shown in part (A), only 1991 caused significant changes to the river bed. Based on this limited database, it seems that only exceptional events had significant impacts on the river bed.

Table 3. Calculations of modelled CVQ_p on the Jokulsá á Fjöllum in north-east Iceland, based on a 24 year gauging record that does not include any jökulhlaups, and adding an artificial year to the record with differing peak discharge magnitudes relative to the recorded peak discharge. The CVQ_p of the raw gauging record is 0.27. Jökulhlaups with 100 times normal peak discharge have been documented from the region (e.g. Snorrason *et al.*, 2002).

With one artificial year added	Synthetic Qp	Model CVQ_p
2 × maximum	877.58	0.420225
4 × maximum	1755.16	0.814732
10 × maximum	4387.90	1.719781
50 × maximum	21939.50	3.625332
100 × maximum	42876.00	4.156576

up to 3 to 4 m thick that are continuous for tens of metres in the flow-parallel direction, were deposited at this site during the 1991 event.

The three types of events summarized above, from 1977 to 2018, are plotted on the annual peak discharge series at Clare on the lower Burdekin River (Fig. 7B). Although only two events fall into the category that caused major bed change, it is evident that exceptional events are required to have any major impact on the sedimentary record of this river. Given the observations summarized above and noting that there are other exceptional events shown in Fig. 7B which pre-date the time series of available aerial imagery, this suggests that events shaping the alluvial record of the Burdekin River occur on intervals of tens of years. GPR data (Fielding *et al.*, 2011) suggest that the most recent of those events (1991) is likely to be largely responsible for what is currently preserved below the bed of the modern river.

The very large 1991 Burdekin River flow event made very little change to the CVQ_p at Clare (Fig. 7B). Conversely, large events in rivers with lower CVQ_p, such as the South Saskatchewan (Fig. 6), have an immediate impact on the CVQ_p, with abrupt rises recorded in 1995 and 2013 (but not in 2005; Sambrook Smith *et al.*, 2010). This raises the question of whether events so anomalous that they abruptly increase the CVQ_p are required in order to have any significant influence on preserved stratigraphy in such systems.

An extreme example of this relationship is provided by glacial outburst floods (or 'jökulhlaups' from the Icelandic). Such phenomena, triggered by sub-glacial volcanic eruptions or breaches of glacial lake dams, entail abrupt, one to three orders of magnitude increase in discharge down glacier-fed rivers (e.g. Snorrason *et al.*, 2002; Alho *et al.*, 2005; Marren *et al.*, 2009; Carrivick & Tweed, 2019). No long-term gauging records that include major jökulhlaups could be found during this study. To circumvent this issue, Table 3 models the effect of superimposing a jökulhlaup of varying magnitude on the annual peak discharge from a 24-year gauging record (that does not include any jökulhlaups) from Jökulsá á Fjöllum in north-east Iceland. The CVQ_p rises from 0.27 for the raw gauge record to >4 if a year is added with a discharge that peaks at 100 times greater than the maximum recorded event (Table 3). Events of this and larger magnitude have been recorded or inferred in the recent past from Jökulsá á Fjöllum (Alho *et al.*, 2005) and Skeiðarársandur, southern Iceland, in 1996 (Snorrason *et al.*, 2002). Major historical and older Holocene jökulhlaups have been shown to leave a lasting imprint on the landscape in terms both of erosional and (importantly) depositional features (e.g. Maizels, 1989; Russell & Knudsen, 2002; Cassidy *et al.*, 2004; Alho *et al.*, 2005; Duller *et al.*, 2008; Marren *et al.*, 2009).

A case study: the Platte River drainage basin, central USA

A case study of the Platte River drainage basin (220 000 km^2; Fig. 8) in the central Great Plains region of the USA is used here to evaluate spatial and temporal changes in CVQ_p and their potential impact on alluvial records. This system is coincidently an area where several formative studies in fluvial lithofacies analysis were undertaken by numerous researchers, and those study sites are marked on Fig. 8. The Platte has two main threads, the North and South Platte rivers (Fig. 8), both of which rise in the Front Range, Rocky Mountains of Wyoming and Colorado, and flow broadly eastward, converging in western Nebraska before joining the Missouri River near Plattsmouth in south-east Nebraska. There are several major tributaries in the upstream portion of the basin, including Big Thompson River, Bijou and Lodgepole creeks on the South Platte, and the Laramie River and Sweetwater Creek on the North Platte. Downstream of the confluence of the North and South Platte, there are several more major tributaries including the Loup and Elkhorn rivers. Several

dams have been built on the upper parts of the system, notably Lake McConaughy on the North Platte River, completed in 1941. Numerous gauging stations, some with over 100 years of record, provide a plethora of discharge data throughout the drainage basin (Fig. 8), facilitating an analysis of CVQ_p patterns in time and space. This plethora of data largely overcomes the problems that arise if one (or more) gauging station record is incomplete or 'suspect' for individual discharge events (peak discharge may be unreliable in gauging data because it may exceed the measuring range of the gauging station and consequently require an estimate).

A lot of sedimentological and stratigraphic data are available for Bijou Creek (McKee *et al.*, 1967; Costa & Jarrett, 2008), the confluence of the Roaring River and Fall River (Jarrett & Costa, 1986; Blair, 1987), the Big Thompson River (Kimbrough & Holmes Jr., 2015), and for the mainstem Platte River (Smith, 1970, 1971a,b; Joeckel & Henebry, 2008; Horn *et al.*, 2012a,b; Joeckel *et al.*, 2015) and the Calamus River (Bridge & Gabel, 1992; Gabel, 1993; Bridge *et al.*, 1995). These well-known study sites are indicated on Fig. 8.

In general, CVQ_p has fluctuated modestly over the periods of record in the mainstem channel, as exemplified by the gauging stations at Overton and Duncan, Nebraska (Figs 8, 9A and 9B). The record at Louisville, Nebraska (Fig. 9C), on the other hand, shows a large upward shift in 2019, after a major flow event in that year that resulted from exceptional early spring rainfall combined with rapid melting of winter snow accumulation. This event emanated from the Elkhorn River catchment (Fig. 8). This highlights the impact that rare flow events can have on the CVQ_p. Several such runoff events have occurred in different parts of the Platte River catchment over the period of record. The CVQ_p 'signature' of specific events was tracked, including the June 1965 (tributaries and South Platte River in eastern Colorado and western Nebraska), July 1982 (Roaring River to Big Thomson River) and March 2019 events (Elkhorn and lower Platte rivers), to determine how far the influence of a single precipitation and runoff event can extend. The 2013 flow event in the Big Thompson and South Platte rivers, which caused an estimated 3 billion US$ damage to property and infrastructure (Kimbrough & Holmes Jr., 2015) in the Front Range canyon and adjacent plains communities in eastern Colorado (Fig. 8), was also tracked. Figures 10 to 13 show the characteristics of the CVQ_p response to the runoff events in 1965, 1982, 2013 and 2019, respectively. These maps show: the portion of the basin where there was a noticeable effect on the CVQ_p based on gauging records (the most downstream station shown being the lowest station where a change is evident); the annual peak discharge record at selected gauging stations together with running values of CVQ_p; the relative size of the change in CVQ_p (size of coloured circle indicates minor, moderate and major changes, respectively); and the date when peak discharge was recorded at the selected gauging stations. In some cases, the CVQ_p rose to levels well beyond the long-term values used to characterize river systems in Table 2. For every gauging station shown in Figs 10 to 13, the event in question was the peak discharge for the given year.

The South Platte River event of June 1965 (Fig. 10) arose from heavy precipitation in the western tributary catchments, with the flood peak moving downstream through the area over five or six days. A change in the CVQ_p resulting from this event is seen as far as the town of North Platte, 250 km downstream (Costa & Jarrett, 2008). The biggest effects were felt in the tributary streams such as Kiowa, Plum and Bijou creeks (Fig. 10), although gauging records there are somewhat incomplete. Costa & Jarrett (2008) estimated peak discharge indirectly at 7759 m^3 s^{-1} in Bijou Creek. McKee *et al.* (1967) provide detailed sedimentological data on the effects of this event. They documented the cutting and filling of new channels at multiple locations, with extensive deposition of up to 4 m of sands internally dominated by upper flow regime stratification. It is notable that this case study became the basis for one of Miall's (1977) vertical sequence facies models for braided river deposits. The record of this event at Bijou Creek is unquestionably that of a high to very high CVQ_p system.

A flash flood on the Roaring River in the high Rocky Mountains occurred on 15 July 1982 as a result of dam failure (Jarrett & Costa, 1986; Blair, 1987). A hyperconcentrated flow descended the Roaring River and constructed a new alluvial fan at the confluence with the Fall River (a tributary of the Big Thompson River; Fig. 11). Peak discharge on the Roaring River was estimated as 340 m^3 s^{-1} (Jarrett & Costa, 1986). This event had a major impact on the CVQ_p for only a few kilometres downstream of the confluence

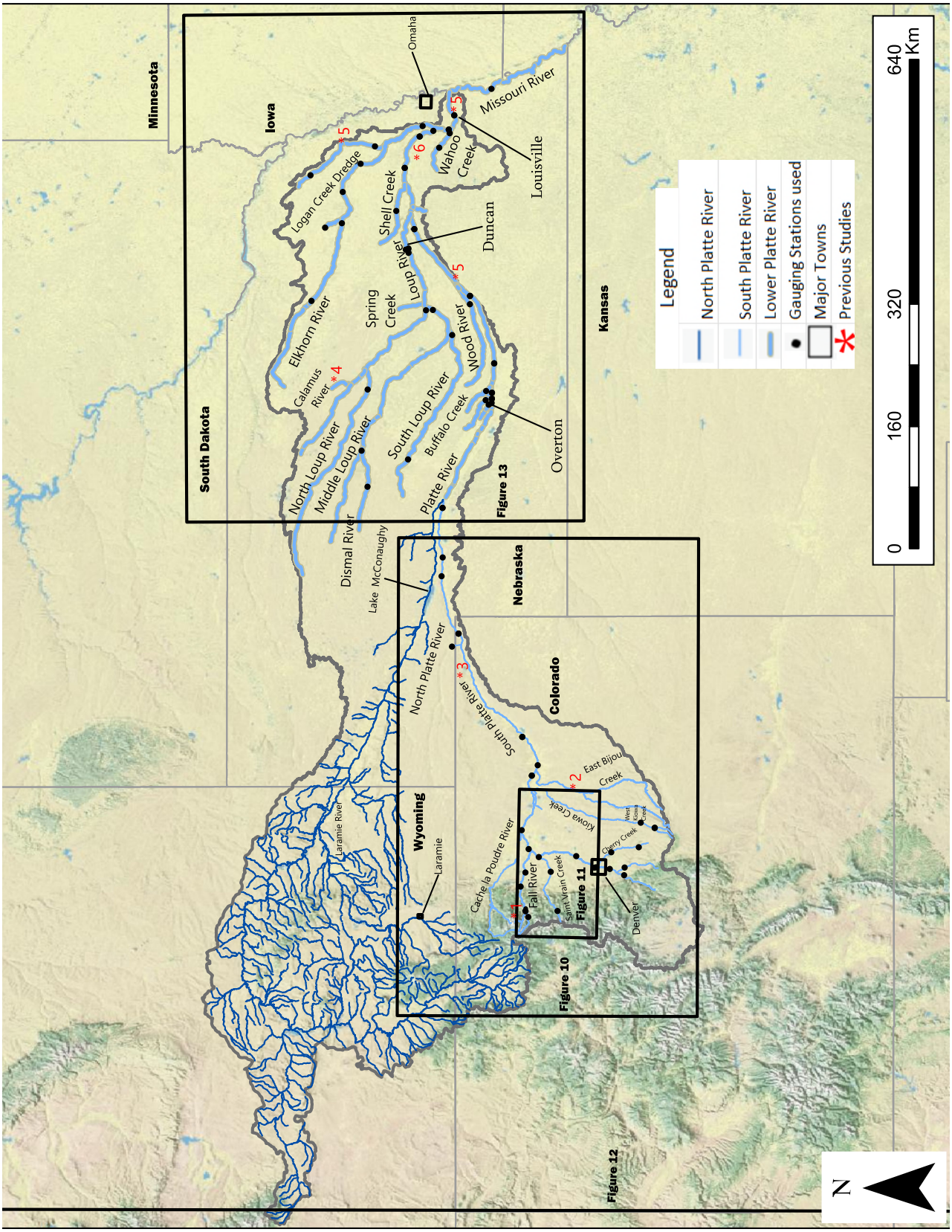

Fig. 8. Map of the Platte River drainage basin in central USA, showing the principal watercourses and other cultural and geographic features, including gauging stations. The locations of published facies studies on the Platte River and its tributaries are shown by red stars: (1) Blair, 1987; (2) McKee *et al.*, 1967; (3) Joeckel *et al.*, 2015; (4) Bridge & Gabel, 1992; Gabel, 1993; Bridge *et al.*, 1998; (5) Horn *et al.*, 2012a,b; (6) Smith, 1971a,b. In other publications, N.D. Smith reported observations and data from multiple locations along the Platte River. Black dots denote the locations of gauging stations used in this study.

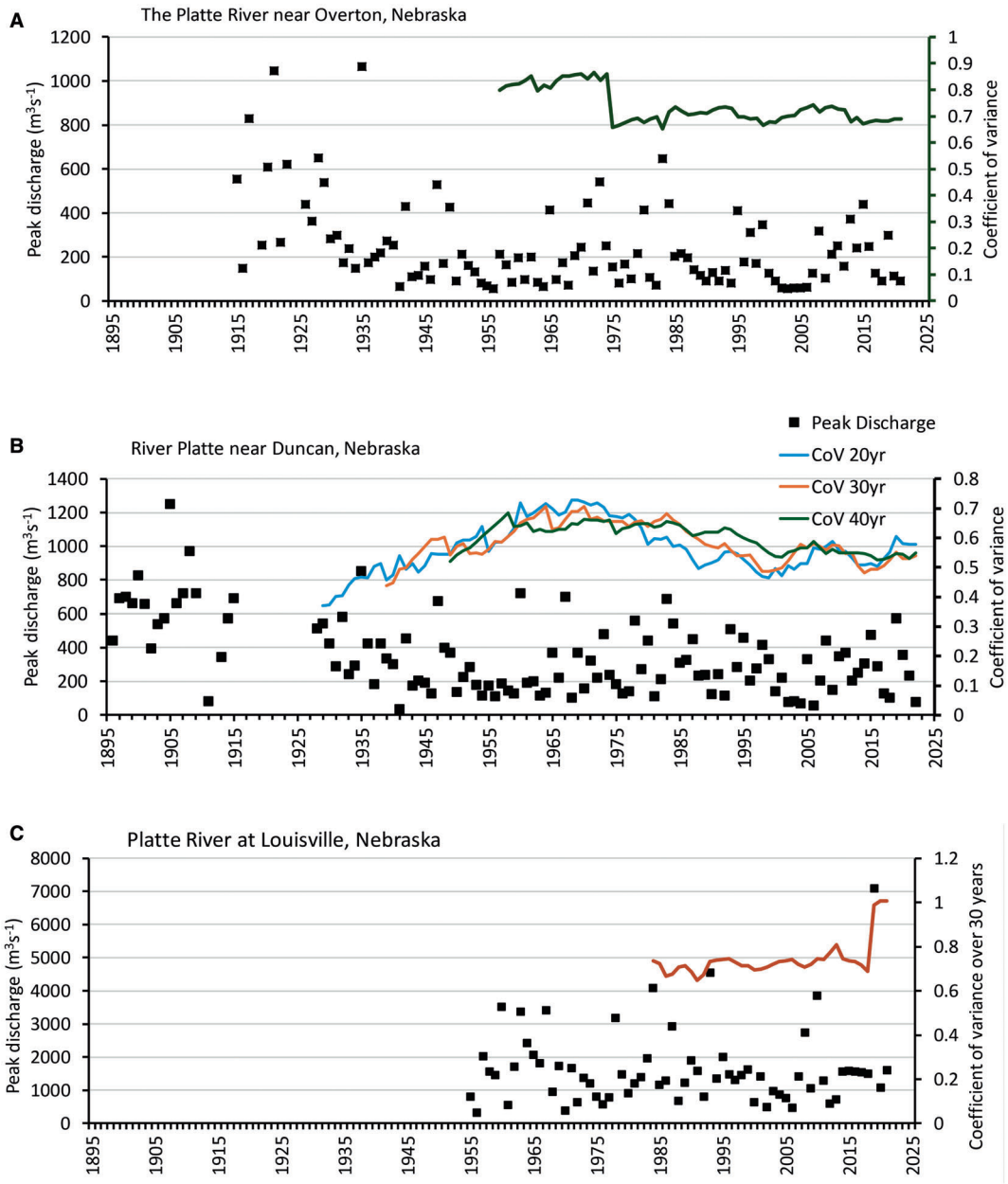

Fig. 9. Plots of annual peak discharge and CVQ_p, with 30 and 40 year moving values, for Overton, Duncan and Louisville, Nebraska, on the Platte River, central USA (see Fig. 8 for locations).

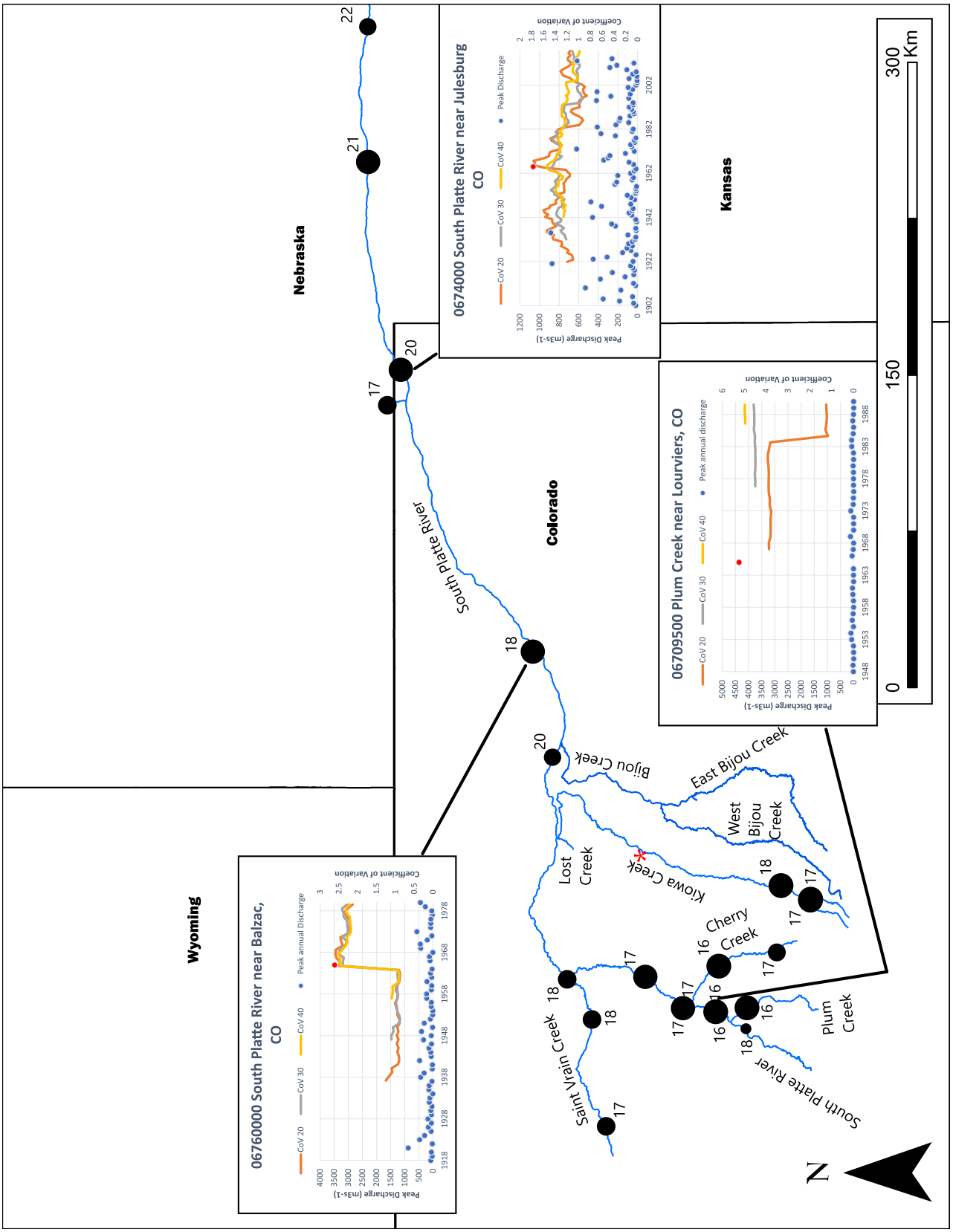

Fig. 10. Map of the area of the South Platte River system where the 1965 flow event had a significant impact on the CVQ_p. The size of black circles indicating the relative size of the change in CVQ_p (small = minimal, medium = moderate, large = major) and the associated number is the date in June 1965 when the peak discharge was measured at that site. Graphs show the record of peak annual discharges from selected gauging stations, with a red dot denoting the June 1965 event. In each case, that event was the maximum discharge in that year at that site. The 20, 30 and 40 year moving CVQ_p values are shown for each gauging record. Red star marks the site of the study of McKee *et al.* (1967).

of the Roaring and Fall rivers, but a minor influence can be recognized as far as Kersey, Colorado (Fig. 11). The event caused the CVQ_p value to rise abruptly from *ca* 0.5 to *ca* 3.5 in a station close to the Roaring River, moving the system into an entirely different class of CVQ_p. The major depositional effects, which were formed as a direct consequence of this event, were restricted to the Roaring River and the alluvial fan formed at the confluence with the Fall River (Jarrett & Costa, 1986; Blair, 1987). The deposit was up to 14 m thick (Blair, 1987). Sand and gravel with upper flow regime sedimentary structures record that the flow was at least locally supercritical, hyperconcentrated and turbulent. The Roaring River alluvial fan is a single event deposit that represents an extreme in the spectrum of sedimentological responses to individual runoff events. These now classic deposits correlate therefore with CVQ_p of 3 or higher (Fig. 11). This stresses the importance of using the appropriate interval values of CVQ_p.

The 2013 Big Thompson River flood (Kimbrough & Holmes Jr., 2015) is comparable to an earlier event in 1976, and like the earlier event it affected the canyon reach from Estes Park to the foot of the Front Range greatly (Fig. 12). Precipitation in this case was more widely distributed and continued for longer than in the 1976 event, leading to an estimated peak discharge of 454 $m^3\ s^{-1}$ at the mouth of the canyon (Kimbrough & Holmes Jr., 2015). Sustained precipitation also caused extensive flooding across the western Great Plains, and the event had an impact on CVQ_p down the entire length of the Platte River to the confluence with the Missouri River (Fig. 12), taking almost a month for the flood peak to move that far. Kimbrough & Holmes Jr. (2015) note extensive geomorphic changes in the Big Thompson River canyon, and Joeckel *et al.* (2015) document extensive sedimentological change to the South Platte and Platte River as a direct result of this event. A series of changes were noted, some entailing accumulations of large, woody debris or of sediment around vegetation obstacles and localized scour. Joeckel *et al.* (2015) suggested that this array of effects could be considered as a signature of a major flow event in a river like the Platte.

The 2019 flow event on the eastern Nebraska tributaries of the Platte River (Loup Rivers, Elkhorn River, principally) affected a broad area and can be recognized in gauging records as far as the Missouri River below the confluence with the Platte (Fig. 13). This flow event was caused by widespread, heavy precipitation across eastern Nebraska and surrounding regions, and led to extensive flooding (Fig. 14A). The flood peak moved downstream on several tributaries and the mainstem channel simultaneously. This event caused an abrupt increase in the CVQ_p at numerous gauging stations across the region (Fig. 13). It caused major changes in the arrangement of channel sediments in the braided, lower Platte River. Field observations near Louisville, Nebraska, in 2021 indicate the internal architecture of 2019 sand bar deposition was quite heterogeneous, and involved some upper flow regime structures as well as low-angle dune (cf. Cisneros *et al.*, 2016; Bradley & Venditti, 2017) cross-stratification (Fig. 14B and C). The subsurface architecture of lower Platte River sediments in the same area was interpreted by Horn *et al.* (2012a) to record repeated erosional truncation of prior deposits by successive annual events, but the 2019 record may have overprinted this pattern.

Taken as a set, these records of events illustrate four important points. Firstly, at least five events over the past 60 years have had a significant influence on different parts of the Platte River system, and have left a lasting record of change in the alluvial stratigraphy, at least locally. Secondly, it could be argued, given the background sediment accumulation pattern established by Horn *et al.* (2012a), that events causing an abrupt and substantial increase in

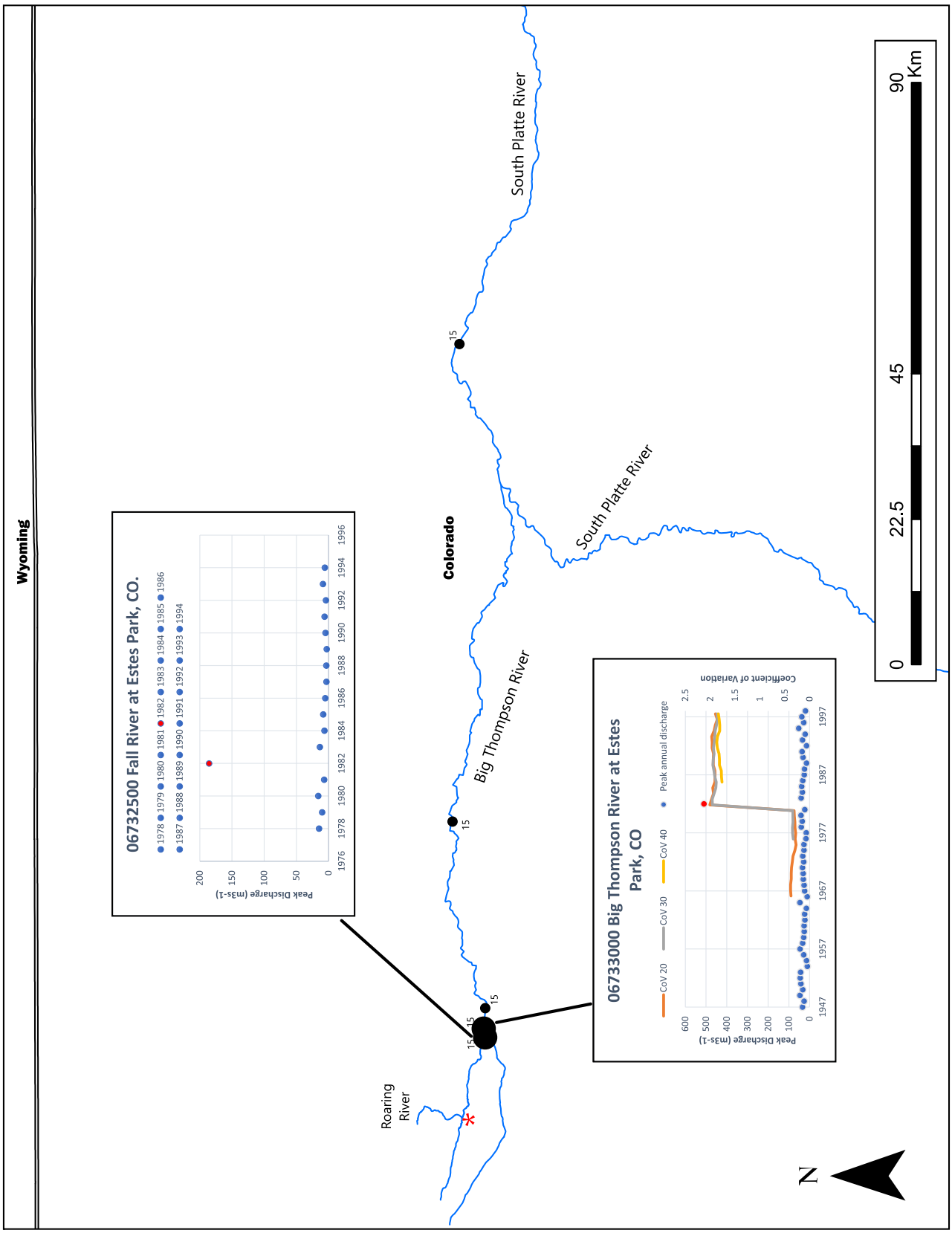

Fig. 11. Map showing characteristics of the anomalous 1982 flow event on the Roaring, Fall and Big Thompson rivers. The map covers only the extent of the basin where the event caused an increase in the CVQ_p, with the size of black circles indicating the relative size of the CVQ_p change (small = minor, medium = moderate, large = major) and the associated number representing the date in July 1982 when the peak discharge was measured at that site. Graphs show the record of peak annual discharges from selected gauging stations, with a red dot denoting the July 1982 event. In each case, that event was the maximum discharge in that year at that site. 20, 30 and 40 year moving CVQ_p values are shown for each gauging record. Red star marks the site of the study of Blair (1987).

the CVQ_p are perhaps required in order to leave a lasting recognizable record of an individual event. Thirdly, over the timeframes that individual channels or channel belts are active (hundreds to thousands of years), the relative frequency of anomalous events (that might seem anomalous in terms of local human experience, but broadly tens of years) might be such that they leave the dominant imprint on the alluvial architecture. This is consistent with the characteristics of high CVQ_p systems in general, and with the classification of the Platte River as a high CVQ_p system from its discharge record (Table 2). Fourthly, the spatially and temporally heterogeneous distribution of individual flow events and their effects on sedimentation can be expected to affect the entire system over a sufficiently long timeframe (hundreds to thousands of years, beyond the limit of gauging records). Thus, it is concluded that, using the Platte River drainage basin as an example, river systems will, over the full span of time they are active, form and preserve an alluvial record that reflects their inter-annual peak discharge variability.

A NEW GENERATION OF FLUVIAL FACIES MODELS

The data in Table 2 and the insights gained from the Platte River drainage basin indicate that the CVQ_p is a statistic that correlates robustly with alluvial deposit characteristics, and reflects the environmental characteristics of the formative system. It can therefore be used as the basis for a new set of fluvial facies models and is largely independent of planform, and that have predictive or interpretive value. These models can be used along with a traditional, planform-based view, or as an alternative to that approach. It is acknowledged that the new models do not specifically inform predictions of cross-sectional channel body dimensions, such as are useful in subsurface resource exploration and management (cf. Fielding & Crane, 1987; Gibling, 2006; Colombera *et al.*, 2014). Furthermore, planform-based models can better address macroform geometry of alluvial channel fills. However, the CVQ_p-based models may allow more meaningful interpretation of palaeoenvironmental conditions and changes.

It is suggested that facies models based on CVQ_p correlate more significantly with alluvial architectural style than models based on particular climatic forcing mechanisms, such as monsoons (Plink-Björklund, 2015, 2019). Indeed, Table 2 demonstrates that rivers formed in terrains subjected to monsoonal variations display a range of CVQ_p values similar to many rivers in other climatic zones. Some monsoonal rivers (for example, Brahmaputra/Jamuna, Ganges), perhaps counter-intuitively, show quite low values of CVQ_p, and their deposits are internally dominated by lower flow regime bedforms and structures (Best *et al.*, 2003; Shan *et al.*, 2020). Plink-Björklund (2015) considered monsoonal rivers and those in other subtropical domains as a single class of rivers, but the CVQ_p data show that the two display quite different characteristics. The array of cross-sectional models proposed by Plink-Björklund (2015, fig. 24) and interpreted to reflect a gradient of discharge 'flashiness' are not linked to the deposits of any modern rivers. Figure 3 shows CVQ_p plotted against degrees of latitude north or south of the Equator and demonstrates little relationship between latitude and CVQ_p. It also evident from Fig. 3 that the rivers surveyed with the highest values of CVQ_p (within the database) are in deserts and lie mostly in the range 20 to 35 degrees of latitude, corresponding to zones around the fringes of the world's low-latitude deserts that experience subhumid to semiarid climates and often highly unpredictable precipitation (see also Table 2). Facies models based on peak discharge variance, then, do not provide a diagnosis of latitudinal setting but contribute to an understanding of formative environment

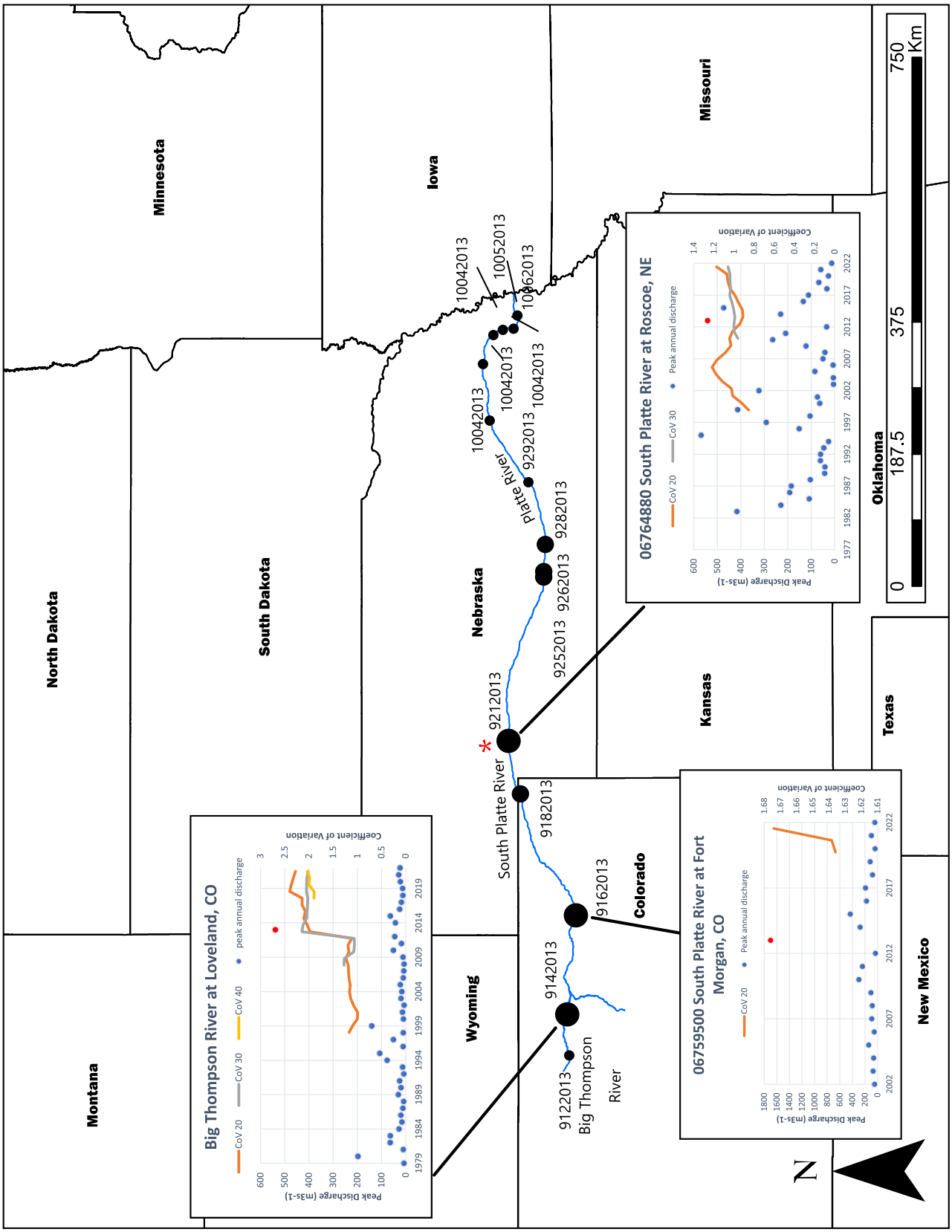

Fig. 12. Map showing characteristics of the anomalous 2013 flow event on the Big Thompson River. The map covers only the extent of the basin where the event caused an increase in the CVQ_p, with the size of black circles indicating the relative size of the CVQ_p change (small = minor, medium = moderate, large = major) and the associated number representing the date in September or October 2013 when the peak discharge was measured at that site. Graphs show the record of peak annual discharges from selected gauging stations, with a red dot denoting the September 2013 event. In each case, that event was the maximum discharge in that year at that site. 20, 30 and 40 year moving CVQ_p values are shown for each gauging record. Red star shows the location of the study of Joeckel *et al.* (2015).

including climatic regime. Further information on palaeoclimatic parameters could be derived from a variety of geochemical proxies now available (e.g. Algeo & Liu, 2020; Dinis *et al.*, 2020) in order to facilitate an integrated palaeoenvironmental analysis.

The following passages give details of facies models for the deposits of low, moderate, high and very high/ultra-high discharge variance fluvial systems, based on examples from modern rivers (Table 2) and with illustrations of equivalent successions from the rock record (Figs 15 to 18). A summary of the characteristics of low, moderate, high and very high/ultra-high CVQ_p river channel fills is provided in Fig. 19. This builds on the preliminary analysis presented by Fielding *et al.* (2018). The CVQ_p classes documented herein are largely independent of planform, sediment grain-size and scale. Some examples are single storey channel bodies, whereas others are multi-storey or multi-lateral. Controls on such larger-scale architecture are distinct from channel-forming and channel-filling processes, viz. accommodation rate, sediment supply rate and avulsion rate (Allen, 1978, 1979; Bridge & Leeder, 1979; Mackey & Bridge, 1995; Karssenberg & Bridge, 2008).

There are some sedimentary structures and features that are common to all CVQ_p classes and considered non-diagnostic. Such features are not included in the descriptions below. They include ripple cross-lamination and climbing ripple cross-lamination, and soft-sediment deformation structures such as overturned bedding, convolute bedding and load structures. The examples cited and illustrated avoid those where there is evidence for tidal modulation of fluvial outflow or backflow due to flood tidal movement, because tidal action is known to be a major contributor to facies heterogeneity in coastal river systems (Davis & Dalrymple, 2012). The categories are defined by somewhat arbitrary CVQ_p boundaries, informed by changes in the preserved facies assemblage of rivers surveyed in Table 2. As demonstrated in a previous section, CVQ_p varies both spatially and temporally in the same system, and so ancient alluvial successions might be expected to preserve elements of more than one style, or to fluctuate from one style to another.

Deposits of rivers with low CVQ_p (<0.2 to 0.5)

Rivers with low values of CVQ_p (Table 2) span the full range of planform styles, of dimensions and of latitude on the modern Earth's surface. Average grain-size is variable, ranging from mud to gravel, but there is minimal variability in lithology within channel fills. Macroform features such as remnants of in-channel bars and channel forms are abundantly and often completely preserved. Deposits of these rivers are dominated by lower flow regime structures, mainly dune-scale cross-bedding of various sizes, with subordinate flat stratification. Examples of modern rivers that epitomize this style include the Amazon, Calamus, Ganges, Jamuna, Mississippi and South Esk (Table 2, Fig. 15A). These are also among the rivers for which the most detailed documentations of sediment body architecture have been derived (e.g. Jordan & Pryor, 1992; Bridge *et al.*, 1995, 1998; Best *et al.*, 2003; Galeazzi *et al.*, 2018; Almeida *et al.*, 2024). Large woody debris is often seen washing down many of these modern rivers but it appears to be relatively poorly preserved in the sedimentary record. Trees may grow densely on bank tops and complex bar tops, and roots are seen penetrating down into older channel deposits, but tree trunks are not found rooted within channel deposits.

Many ancient examples of alluvial deposits that correspond to the low CVQ_p style have been documented (Fig. 15B to G). Indeed, this remains the archetypal alluvial channel body style in the minds of the majority of sedimentary

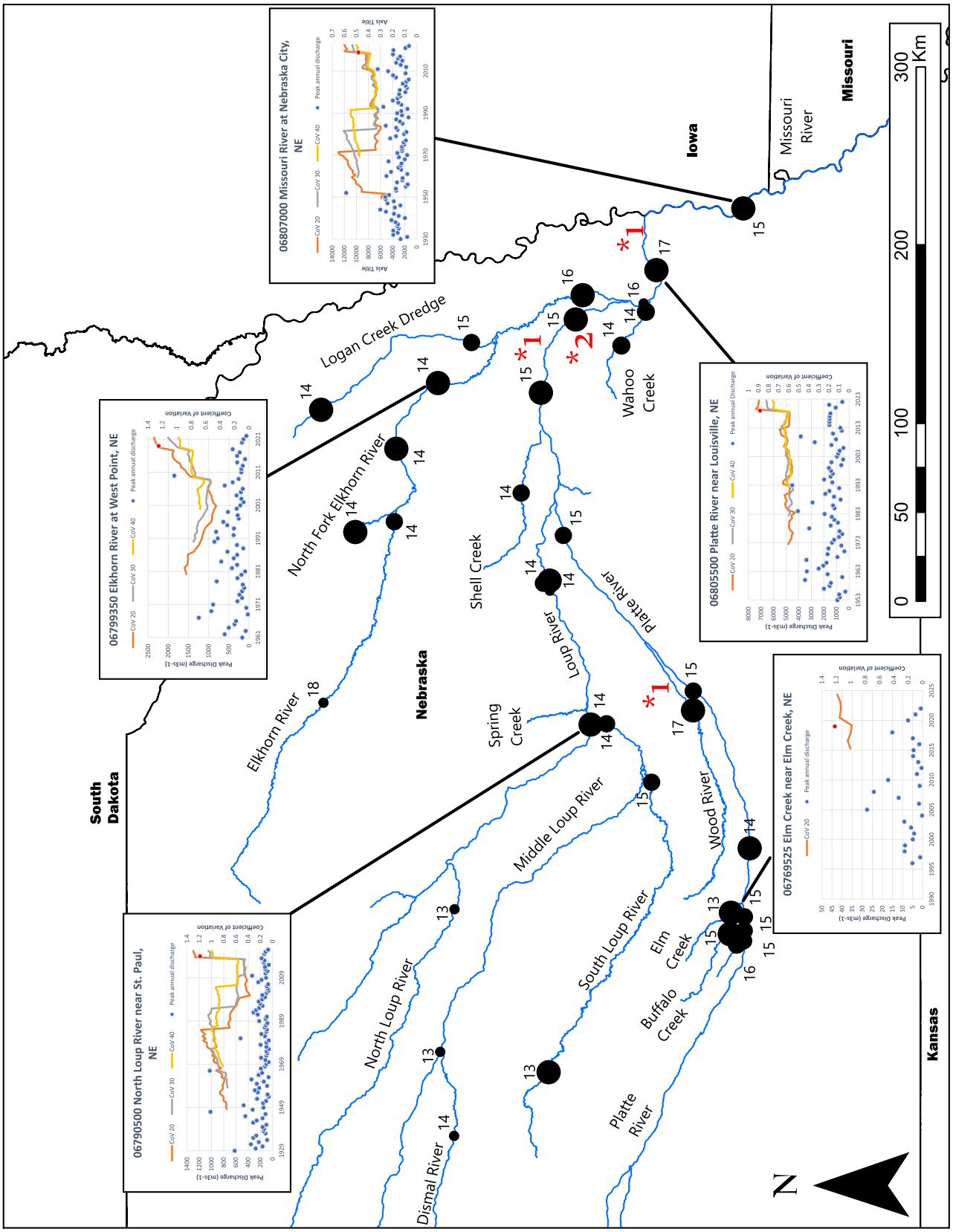

Fig. 13. Map showing characteristics of the anomalous 2019 flow event on the Platte River and tributaries in eastern Nebraska. The map covers only the extent of the basin where the event caused an increase in the CVQ_p, with the size of black circles indicating the relative size of the CVQ_p change (small = minor, medium = moderate, large = major) and the associated number representing the date in March 2019 when the peak discharge was measured at that site. Graphs show the record of peak annual discharges from selected gauging stations, with a red dot denoting the March 2019 event. In each case, that event was the maximum discharge in that year at that site. 20, 30 and 40 year moving CVQ_p values are shown for each gauging record. Red stars show the location of studies by: (1) Horn *et al.* (2012a,b); and (2) Smith (1971a,b).

Fig. 14. (A) Aerial view of flood on Elkhorn River, Nebraska, upstream of the confluence with the Platte River, 16 March 2019. (B) and (C) Field photographs of bar deposits on the lower Platte River near Louisville, NE, that were formed in the 2019 event. Note the dominance of low-angle dune cross-bedding and flat/low-angle stratification in the cutbank deposits. Vertical section *ca* 1.5 m in each case.

geologists. Historically, ancient fluvial sediment bodies that did not conform to this style were either regarded as oddities and largely ignored, or in some cases not even recognized as recording channel deposits. The examples discussed here and illustrated in Fig. 15 are either from formations that conform to this style *in toto* or in part. Among these are the many well-exposed sandstone-dominated channel bodies from the lower to middle Pennsylvanian (Namurian/Westphalian) succession of central and northern England (Fielding, 1986; Guion & Fielding, 1988; Guion *et al.*, 1995; Keogh *et al.*, 2005) and south Wales (Hartley, 1993; Hampson, 1998; George, 2000). Channel sandstone bodies are internally dominated by cross-bedding (Fig. 15B) and show excellent preservation of macroform architecture (e.g. Haszeldine, 1983). The palaeoclimate

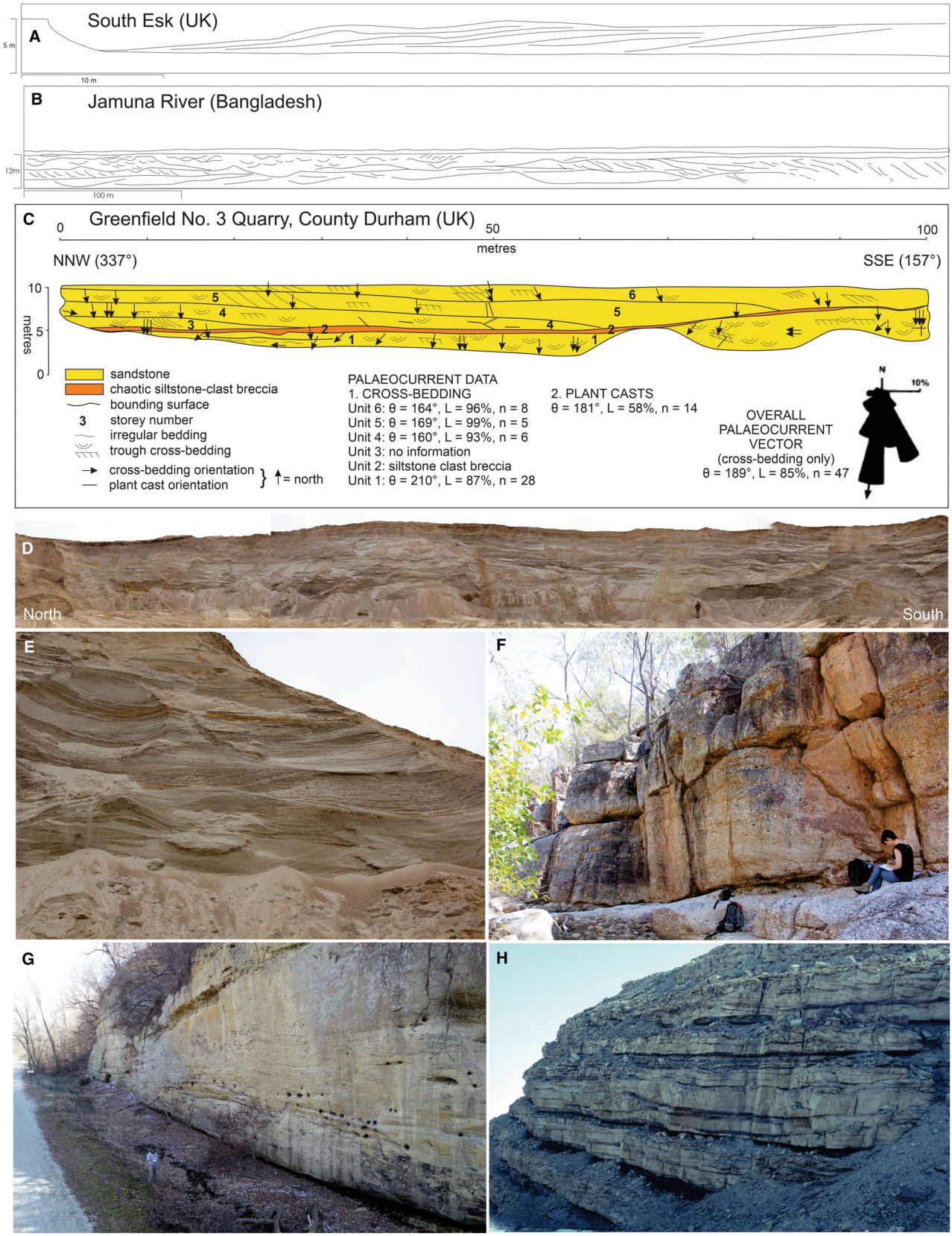

Fig. 15. Examples of low CVQ_p river deposits. (A) Line drawing interpretation of GPR data through a sand-dominated point bar deposit on the South Esk River of Scotland, showing well-preserved, macroform cross-bedding related to point bar migration. Redrawn from Bridge *et al.* (1995). (B) Line drawing interpretation of GPR data through a sand-dominated, mid-channel bar on the Jamuna River of Bangladesh, showing an abundance of dune-scale cross-bedding, and macroform features such as major scour surfaces and bar front slipface cross-bedding (right end). Note vertical exaggeration. Redrawn from Best *et al.* (2003). (C) Line drawing and interpretation of a quarry face exposing a channel body in the lower Westphalian A of the Durham coalfield, north-east England, again showing an abundance of cross-bedding and well-preserved macroform features (channel floor scour surface, storey-bounding bar accretion surfaces). Redrawn from Fielding (1986). (D) Photomosaic of pit face at Powell, Nebraska, USA, exposing pervasively cross-bedded Pleistocene gravelly sands that constitute multi-storey incised-valley fills. Person for scale 1.8 m. (E) Close-up view of the southern end of the pit face in (D), showing pervasive dune-scale cross-bedding. Bones and teeth of woolly mammoths were also found at this locality. 3 m vertical section shown. (F) Cross-bedded conglomerates and gravelly sandstones of the Mississippian Mount Hall Formation in the Drummond Basin, Queensland, Australia. Backpack 0.6 m high. (G) Cross-bedded sandstones forming part of the uppermost Pennsylvanian Indian Cave Sandstone at Peru in south-east Nebraska, USA, a multi-storey incised-valley fill (one bounding surface is visible in the upper part of the face). Drone pilot 1.65 m. (H) A series of sandstone channel fills dominated by dune-scale cross-bedding and showing channel-scale bedding features in the upper Permian Bainmedart Coal Measures of the Prince Charles Mountains, East Antarctica. 30 m section exposed.

during this time, at the sites described, is widely regarded to have been humid and tropical (Schopf, 1973; Besly & Turner, 1983). Interestingly, the overlying, upper Pennsylvanian (Stephanian/Autunian) succession in the English central Pennine Basin preserves a record of gradually changing fluvial style dominated by moderate to high CVQ_p alluvial styles, and is interpreted to have accompanied a change to a drier, more seasonal tropical palaeoclimate (Besly, 1988; Glover & Powell, 1996). Other illustrated examples of the low CVQ_p alluvial style (Fig. 15) include sand and gravel Pleistocene incised valley-fills in Nebraska, central USA (Stanley & Wayne, 1972), sandy incised valley-fill of the uppermost Pennsylvanian Indian Cave Sandstone of south-east Nebraska (Fischbein *et al.*, 2009) and the sandy, upper Permian Bainmedart Coal Measures channel deposits of East Antarctica (Fielding & Webb, 1996; McLoughlin & Drinnan, 1997).

Commercial gravel pits near Fairbury, Nebraska, expose multi-storey sand and gravel deposits up to 20 m thick that occupy incised topography below the present-day landscape of the Great Plains (Fig. 15C and D). They are internally dominated by trough cross-bedding at various scales, and also preserve large siltstone blocks (interpreted to have slumped into channels from nearby banks), and bones and teeth of woolly mammoths. Pleistocene palaeoclimate of this area has been interpreted as cool temperate to cold with cycles of glaciation, accompanied by alternating periods of humid/mild and arid/cold conditions inferred from fossil and other data (Stanley & Wayne, 1972; Roy *et al.*, 2004; Muhs *et al.*, 2008). The palaeogeographical scenario for the Fairbury incised-valley fill deposits is likely comparable to coarse bedload rivers draining the modern, glaciated and mountainous north-west of North America (for example, Kicking Horse, Fraser and Mackenzie rivers, which show low values of CVQ_p: Table 2).

The Mississippian Mount Hall Formation of the Drummond Basin in central Queensland, Australia, comprises a regionally widespread sheet of sandstone and conglomerate-dominated alluvial deposits up to 3 km thick (Sobczak *et al.*, 2019). Erosionally-bounded channel bodies are internally dominated by dune-scale cross-bedding with minor components of other sedimentary structures (flat stratification with clast imbrication, notably; Fig. 15E). During the Mississippian, eastern Australia lay in the southern temperate latitudes and is thought to have experienced humid climate conditions, based on preserved flora and fauna. The Mount Hall Formation is similar in many ways to the deposits of some modern, broad gravelly alluvial streams such as those in the Canterbury Plains, New Zealand (Moreton *et al.*, 2002; Leckie, 2003), and in Alaska (Lunt *et al.*, 2004; Lunt & Bridge, 2004; Tye, 2004).

The Indian Cave Sandstone as exposed near Peru, Nebraska (Fig. 15F), has a multi-storey

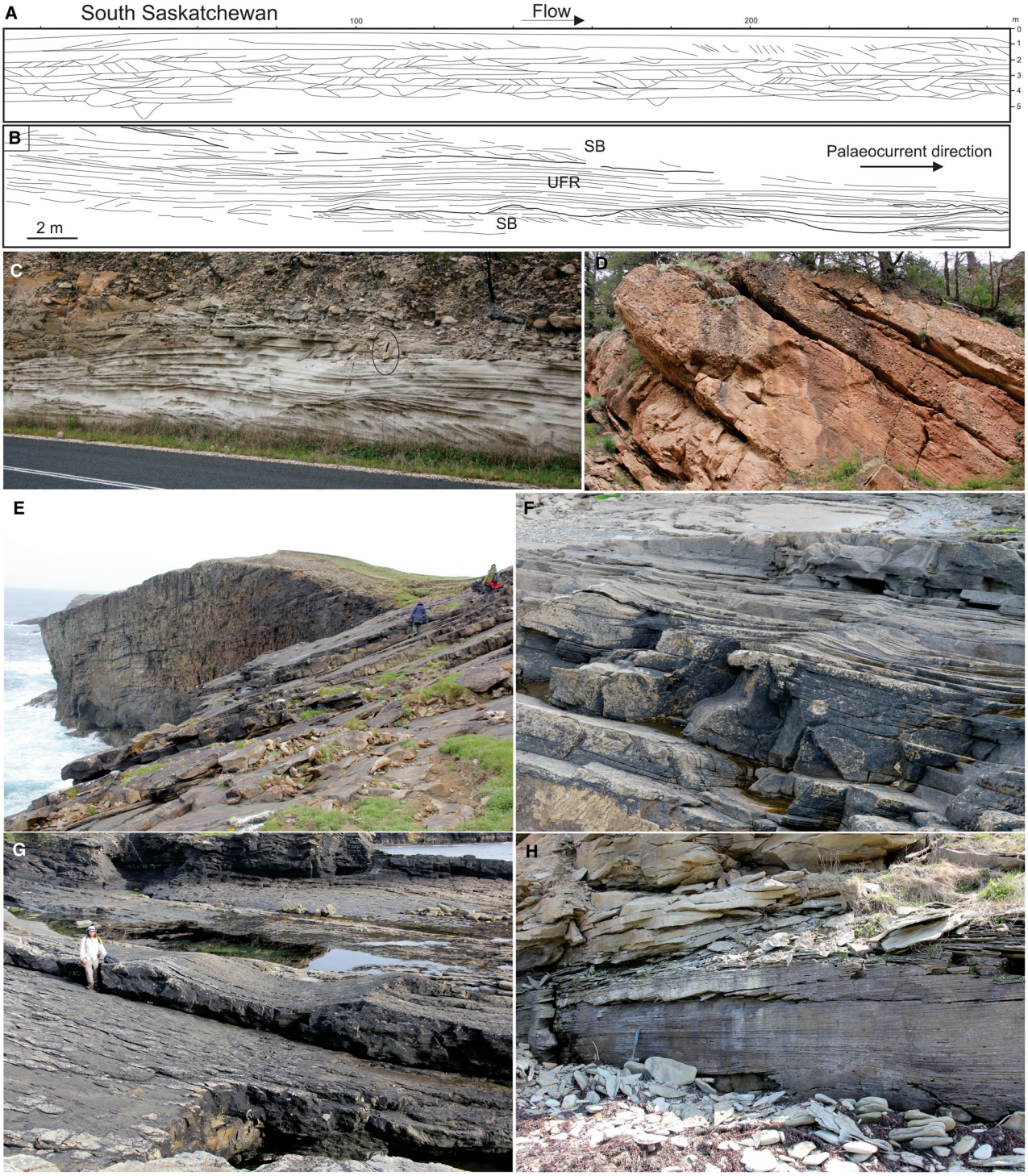

Fig. 16. Examples of moderate CVQ_p river deposits. (A) Line drawing interpretation of GPR data through sandy alluvium of the South Saskatchewan River in Canada (from Sambrook Smith *et al.*, 2006), showing common dune-scale cross-bedding but an increased abundance of flat and low-angle stratification, minor channel scours and other bedding features relative to the low CVQ_p style (compare with A). Note vertical exaggeration. (B) Line drawing interpretation of a photomosaic taken of part of the upper Permian Colinlea Sandstone near Springsure, Queensland, Australia (from Fielding, 2006). Note the preservation of lower and upper cross-bedded intervals (labelled SB for Sandy Bedform, in the classification of Miall, 1985) separated by a central interval dominated by upper flow regime stratification (labelled UFR). No vertical exaggeration. (C) Close-up view of the central part of (B), showing undulatory stratification with local development of backsets. Hammer for scale 0.3 m (circled). (D) Outcrop view of part of the Upper Cretaceous Indianola Group in Chicken Creek canyon, Utah, western USA. The view shows a stack of erosionally-based conglomerate and sandstone bodies, internally dominated by flat and low-angle stratification with lesser cross-bedding. About 10 m of vertical section is visible. (E) Coastal cliff exposures of sandstone-dominated channel fills in the lower Pennsylvanian Kilkee Cyclothem north of Kilkee, western Ireland. Geologists for scale in the foreground are walking across a zone of undulatory, possible antidunal bedding. The entire body, 27 m thick and erosionally-based, is visible in the cliff face where dune-scale bedding and upper flow stratification are preserved in equal proportions. (F) Close-up view of part of a train of small antidunes in channel deposits of the Kilkee Cyclothem near Cleedagh Bridge, western Ireland. Palaeoflow was towards the right, and the antidunes preserve an amplitude of 8 cm and wavelength of 110 to 180 cm. (G) Large, near-symmetrical bedwaves on the top surface of a channel sandstone at the same locality as (F). Palaeoflow was towards the right. Geologist for scale 1.8 m. (H) Flat and undulatory stratification passing laterally into small-scale cross-bedding in the Pennsylvanian South Bar Formation, Victoria Mines, Atlantic Canada. Hammer for scale 0.25 m.

architecture, with channel deposits dominated by unidirectional trough cross-bedding and preservation of macroform architectural features (Fischbein *et al.*, 2009). This and other out-of-context, incised-valley fills in the Pennsylvanian of the US Interior basins form parts of repetitive stratal cycles ('cyclothems') that are thought to record a far-field, palaeotropical response to Gondwanan glacial cycles on orbital frequencies during the late Palaeozoic Ice Age (Wanless & Shepard, 1936; Heckel, 2008). Although the lowstands of these cycles are characterized by evolved palaeosols that relate to hot and strongly seasonal climates (e.g. Joeckel, 1994; Rosenau *et al.*, 2013a,b), filling of incised topography by fluvial systems during late lowstand to early transgressive conditions happened under more equable and humid climate (e.g. Feldman *et al.*, 2005; Fielding *et al.*, 2020).

The sandy channel bodies of the upper Permian Bainmedart Coal Measures in the Prince Charles Mountains, East Antarctica (Fig. 15G), are internally dominated by dune-scale cross-bedding and display well-preserved channel-scale macroform features (Fielding & Webb, 1996; McLoughlin & Drinnan, 1997). According to these authors, the succession formed in a cold temperate, humid climate affected by cyclicity that operated on orbital frequencies during which sediment and water discharge varied. By comparison with the modern exemplars, these streams operated under conditions of low interannual discharge variability.

The above-cited and illustrated examples of the low CVQ_p alluvial style encompass a variety of interpreted planform styles, formed at a variety of interpreted palaeolatitudes and under a range of climatic conditions. Additional examples that are fully evident from detailed architectural data provided by researchers include Upper Carboniferous sandy channel bodies in Northumberland, England (Haszeldine, 1983), Devonian 'Brownstones' of the Welsh Borderlands (Allen, 1983), and sandy, coastal braidplain deposits of the Triassic Hawkesbury Sandstone in the Sydney Basin, eastern Australia (Conaghan & Jones, 1975; Rust & Jones, 1987; Miall & Jones, 2003).

Deposits of rivers with moderate CVQ_p (0.5 to 0.8)

Rivers with moderate CVQ_p values span a range of latitudes, climatic zones, sediment grain-sizes and planforms (Table 2). Data from the bed and subsurface of the examples in Table 2 and other rivers indicate that although dune-scale cross-bedding is still a prominent constituent of the alluvium, upper flow regime structures are also abundantly preserved. Macroform architecture is less completely preserved/identifiable in the subsurface structure of these rivers, in

comparison to that of low CVQ_p rivers (Fig. 16A). There is a degree of lateral lithological heterogeneity in channel deposits and a greater involvement of large woody debris than observed in low variance river deposits (Table 2). Modern examples of moderate CVQ_p systems include the Platte, South Saskatchewan, Congaree and Wabash rivers (Table 2).

Many ancient examples of alluvium preserving characteristics of the moderate CVQ_p style exist (Fig. 16). These include the fluvial facies of the upper Permian Colinlea Sandstone in Queensland, north-east Australia (Fielding, 2006), parts of the Upper Cretaceous Indianola Group in Utah, western USA (Lawton, 1982), the lower Pennsylvanian Central Clare Group coastal alluvial channel fills of western Ireland (Best & Wignall, 2016), and the lower part of the basal Pennsylvanian South Bar Formation of Cape Breton, Atlantic Canada (Rust & Gibling, 1990).

The early Lopingian was a time of cold temperate climate in eastern Australia, which was then in high southern latitudes, and affected at higher altitudes by the P4 glaciation (Fielding *et al.*, 2023). Fluvial deposits of the Colinlea Sandstone (Fig. 16B and C) form part of a thick and extensive, coarse-grained alluvial to deltaic sediment accumulation at the western margin of the Bowen Basin of Queensland (Fielding *et al.*, 2019a). The internal architecture of channel deposits includes excellent examples of upper flow regime structures (for example, Fig. 16C, and see Fielding, 2006). Macroform structures are more difficult to identify and appear less well-preserved (Fig. 16B and C). Comparison with modern river examples (Table 2) suggests that discharge conditions were somewhat variable on an inter-annual basis.

The Upper Cretaceous Indianola Group accumulated in the proximal foreland of the Western Cordilleran Foreland Basin of North America. It includes coarse-grained alluvium shed eastward into the foredeep from the rising Sevier Orogen (Lawton, 1982). The palaeoclimate is interpreted to have been warm temperate and seasonal, at mid-latitudes (Wolfe & Upchurch, 1987; Burgener *et al.*, 2023). Cyclical facies variations in correlative coastal fluvial successions further down-palaeoslope (Masuk Formation: Corbett *et al.*, 2011; Hess & Fielding, 2020; and see below) suggest a repetitive climatic cyclicity from high to low discharge variance conditions over the timeframes of channel activity (hundreds to thousands of years). The Indianola Group alluvium preserves gravelly and sandy channel deposits with common upper flow regime sedimentary structures (for example, Fig. 16D), suggesting that discharge variability is also recorded in the upslope parts of the palaeodrainage system.

The basal Pennsylvanian Central Clare Group of western Ireland preserves a number of erosionally-based sandstone-dominated channel bodies that are believed to have formed on a lowland, coastal alluvial plain that fed river-dominated deltas in the Shannon Basin (Best & Wignall, 2016). Palaeoclimate is believed to have been tropical and humid (Schopf, 1973; Besly & Turner, 1983). In addition to abundant dune-scale cross-bedding, the channel bodies contain common upper flow regime structures, including antidunal bedding at various scales (Fig. 16E to G). A feature of these exposures is the preservation of trains of small antidunes (Fig. 16F) and form sets of large, undular bedwaves (Fig. 16G). Based on comparison with modern systems, it can be inferred that formative streams experienced moderate levels of inter-annual discharge variability.

The lower to middle Pennsylvanian South Bar Formation in the Sydney Basin of Atlantic Canada is a thick (*ca* 1000 m), sandstone-dominated succession that is interpreted to have formed in coastal alluvial plain environments (Rust & Gibling, 1990; Gibling *et al.*, 2010; Allen *et al.*, 2014). A gradual upward transition through the unit was noted by these authors and interpreted as a record of a progressively more seasonal climate, leading to a change in preserved facies to those representing a more freely-drained alluvial surface. Channel sandstone bodies in the lower and middle parts of the unit are composed of an array of dune-scale cross-bedding and moderately abundant upper flow regime structures (for example, Fig. 16H), with sporadic preservation of *in situ*, upright tree fossils. These facies are interpreted to record a discharge regime characterized by moderate levels of inter-annual discharge variability, and they pass upward into a style more reminiscent of high levels of CVQ_p (see below).

The above examples span a variety of channel planform styles, and a range of palaeoclimate and palaeolatitude, emphasizing the point that the CVQ_p classification is somewhat independent of these variables. Other examples evident from the literature include elements of the Permian Vrchlabí Formation of the Czech Republic

(Schöpfer *et al.*, 2022), Ordovician glaciofluvial deposits spectacularly exposed in north Africa (Ghienne *et al.*, 2010; Girard *et al.*, 2012) and Pleistocene glaciofluvial deposits from western Europe (Lang *et al.*, 2021).

Deposits of rivers with high CVQ_p (0.8 to 1.5)

Rivers with high values of CVQ_p include rivers in a range of latitude and climatic zone (for example, Platte, Powder, Burdekin, Loup, Bijou Creek), but have in common that they flow through terrains that experience strongly seasonal and somewhat irregular precipitation patterns (Table 2; Fig. 17). These rivers also span a large range of planform style, and calibre of transported sediment. They show a greater degree of lateral heterogeneity in river bed and channel fill lithology than their lower CVQ_p counterparts. Bedforms and sedimentary structures include a sizeable proportion of upper flow regime structures (Fig. 17A and H; plane beds, antidunes, localized trough-like scour fills, and in places stratification relatable to chutes-and-pools and even cyclic steps), and macroform features on channel scales are difficult to identify (poorly preserved) relative to lower CVQ_p systems. They mostly include arborescent river bed vegetation to some extent, and preserve abundant large woody debris and *in situ* tree stumps in their alluvial record. Exceptions to this are the jökulhlaup (glacial outburst flood) deposits documented from polar tundra regions (e.g. Maizels, 1989; Russell & Knudsen, 2002; Duller *et al.*, 2008; Marren *et al.*, 2009), that largely lack vegetation. They are nonetheless dominated by upper flow regime stratification, including abundant antidune and chute-and-pool deposits.

Several ancient alluvial successions can be interpreted to have formed under high CVQ_p conditions, by comparison with the characteristics of modern exemplars (Fig. 17). These include the Pennsylvanian upper South Bar Formation of Cape Breton, Atlantic Canada (Allen *et al.*, 2014), the Pennsylvanian Boss Point and Little River formations of the Cumberland Basin, Nova Scotia, Atlantic Canada (Allen *et al.*, 2013), and the upper Permian Newcastle and Illawarra Coal Measures of the Sydney Basin, Australia (Fielding *et al.*, 2021).

The upper part of the lower to middle Pennsylvanian South Bar Formation in the Sydney Basin of Atlantic Canada is characterized by fluvial sediment bodies that preserve dominantly upper flow regime sedimentary structures, preserve little evidence of identifiable macroform architecture in channel bodies, display some lateral lithological variability, and preserve common, fossil tree stumps (Fig. 17B and G). The upward change noted previously into this fluvial style is interpreted to represent a gradual change towards a more strongly seasonal climate that entailed greater extremes of temperature and precipitation, and higher CVQ_p (Rust & Gibling, 1990; Gibling *et al.*, 2010; Allen *et al.*, 2014).

The basal Pennsylvanian Boss Point and Little River formations of the Joggins area, mainland Nova Scotia (Browne & Plint, 1994; Calder *et al.*, 2005; Fielding *et al.*, 2011; Allen *et al.*, 2013; Rygel *et al.*, 2015), preserve channel sandstone bodies in which upper flow regime structures dominate. There is lateral lithological heterogeneity, macroform architecture is difficult to identify and poorly preserved, and fossil tree stumps occur in channel facies (for example, Fig. 17C and D). Reddened palaeosols indicative of emergent, freely-drained floodplain settings are increasingly common upward through the succession. This interval was used by Fielding *et al.* (2018, fig. 9) as an example of progressive change from low, through moderate, to high CVQ_p alluvial style, and is also accompanied by a change in sediment dispersal direction, as indicated by palaeocurrent measurements from sedimentary structures. Allen *et al.* (2013) and Fielding *et al.* (2011, 2018) interpreted this succession as recording a progressive trend from a humid, tropical palaeoclimate to a more strongly seasonal climate that involved lengthy dry periods. The overlying Joggins Formation records a change back through moderate to low CVQ_p alluvial style and includes coal seams, both properties interpreted by the above-mentioned authors as recording a return to a more equable, humid palaeoclimate.

The upper Permian coal-bearing formations of the Sydney Basin, New South Wales, eastern Australia (Illawarra and Newcastle Coal Measures; Bamberry *et al.*, 1995; Diessel, 1980), formed in high southern palaeolatitudes. They preserve a spectrum of lithologically heterogeneous channel bodies in which upper flow regime sedimentary structures and fossil *in situ* tree stumps are common (for example, Fig. 17E and F). Macroform features are preserved in some bodies, notably large lateral accretion sets, whereas others preserve little in the way of identifiable macroform architecture (Fielding *et al.*, 2021). These channel bodies are

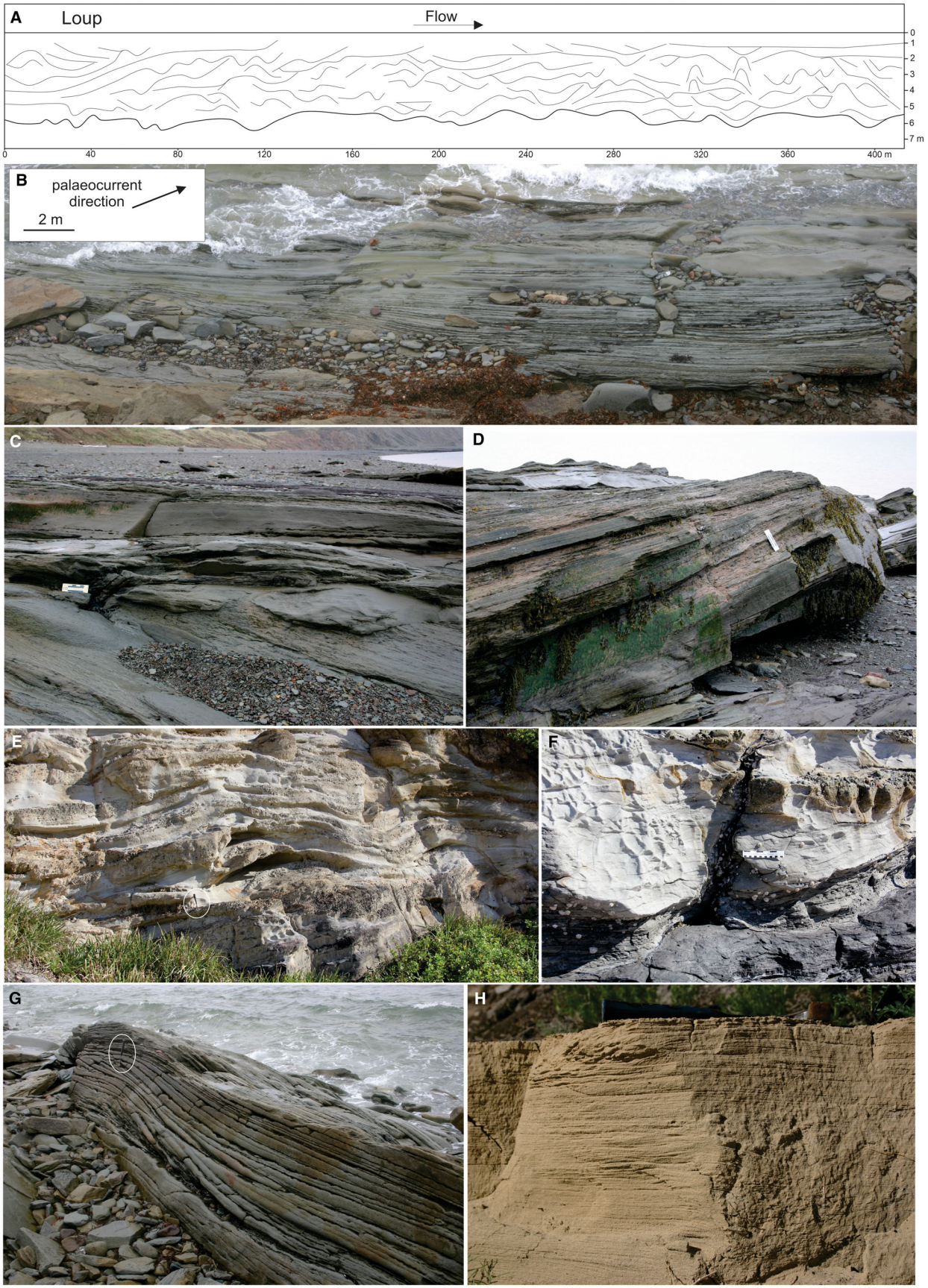

Fig. 17. Examples of high CVQ_p river deposits. (A) Line drawing interpretation of GPR data from a braid bar of the Loup River in Nebraska, central USA (from Fielding *et al.*, 2018). Note the diversity of preserved bedding structures and paucity of dune-scale cross-bedding relative to Figs 15A and 16A. Point diffractions near the downstream end of the transect are likely tree stumps or large, woody debris. Note vertical exaggeration. (B) Photomosaic of a sandstone channel fill body from the upper part of the Pennsylvanian South Bar Formation at Victoria Mines, Atlantic Canada. Note the dominance of flat and low-angle stratification. Scale and palaeoflow direction indicated. (C) Close-up view of an *in situ*, small, tree stump (immediately to the right of the 0.15 m scale card) inclined in the down-palaeoflow direction and encased in a sandstone channel fill in the lower Pennsylvanian Little River Formation near Joggins, Atlantic Canada. Palaeoflow was from left to right as indicated by the cross-set in the lower right of the field of view, while the tree fossil is overlain by antidunal, convex-upward stratification. (D) View of low-angle backset cross-stratification in a channel sandstone, same formation and locality as for (C). Palaeoflow direction was from left to right as indicated by interbedded foreset cross-bedding. Scale card 0.15 m. (E) Long-wavelength antidunal bedding in a composite fluvial channel fill of the uppermost Permian Karignan Conglomerate at Ghosties Beach, New South Wales, Australia. The convex-upward bedset preserves evidence of both down-palaeoflow migration (right to left, as indicated by cross-bedding in the section below the antidunal bedding), and aggradation at a supercritical angle with respect to the stoss side slope of the formative bedform. Hammer (circled) 0.25 m. (F) *In situ*, upright tree fossil rooted into the base of the same channel body as shown in part (E), same locality. The tree fossil extends for *ca* 0.6 m upward into coarse-grained, gravelly sandstone, and is interpreted to have lived in the formative channel floor. Scale bar 0.15 m. (G) Close-up view of low-angle dune-scale cross-bedding passing down-palaeocurrent (left to right) into undulatory, upper flow regime stratification in the upper part of the Pennsylvanian South Bar Formation at Victoria Mines, Atlantic Canada. Hammer (circled) 0.25 m. (H) Fine sand deposits in the cutbank of the modern Sweetwater Creek, Utah, western USA, showing abundant flat and low-angle stratification with local backset bedding (flow direction left to right). Hammer lying flat on bank top is 0.25 m long.

interpreted as the product of a palaeoclimate that was initially cold temperate but became warmer and progressively more seasonal over the last 1 Myr of the Permian, culminating in abrupt warming at the end-Permian (Fielding *et al.*, 2019b; Frank *et al.*, 2021; Wu *et al.*, 2021).

As with other CVQ_p classes, these examples span a range of palaeoclimatic and latitudinal zones, channel sizes and planforms. They are all interpreted from independent evidence to have formed under strongly seasonal climates, however. Other examples from the literature include channel bodies in the Silurian–Devonian Jaicós Formation of Brazil (Manna *et al.*, 2021), elements of the Permian Vrchlabí Formation of the Czech Republic (Schöpfer *et al.*, 2022), the Triassic Dockum Group of Texas, south-west USA (Walker & Holbrook, 2023), the Palaeogene Green River Formation of Utah (Gall *et al.*, 2017; Wang & Plink-Björklund, 2019, 2020) and the Palaeogene Poison Canyon Formation of south-west USA (Schwartz *et al.*, 2021).

Deposits of rivers with very high (1.5 to 2.0) CVQ_p

Modern rivers with very high CVQ_p are mostly in mid to low-latitudes and are predominantly found in areas that experience strongly seasonal, and erratic precipitation patterns. Some flow through dryland terrains, but examples of this class are also preserved in some polar, glacier-fed rivers subject to glacial outburst floods (jökulhlaups). Examples include rivers with a range of size, planform and sediment type (for example, upper Burdekin, Orange, Nueces: Table 2; Fig. 18). The deposits of these rivers are quite unlike those of the low and moderate CVQ_p styles. They preserve: (i) a dominance of upper flow regime sedimentary structures and often unstratified or diffusely stratified beds of sand and gravel, with only locally-developed dune-scale cross-bedding (Fig. 18A and B); (ii) limited to no macroform structure; (iii) a lot of lateral lithological heterogeneity; and, in some of these, (iv) an abundance of evidence of in-channel woody plant growth (in the form of *in situ* stumps and trunks, roots, and locally derived, large woody debris; Fig. 18C). Pedogenically modified mud partings, often with desiccation features (for example, Fig. 18D), are common within the channel fills of these rivers, and bioturbation is also locally abundant throughout channel fills.

Ancient examples of the very high CVQ_p fluvial style include the Permo–Triassic boundary succession of the eastern Ordos Basin, north China (Fig. 18E and F), parts of the Upper

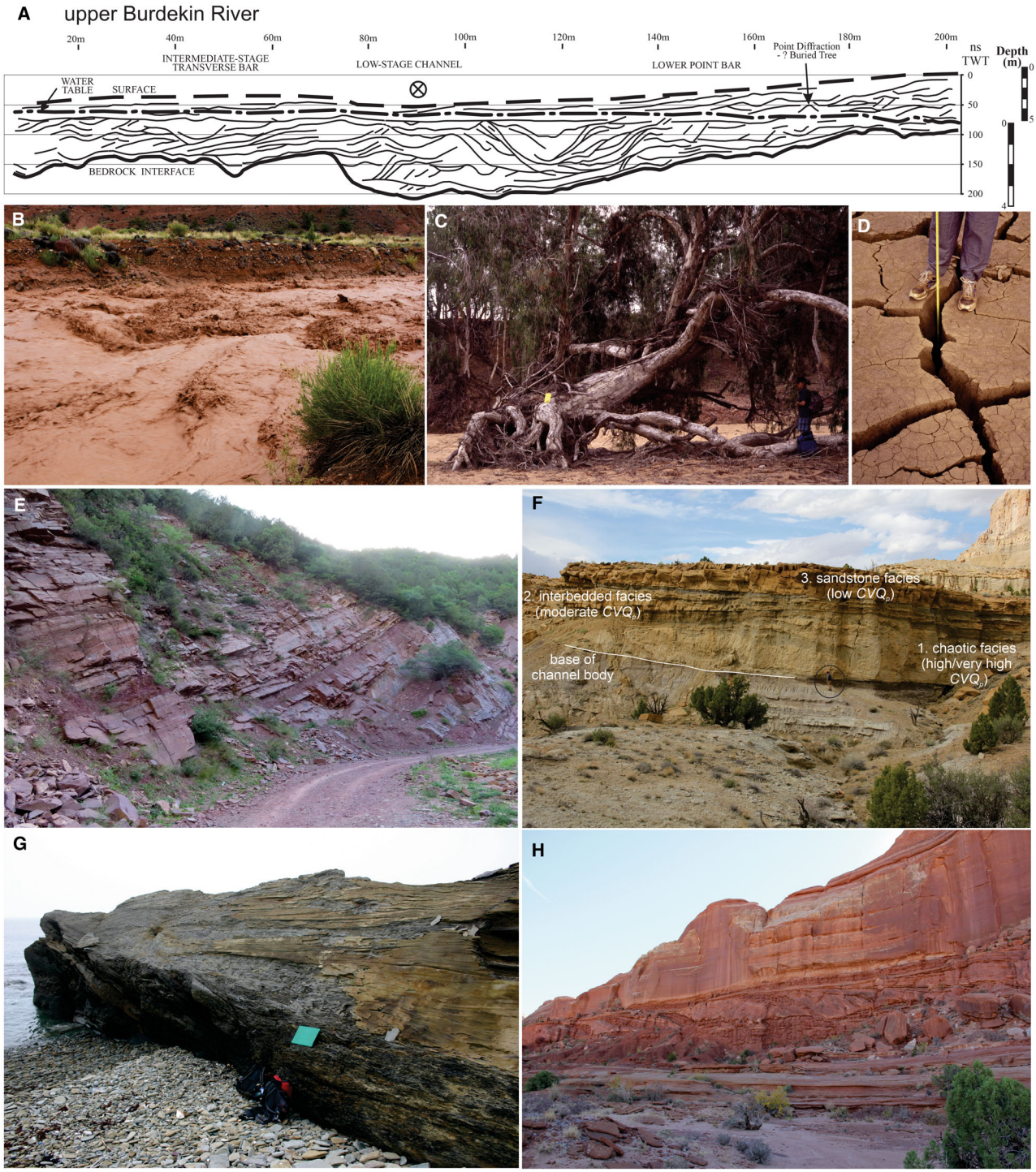

Fig. 18. Examples of very high and ultra-high CVQ_p river deposits. (A) Line drawing interpretation of GPR data across the upper Burdekin River at Dalrymple, Queensland, Australia (flow into the plane of the illustration; from Fielding *et al.*, 1999). A variety of bedding features is imaged, including deep trough scours, flat and low-angle stratification including antidunal bedding, and evidence of buried, *in situ*, trees. Although much of the river bed sediment is sand with minor gravel, pedogenically-modified mud partings are also commonly preserved in cut-bank exposures. (B) View of a flash flood in a small watercourse near Torrey, Utah, western USA (exposed cut-bank is 2.0 m high). Note the highly sediment-charged (strongly coloured) nature of the water and the presence of standing and upstream-breaking waves on the water surface. This event caused significant erosion of the bed, then formation of a massive, mostly unstratified, mud-rich, sand and gravel deposit. (C) Prostrate, living *Melaleuca* (paperbark) tree estimated to be over 100 years old (Fielding *et al.*, 1997) in the bed of the upper Burdekin River. Tree is inclined in the downstream direction (left to right). Notebook 0.20 m for scale. (D) Desiccated mud bed in a hollow of the upper Burdekin River bed. Tape measure indicates that polygonal cracks are at least 0.40 m deep. (E) Composite sandstone body of the basal Triassic Liujiagou Formation at Shuiyuguan, Shanxi province, north China. The composite body includes laterally discontinuous, reddened and pedogenically modified mudrock partings (for example, left foreground), and the sandstone is internally dominated by flat and low-angle stratification. About 25 m of vertical section shown. (F) View of a composite, multi-storey channel fill in the Upper Cretaceous Masuk Formation at Blind Trail in the Henry Mountains, Utah, western USA. The lower storey is composed of mixed silt/sandstone, is crudely bedded, and preserves macroform dipping surfaces interpreted as a lateral accretion set. This lower storey is interpreted to record sediment accumulation from high-concentration, flashy flow events such as are typical of very high CVQ_p rivers. Overlying this are interbedded facies and sandstone facies, interpreted, respectively, to record moderate and low CVQ_p conditions. Geologist (circled) 1.8 m high. (G) View of a fluvial channel body from the Pennsylvanian Sydney Mines Formation at Long Beach, Atlantic Canada. The lithology passes laterally from sandstone into root-penetrated siltstone, and the body is internally dominated by flat and low-angle stratification. Green file is 20 cm high. (H) Interbedded and admixed sandstone/siltstone body comprising the Dewey Bridge Member (Doelling, 2003) north-west of Moab, Utah, western USA. This body, above the aeolian Navajo Sandstone (lower pavements) and below the cliff-forming, mainly aeolian Entrada Formation (upper massive cliff), shows clinoform bedding that can be interpreted as a lateral accretion set. The Dewey Bridge Member is interpreted here as the deposit of a river channel that crossed a semiarid plain and reworked mainly aeolian deposits in intermittent, possibly high-concentration flow events. Cliff is 25 to 30 m high.

Cretaceous Masuk Formation in southern Utah (Fig. 18F and G), and parts of the Pennsylvanian Sydney Mines Formation (Fig. 18G and H) of Cape Breton, Atlantic Canada (Allen *et al.*, 2014; Hess & Fielding, 2020; Shao *et al.*, 2024).

Sandstone bodies of the basal Triassic Liujiagou Formation at Shuiyuguan, Shanxi province, north China (Shao *et al.*, 2024) illustrate a change in alluvial style from the underlying upper Permian fluvial strata (in which fluvial channel deposits are dominated by dune-scale cross-bedding) to thick, tabular sandstone bodies with a sheet-like architecture (Fig. 19E). These bodies are internally dominated by flat and low-angle stratification with convex-upward elements. The sandstone bodies also contain abundant reddened mudstone partings, desiccation cracks and common bioturbation (Fig. 19F). They are interpreted to record fluvial sediment accumulation in channels with high values of CVQ_p. These conditions evidently became prevalent following environmental changes at the Permo–Triassic boundary. Similar changes in alluvial style have been noted by other researchers at the same level in North China (e.g. Zhu *et al.*, 2019, 2020).

The lower storeys of composite channel fill bodies in the Campanian Masuk Formation of the Henry Mountains, southern Utah, USA, are composed of a massive and soft-sediment-deformed sandstone–siltstone mixture (Fig. 19F). Macroform dipping surfaces are visible but very few primary sedimentary structures are preserved. The admixed lithology contains abundant plant debris and locally large, irregularly shaped, clasts of intraformational siltstone (Corbett *et al.*, 2011; Hess & Fielding, 2020). These chaotic channel fills are interpreted to have formed under a strongly seasonal and erratic runoff regime that gave rise to intermittent, highly sediment-charged flood flows with inherently very high CVQ_p. They form the basal part of tripartite, composite channel bodies that preserve what Hess & Fielding (2020) interpreted as climate-induced cyclicity.

The Pennsylvanian Sydney Mines Formation of Cape Breton, Atlantic Canada, contains a range of ancient channel body types (Batson & Gibling, 2002; Gibling *et al.*, 2004; Allen *et al.*, 2014). Among them are erosionally-based, laterally heterogeneous bodies of sandstone and

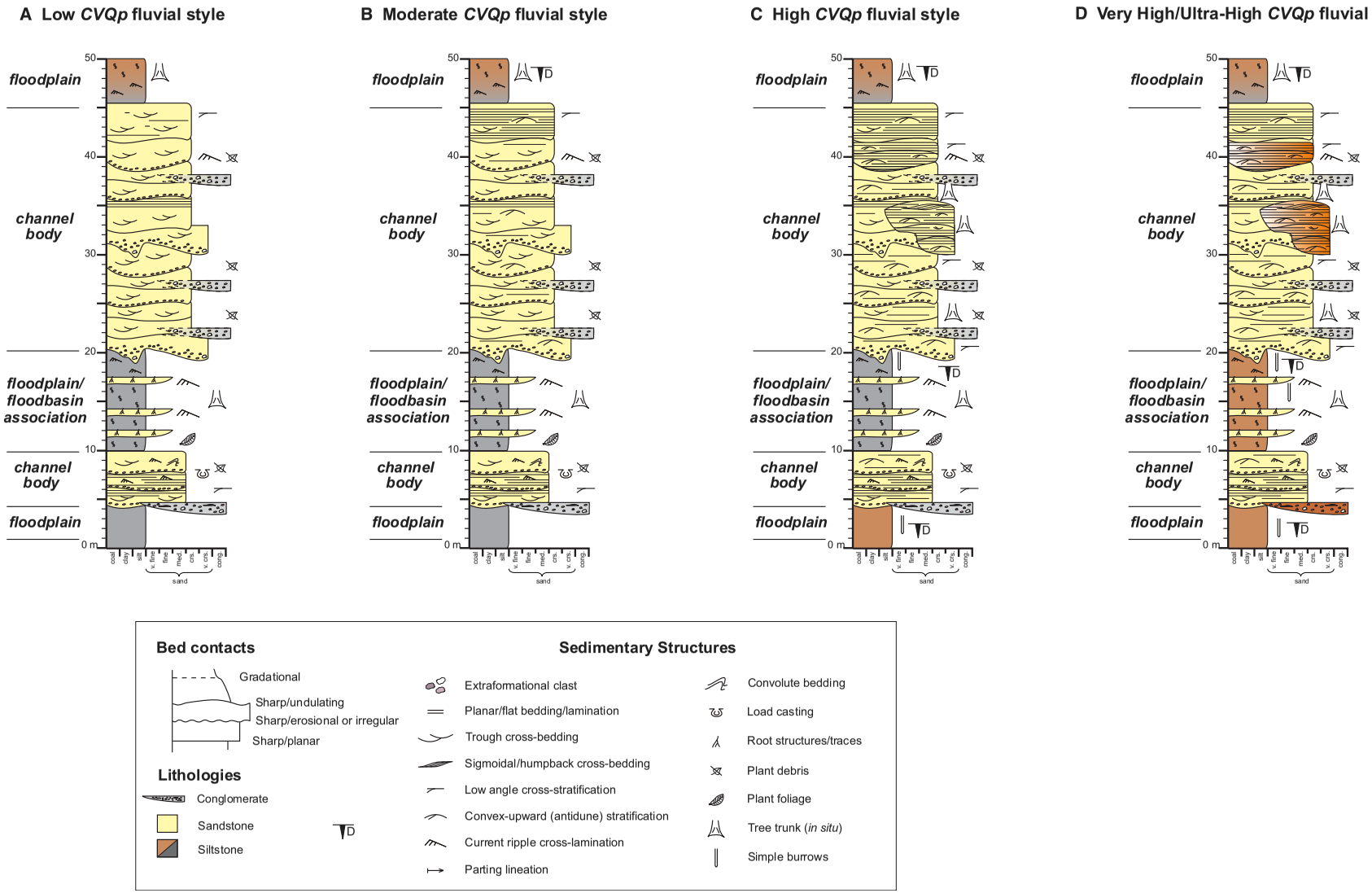

Fig. 19. Facies models for low, moderate, high and very high CVQ_p river systems (modified from Fielding *et al.*, 2018). The summaries are in the form of vertical graphic logs and not cross-sectional line drawings of stratal architecture because there is expected to be considerable variability in the latter within each category. Each log is designed to show approximately the same proportion and thickness of channel deposits and similar grain-size distribution, since channel body size and sediment calibre are not defining characteristics. See also Table 1 for a list of defining characteristics of these fluvial styles.

siltstone, containing discontinuous, pedogenically modified red mudstone partings (Fig. 19G). Internally, these bodies are dominated by flat and low-angle stratification, including antidunal bedding, along with soft-sediment deformation and abundant, *in situ*, upright tree stump fossils (Fielding *et al.*, 2009; Allen *et al.*, 2014). They are interpreted as channel fills formed in hydrological conditions with very high CVQ_p, in strongly seasonal, subtropical climates subject to erratic precipitation and runoff.

Other examples of the very high CVQ_p alluvial style evident from the literature include the Triassic Dockum Group of Texas, south-west USA (Walker & Holbrook, 2023), the Palaeogene Green River Formation of Utah (Gall *et al.*, 2017; Wang & Plink-Björklund, 2019, 2020), and the Palaeogene Poison Canyon Formation of south-west USA (Schwartz *et al.*, 2021).

Deposits of rivers with ultra-high (>2.0) CVQ_p

An additional category is proposed to classify deposits of desert wadis and other extremely infrequent events in different streams [such as the Roaring River, Colorado dam burst flood of 1982 (Fig. 11) and some jökulhlaups] as those characterized by ultra-high CVQ_p (>2.0; Table 2). Such deposits preserve predominantly upper flow regime stratification, are highly variable lithologically, show little recognizable macroform structure preservation, and may preserve remnants of trees *in situ* in channel deposits. They are also commonly composed of mixed sand and mud lithologies. It is likely that most streams in deserts would fall into this category, but there is very little reliable gauging data. In such streams, the bed may be dry most years and sediment-transporting flows occur rarely. Modern examples include the rivers crossing the Namib Desert of south-west Africa (Stanistreet & Stollhofen, 2002; Krapf *et al.*, 2003), the wadis of Oman (Fryberger *et al.*, 2016; Kocurek *et al.*, 2020), and the 'Channel Country' rivers of central Australia (for example, Cooper Creek; Table 2; Nanson *et al.*, 1986; Gibling *et al.*, 1998). The latter is an example of desert systems in which sediment is transported as sand-sized mud aggregates.

An ancient example of the ultra-high CVQ_p alluvial style is given by part of the Jurassic Dewey Bridge Member near Moab, Utah (Fig. 18H). The Jurassic Dewey Bridge Member (arguably part of the Carmel Formation; Doelling, 2003) occurs above the aeolian Navajo Sandstone and below the aeolian Entrada Sandstone in mesas north-west of Moab, Utah (USA). The upper part of this unit includes erosionally-based sandstone/siltstone bodies that have crudely-defined clinoform sets up to 10 m thick (Fig. 18H). Within the units defined by dipping surfaces, the channel fill lithologies are predominantly composed of mixed sand-sized and silt-sized particles, preserve root traces and diffuse bioturbation, and abundant soft-sediment deformation including desiccation cracks. Beds are massive, vaguely stratified, and only locally well-stratified with rare cross-bedding. These bodies are interpreted here as channel fills that were in part laterally accreted (or, conceivably, downstream-accreted) and crossed a semiarid, coastal alluvial plain characterized by high discharge variance. Formative flows at times transported high concentrations of suspended sediment, giving rise to the massive and vaguely stratified facies (cf. Baas *et al.*, 2016).

Other published examples of very high to ultra-high CVQ_p fluvial channel sediment bodies include elements of the Triassic Dockum Group of Texas, south-west USA (Walker & Holbrook, 2023), Palaeogene deposits of the south-west USA (Gall *et al.*, 2017; Plink-Bjorklund, 2019; Zellman *et al.*, 2020) and Pleistocene alluvium in Namibia (Smith *et al.*, 1993).

New facies models for the deposits of low, moderate, high and very high/ultra-high CVQ_p fluvial channel fills

New facies models for the deposits of low, moderate, high and very high/ultra-high CVQ_p fluvial channel fills are given in Fig. 19 in the form of summary vertical graphic logs, in the hope that this will stimulate further research on the topic. The graphic logs are constructed in order to preserve a consistent proportion of channel bodies versus overbank facies, so as not to introduce a lithological bias. Nonetheless, because the degree of internal lithological heterogeneity in channel bodies increases with increasing CVQ_p, the graphic logs showing high and very high/ultra-high CVQ_p fluvial styles incorporate this characteristic. No illustrations of cross-sectional channel body architecture are shown because this is a highly variable property both within and between CVQ_p classes. Rather, the emphasis is on variations in the internal properties of channel deposits in the different classes. The models are independent of climatic zone (with the above caveat concerning the location of many high/ultra-high CVQ_p rivers in semiarid and arid zones) and independent of channel size.

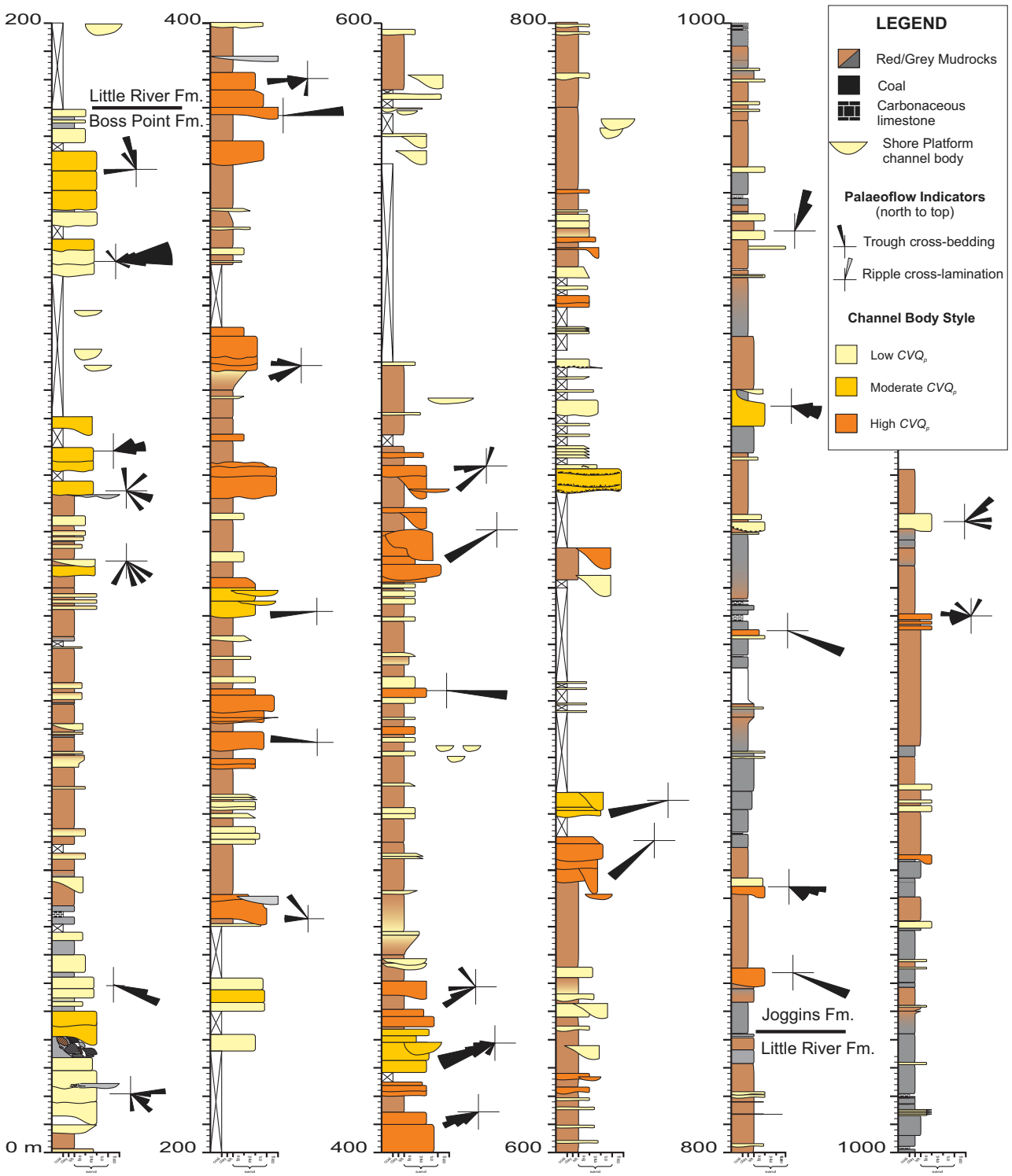

Fig. 20. Example of stratigraphic variation in CVQ_p, from the Pennsylvanian of the Cumberland Basin, Atlantic Canada (modified from Fielding *et al.*, 2018). Shown is the uppermost 200 m of the Boss Point Formation, the entire Little River Formation, and the lowermost part of the Joggins Formation, totalling about 1150 m of section (see Allen *et al.*, 2013, for more information). From the base upward, there is a progressive change from Low CVQ_p, through Moderate, to High CVQ_p alluvial style and then back through Moderate to Low CVQ_p style. This cycle of change is concordant with changes in sediment dispersal directions as indicated by palaeoflow data shown in rose diagrams. The stratal cycle is interpreted to record changes in palaeoclimatic conditions associated with a change in the palaeogeography of the region.

Deposits of the low CVQ_p alluvial style are characterized by channel fills with clearly preserved macroform elements (channel forms, bar accretion surfaces), a preponderance of dune-scale cross-bedding, relatively consistent lithology within channel fills, and a limited role for vegetation in channel fills. In the moderate CVQ_p style, those channel fills show somewhat muted macroform architecture, preserve a significant proportion of upper flow regime sedimentary structures, may show in-channel, lateral lithological changes, and may preserve remnants of woody vegetation within channel fills. Deposits of the high CVQ_p style lack obvious macroform architectural elements, preserve a preponderance of upper flow regime structure, show common lateral lithological changes within channel fills, and preserve common evidence of *in situ* tree establishment in the formative channels along with abundant large, woody debris. The very high CVQ_p style is also characterized by little or no macroform element preservation and a sheet-like architecture, dominance of upper flow regime structures to the virtual exclusion of lower flow regime structures, common admixed sand/mud/gravel lithologies, common fine-grained partings with desiccation, bioturbation and pedogenic modification features, and abundant evidence of *in situ* tree growth in channels. The ultra-high CVQ_p style records mainly the deposits of desert streams, which display the features noted for the high CVQ_p style but lack significant evidence for *in situ* tree growth and are interbedded with aeolian deposits.

The new models can be used in isolation or in combination with 'traditional' planform-based models. As stated earlier, planform-based models can inform some aspects (such as cross-sectional channel body geometry) that CVQ_p models cannot address. It is also likely that planform-based models are more useful in evaluations of low and moderate CVQ_p river deposits where macroform structure is more overtly visible. However, CVQ_p-based models such as those presented here are the only ones that incorporate the full range of environmental conditions under which rivers operate (dryland to perhumid). They furthermore allow insights that planform-based models cannot, as is expanded upon below.

Applications of the new facies scheme

Recognition of one of the above-documented, peak discharge variance-based, fluvial styles in an ancient succession allows an interpretation of the type of runoff under which that deposit formed. This may assist the interpretation of palaeoenvironmental conditions for an ancient succession. Just as useful, however, is the recognition of changes in style through a stratigraphic succession, either progressively or repetitively in multiple stratal cycles. Recognition of progressive change can speak to a broad, long-term change in palaeoclimate, whereas cyclical repetitions of fluvial style changes can inform an understanding of shorter-term climate cyclicity, for example on Milankovitch frequencies. These applications are illustrated with two examples from the authors' experience; the Pennsylvanian succession of the Cumberland Basin, Nova Scotia, Canada, and the cyclical Upper Cretaceous Masuk Formation of Utah, western USA.

A log of the 1200 m interval from the upper Boss Point Formation to Joggins Formation (Fig. 20) in the Cumberland Basin, mainland Nova Scotia (Allen *et al.*, 2013; Fielding *et al.*, 2018), shows preservation of a progressive upward change from low CVQ_p, through moderate, to high CVQ_p fluvial style, and then back again to low CVQ_p style. No precise timing constraints are available for this succession. It was, however, accumulated rapidly during a phase of subsurface salt withdrawal (Waldron & Rygel, 2005), and may represent a time period of the order of <1 Myr. The changes are accompanied by concordant variations in sediment dispersal directions, as indicated by palaeoflow measurements from sedimentary structures, suggesting that climatic change may have accompanied changes in palaeogeography. Previous evaluations of these formations by a variety of researchers did not identify such a long-term cyclicity in palaeoenvironmental conditions, highlighting the potential of this approach for identifying subtle or gradual shifts in (palaeo)-environmental conditions.

Composite channel fill bodies preserved in the Campanian Masuk Formation (Eaton, 1990) in the Henry Mountains of Utah, USA, show a tripartite stacking pattern (Fig. 18F), with a basal chaotic storey overlain by an interbedded sandstone–siltstone unit with Inclined Heterolithic Stratification (IHS), in turn overlain by a sandstone interval (Corbett *et al.*, 2011; Hess & Fielding, 2020). This pattern is more or less repeated several times through the formation, giving rise to sheet-like, composite channel bodies that are significantly broader in a cross-palaeoslope direction than would be predicted from dimensions of single channel fills in those

bodies. Corbett *et al.* (2011) and Hess & Fielding (2020) interpreted these composite bodies as the product of climatically-driven cycles that initially formed chaotic, mixed and unstratified deposits characteristic of the high CVQ_p fluvial style (Fig. 18F). Over time, this was superseded by more stratified and well-bedded, more grain-size-segregated deposits referable to moderate and low CVQ_p styles. The preservation of this tripartite stacking pattern in several successive, composite channel bodies allows the identification of climatic cycles during the Campanian of the Western Cordilleran Foreland Basin that operated on the timescales of channel filling (likely hundreds to thousands of years, or sub-Milankovitch frequency).

The above examples provide illustrations of the ways in which CVQ_p-based facies models could be used to assist in palaeoenvironmental analyses of ancient successions. Previously-formulated, planform-based facies models cannot provide such interpretive value. The new models presented here also fulfil most of the criteria cited by Walker (1979) and more recently by Miall (2010) as to the roles of facies models in general.

CONCLUSIONS

The concept of using fluvial discharge statistics, and specifically the coefficient of inter-annual peak discharge variance (CVQ_p), as a basis for better understanding alluvial stratigraphy is explored in depth, following the initial proposal of Fielding *et al.* (2018). More rivers for which both good quality, long-term discharge records, and data on surface and subsurface deposit characteristics are known have been used to compile an expanded database. This database demonstrates the strong correlation between CVQ_p and alluvial architecture, and suggests that the nature of the flow history in a river on historical timescales (tens to hundreds of years) exerts a strong control on deposit character. That said, CVQ_p can be both spatially variable along a single river and, depending on the interval over which CVQ_p is calculated, it is temporally variable on timescales of tens of years, suggesting that that more work is needed to understand the gauging record length that is needed to calculate a CVQ_p that will be representative of alluvial deposit character. This also stresses the care needed in defining what age the sediments are to be able to correlate with the appropriate interval of discharge record to calculate variance. Herein, Fielding *et al.*'s (2018) CVQ_p class boundaries have been modified and two additional classes added (very high and ultra-high). It is acknowledged that these classes have arbitrarily defined boundaries that in reality might be regarded as fuzzy. It is hoped that this study stimulates research into the existence or otherwise of inherent thresholds that could form more natural boundaries to classes (or indeed a different statistic of discharge to do this).

A case study using gauging records and sedimentological studies from the Platte River drainage basin in central USA illustrates these patterns explicitly, and shows that individual, high flow events can have a disproportionate influence on alluvial records. Specific flow events from the past hundred years are documented to have changed the character of the preserved alluvial record at several sites within this basin. These patterns indicate that the higher the CVQ_p on a river or portion of a river, the more likely it is that features related to the high and very high CVQ_p river classes documented herein will be preserved.

A series of facies models is proposed to account for rivers that formed under low, moderate, high, very high and ultra-high CVQ_p conditions. The class boundaries, modified from those proposed by Fielding *et al.* (2018), are arbitrary and gradational, such that an ancient succession might preserve elements of more than one of the classes. With increasing CVQ_p, alluvial records preserve a lower proportion of dune-scale cross-bedding, and a higher proportion of upper flow regime sedimentary structures, together with less conspicuous macroform structure, greater lateral lithological heterogeneity, and greater evidence of channel bed growth of woody vegetation within channel facies (at least, since the evolution of woody plants). At the very highest variance there may be a reduction in woody material as a result of some deposits of the class being deposited in extremely arid conditions where vegetation is sparse. These new facies models are independent of channel planform, and provide more potential for interpreting ancient palaeoenvironmental conditions than do planform-based models. In the lower CVQ_p types of deposits where macroforms are more easily identified, it may be possible to subdivide channel bodies or parts of bodies on the basis of planform models (but the value of this is debatable).

Spatial, or upward, stratigraphic changes in the CVQ_p-based alluvial style may be used as a means of determining and characterizing palaeoclimatic change in Earth history on a variety of timescales, ranging from those of channel filling (tens to hundreds of years), through Milankovitch orbital frequencies (tens of thousands of years) to longer-term progressive changes perhaps related to continental drift or other processes (hundreds of thousands to millions of years).

It is hoped that the expanded river database and the improved CVQ_p-based facies models will stimulate a new phase of discovery in the analysis of ancient alluvial records, and move the science away from blinkered adherence to classic categorization.

ACKNOWLEDGEMENTS

This paper was an outgrowth from a plenary presentation at the 12th International Conference on Fluvial Sedimentology, held at Riva del Garda, Italy, on 2 to 7 July 2023. The authors are grateful to the Convenor Massimiliano Ghinassi and the Organizing Committee for the initial opportunity to compile and present this research. We are deeply grateful to all of the individuals and organizations that record discharge data and make the data available via the data sources listed below. N. Mountney, J. Holbrook, and an anonymous individual are thanked for their thoughtful and constructive reviews, along with Associate Editor Theresa Schwartz and Editor Piret Plink-Björklund for their handling of the manuscript.

CONFLICT OF INTEREST

The authors declare no conflicts of interest.

DATA AVAILABILITY STATEMENT

A lot of data used in the analysis for this paper were sourced via The Global Runoff Data Centre, 56 068 Koblenz, Germany (https://grdc.bafg.de/GRDC/EN/02_srvcs/21_tmsrs/riverdischarge_node.html) accessed multiple times through 2023–2024. Components of those data originated from a large number of organizations including: Argentina – the Subsecretaría de Recursos Hídricos (SRH). Brazil – National Water Agency (ANA) and the Operador Nacional do Sistema Elétrico (ONS). South Africa – Department of Water and Sanitation (DWA) Namibia – Ministry of Agriculture, Water & Forestry. Japan – Infrastructure Development Institute (IDI). Malaysia – Department of Irrigation and Drainage. Oman – Ministry of Regional Municipalities, Environment & Water Resources (MRMWR). Most of the Australian data were extracted from the Australian Bureau of Meteorology Hydrologic Reference stream gauging Stations (http://www.bom.gov.au/water/hrs/index.shtml) on various dates through 2023–2024 (including some original discharge data from QLD – Department of Regional Development, Manufacturing and Water, NT – Department of Environment, Parks and Water Security). Burdekin river data were supplied by the Queensland Department of Natural Resources and Mines. American data were sourced from the USGS data base (nwis.waterdata.usgs.gov/nwis) accessed on several dates through 2023 and 2034. British river data were obtained from the from the National River Flow Archive Search Data | National River Flow Archive (ceh.ac.uk) accessed on various dates through 2023–2024. Some data for Canadian rivers were sourced from the Environment and Climate Change Canada Historical Hydrometric Data web site (https://wateroffice.ec.gc.ca/mainmenu/historical_data_index_e.html) on various dates in 2023. Ob River data are available from http://www.r-arcticnet.sr.unh.edu/ObservedAndNaturalizedDischarge-Website/. Some data for the Jamuna River were taken from Rahman (2016). A summary of all data used in this analysis is given in Table S1.

REFERENCES

Alexander, J. and **Fielding, C.R.** (1997) Gravel antidunes in the tropical Burdekin River, Queensland, Australia. *Sedimentology*, **44**, 327–337.

Alexander, J., **Bridge, J.S.**, **Gawthorpe, R.L.**, **Leeder, M.R.** and **Collier, R.E.L.** (1994) Holocene meander belt evolution in an extensional basin, SW Montana USA. *J. Sediment. Res.*, **B64**, 542–559.

Alexander, J., **Fielding, C.R.** and **Pocock, G.D.** (1999) Flood behavior of the Burdekin River, tropical north Queensland, Australia. In: *Floodplains: Interdisciplinary Approaches* (Eds Marriott, S.B. and Alexander, J.), *Geol. Soc. London Spec. Publ.*, **163**, 27–40.

Alexander, J., **Herbert, C.M.**, **Fielding, C.R.** and **Amos, K.J.** (2020) Controls on channel deposits of highly variable rivers: Comparing hydrology and event deposits in the Burdekin River, Australia. *Sedimentology*, **67**, 2721–2746.

Algeo, T.J. and **Liu, J.S.** (2020) A re-assessment of elemental proxies for paleoredox analysis. *Chem. Geol.*, **540**, 119549.

Alho, P., **Russell, A.J.**, **Carrivick, J.L.** and **Käyhkö, J.** (2005) Reconstruction of the largest Holocene jökulhlaup within Jökulsá á Fjöllum, NE Iceland. *Quatern. Sci. Rev.*, **24**, 2319–2334.

Allen, J.R.L. (1978) Studies in fluviatile sedimentation: an exploratory quantitative model for architecture of avulsion-controlled alluvial suites. *Sed. Geol.*, **21**, 129–147.

Allen, J.R.L. (1979) Studies in fluviatile sedimentation: an elementary geometrical model for the connectedness of avulsion-controlled channel sand bodies. *Sed. Geol.*, **24**, 253–267.

Allen, J.R.L. (1983) Studies in fluviatile sedimentation: bars, bar-complexes and sandstone sheets (low-sinuosity braided streams) in the Brownstones (L. Devonian), Welsh borders. *Sed. Geol.*, **33**, 533–555.

Allen, J.P., **Fielding, C.R.**, **Rygel, M.C.** and **Gibling, M.R.** (2013) Deconvolving signals of tectonic and climatic controls from continental basins: An example from the Late Paleozoic Cumberland Basin, Atlantic Canada. *J. Sediment. Res.*, **83**, 847–872.

Allen, J.P., **Fielding, C.R.**, **Gibling, M.R.** and **Rygel, M.C.** (2014) Recognizing products of palaeoclimate fluctuation in the fluvial stratigraphic record: An example from the Pennsylvanian to Lower Permian of Cape Breton Island, Nova Scotia. *Sedimentology*, **61**, 1332–1381.

Almeida, R.P., **Galeazzi, C.P.**, **Best, J.L.**, **Ianniruberto, M.**, **Do Prado, A.H.**, **Janikian, L.**, **Mazoca, C.E.M.**, **Tamura, L.N.** and **Nicholas, A.** (2024) Morphodynamics and depositional architecture of mid-channel bars in large Amazonian rivers. *Sedimentology*, **71**, 1591–1614.

Amos, K.J., **Alexander, J.**, **Horn, A.**, **Pocock, G.D.** and **Fielding, C.R.** (2004) Supply limited sediment transport in a high-discharge event of the tropical Burdekin River, North Queensland, Australia. *Sedimentology*, **51**, 145–162.

Arévalo, O.J., **Colombera, L.**, **Mountney, N.P.**, **Basilici, G.** and **Soares, M.V.T.** (2022) Variations in water discharge at different temporal scales in a mud-prone alluvial succession: the Paleocene-Eocene of the Tremp-Graus Basin, Spain. *Sed. Geol.*, **433**, 106122.

Ashworth, P.J., **Best, J.L.**, **Roden, J.E.**, **Bristow, C.S.** and **Klaassen, G.J.** (2000) Morphological evolution and dynamics of a large, sand braid-bar, Jamuna River, Bangladesh. *Sedimentology*, **47**, 533–555.

Baas, J.H., **Best, J.L.** and **Peakall, J.** (2016) Predicting bedforms and primary current stratification in cohesive mixtures of mud and sand. *J. Geol. Soc. London*, **173**, 12–45.

Bamberry, W.J., **Hutton, A.J.** and **Jones, B.G.** (1995) The Permian Illawarra Coal Measures, southern Sydney Basin, Australia: a case study of deltaic sedimentation. In: *Geology of Deltas* (Eds Postma, G. and Oti, M.N.), pp. 153–166. A.A. Balkema, Rotterdam.

Barefoot, E.A., **Nittrouer, J.A.**, **Foreman, B.Z.**, **Hajek, E.A.**, **Dickens, G.R.**, **Baisden, T.** and **Toms, L.** (2022) Evidence for enhanced fluvial channel mobility and fine sediment export due to precipitation seasonality during the Paleocene-Eocene thermal maximum. *Geology*, **50**, 116–120.

Batson, P.A. and **Gibling, M.R.** (2002) Architecture of channel bodies and paleovalley fills in high-frequency Carboniferous sequences, Sydney Basin, Atlantic Canada. *Bull. Can. Petrol. Geol.*, **50**, 138–157.

Bauch, G.D. and **Hickin, E.J.** (2010) Rate of floodplain reworking in response to increasing storm-induced floods, Squamish River, south-western British Columbia, Canada. *Earth Surf. Process. Landf.*, **36**, 872–884.

Besly, B.M. (1988) Palaeogeographic implications of late Westphalian to early Permian red-beds, Central England. In: *Sedimentation in a Synorogenic Basin Complex: The Upper Carboniferous of Northwest Europe* (Eds Besly, B.M. and Kelling, G.), pp. 200–221. Blackie, Glasgow.

Besly, B.M. and **Turner, P.** (1983) Origin of red beds in a moist tropical climate (Etruria Formation, Upper Carboniferous, UK). In: *Residual Deposits* (Ed. Wilson, R.C.L.), *Geol. Soc. London Spec. Publ.*, **2**, 131–147.

Best, J.L. and **Wignall, P.B.** (Eds) (2016) *A Field Guide to the Carboniferous Sediments of the Shannon Basin, Western Ireland*, p. 375. International Association of Sedimentologists, Wiley-Blackwell, Oxford.

Best, J.L., **Ashworth, P.J.**, **Bristow, C.S.** and **Roden, J.** (2003) Three-dimensional sedimentary architecture of a large, mid-channel sand braid bar, Jamuna River, Bangladesh. *J. Sediment. Res.*, **73**, 516–530.

Blair, T.C. (1987) Sedimentary processes, vertical stratification sequences, and geomorphology of the Roaring River Alluvial Fan, Rocky Mountain National Park, Colorado. *J. Sediment. Res.*, **57**, 1–18.

Blodgett, R.H. and **Stanley, K.O.** (1980) Stratification, bedforms and discharge relations of the Platte River, Nebraska. *J. Sediment. Petrol.*, **50**, 139–148.

Bobrovitskaya, N.N., **Skakalsky, B.G.**, **Zubkova, K.M.**, **Dobrotvorskaya, G.I.**, **Petrova, I.V.**, **Tsivjyan, M.V.m.**, **Chistyakova, N.I.**, **Yanuta, V.G.**, **Callender, E.C.**, **Landa, E.R.**, **Meade, R.H.**, **Councell, T.B.** and **Bruce, R.A.** (1997) Hydrologic and hydrochemical data for the Ob-Irtysh and Yenisey River systems of Central Russia, 1954–1988. *U.S. Geol. Surv. Open-File Rep.*, **97–232**, 20.

Bradley, R.W. and **Venditti, J.G.** (2017) Reevaluating dune scaling relations. *Earth Sci. Rev.*, **165**, 356–376.

Bridge, J.S. (1985) Paleochannel patterns inferred from alluvial deposits: a critical evaluation. *J. Sediment. Petrol.*, **55**, 579–589.

Bridge, J.S. (1993a) Description and interpretation of fluvial deposits: a critical perspective. *Sedimentology*, **40**, 801–810.

Bridge, J.S. (1993b) The interaction between channel geometry, water flow, sediment transport and deposition in braided rivers. In: *Braided Rivers* (Eds Best, J.L. and Bristow, C.S.), *Geol. Soc. London Spec. Publ.*, **75**, 13–71.

Bridge, J.S. (2003) *Rivers and Floodplains: Forms, Processes, and Sedimentary Record*, p. 491. Blackwell Science, Oxford.

Bridge, J.S. and **Gabel, S.L.** (1992) Flow and sediment dynamics in a low sinuosity braided river: Calamus River, Nebraska Sandhills. *Sedimentology*, **39**, 125–142.

Bridge, J.S. and **Jarvis, J.** (1982) The dynamics of a river bend: a study in flow and sedimentary processes. *Sedimentology*, **29**, 499–541.

Bridge, J.S. and **Leeder, M.R.** (1979) A simulation model of alluvial stratigraphy. *Sedimentology*, **26**, 617–644.

Bridge, J.S., **Alexander, J.**, **Collier, R.E.L.**, **Gawthorpe, R.L.** and **Jarvis, J.** (1995) Ground-penetrating radar and coring used to study the large-scale structure of point-bar deposits in three dimensions. *Sedimentology*, **42**, 839–852.

Bridge, J.S., **Collier, R.** and **Alexander, J.** (1998) Large-scale structure of Calamus River deposits (Nebraska, USA) revealed using ground-penetrating radar. *Sedimentology*, **45**, 977–986.

Brierley, G.J. (1996) Channel morphology and element assemblages: a constructivist approach to facies modelling.

In: *Advances in Fluvial Dynamics and Stratigraphy* (Eds Carling, P.A. and Dawson, M.R.), pp. 263–298. Wiley, New York, NY.

Bristow, C.S. (1987) Brahmaputra River: channel migration and deposition. In: *Recent Developments in Fluvial Sedimentology* (Eds Ethridge, F.G., Flores, R.M. and Harvey, M.D.), *SEPM Spec. Publ.*, **39**, 63–74.

Bristow, C.S. (1993) Sedimentary structures exposed in bar tops in the Brahmaputra River, Bangladesh. In: *Braided Rivers* (Eds Best, J.L. and Bristow, C.S.), *Geol. Soc. London Spec. Publ.*, **75**, 277–289.

Bristow, C.S. (1996) Reconstructing fluvial channel morphology from sedimentary sequences. In: *Advances in Fluvial Dynamics and Stratigraphy* (Eds Carling, P.A. and Dawson, M.R.), pp. 351–371. Wiley, New York, NY.

Bristow, C.S., **Skelly, R.L.** and **Ethridge, F.G.** (1999) Crevasse splays from the rapidly aggrading, sand-bed, braided Niobrara River, Nebraska: effect of base-level rise. *Sedimentology*, **46**, 1029–1047.

Brown, W.M., III and **Ritter, J.R.** (1971) *Sediment Transport and Turbidity in the Eel River Basin, California*. USGS, Reston, VI.

Browne, G.H. and **Plint, A.G.** (1994) Alternating braidplain and lacustrine deposition in a strike-slip setting: the Pennsylvanian Boss Point formation of the Cumberland Basin, Maritime Canada. *J. Sediment. Res.*, **B64**, 40–59.

Burgener, L., **Hyland, E.**, **Reich, B.J.** and **Scotese, C.** (2023) Cretaceous climates: Mapping paleo-Koppen climatic zones using a Bayesian statistical analysis of lithologic, paleontologic, and geochemical proxies. *Palaeogeogr. Palaeoclimatol. Palaeoecol.*, **613**, 34.

Calder, J.H., **Rygel, M.C.**, **Ryan, R.J.**, **Falcon-Lang, H.J.** and **Hebert, B.L.** (2005) Stratigraphy and sedimentology of early Pennsylvanian red beds at Lower Cove, Nova Scotia, Canada: the Little River Formation with redefinition of the Joggins Formation. *Atlantic Geol.*, **41**, 143–167.

Cant, D.J. (1978a) Bedforms and bar types in the South Saskatchewan River. *J. Sediment. Petrol.*, **48**, 1321–1330.

Cant, D.J. (1978b) Development of a facies model for sandy braided river sedimentation: comparison of the South Saskatchewan River and the Battery Point Formation. In: *Fluvial Sedimentology* (Ed. Miall, A.D.), *Can Soc. Petrol. Geol. Mem.*, **5**, 627–639.

Cant, D.J. and **Walker, R.G.** (1978) Fluvial processes and facies sequences in the sandy braided South Saskatchewan River, Canada. *Sedimentology*, **25**, 625–648.

Carling, P. (2009) Geomorphology and sedimentology of the lower Mekong River. In: *The Mekong: Biophysical Environment of an International River Basin* (Ed. Campbell, I.), pp. 77–110. Elsevier Science, Amsterdam.

Carling, P. and **Leclair, S.F.** (2019) Alluvial stratification styles in a large, flash-flood influenced dryland river: The Luni River, Thar Desert, north-west India. *Sedimentology*, **66**, 102–128.

Carrivick, J.L. and **Tweed, F.S.** (2019) A review of glacier outburst floods in Iceland and Greenland with a megafloods perspective. *Earth Sci. Rev.*, **196**, 20.

Cassidy, N.J., **Russell, A.J.**, **Pringle, J.K.** and **Carrivick, J.L.** (2004) GPR-derived architecture of large-scale Icelandic jökulhlaup deposits, north-east Iceland. In: *Proceedings of the 10th International Conference on Ground Penetrating Radar*, pp. 581–584. IEEE, Delft, Netherlands.

Cisneros, J., **Best, J.**, **van Dijk, T.**, **Paes de Almeida, R.**, **Amsler, M.**, **Boldt, J.**, **Freitas, B.**, **Galeazzi, C.**, **Huizinga, R.**, **Iannirubertо, M.**, **Ma, H.B.**, **Nittrouer, J.A.**, **Oberg, K.**, **Orfeo, O.**, **Parsons, D.**, **Szupiany, R.**, **Wang, P.** and **Zhang, Y.F.** (2016) Dunes in the world's big rivers are characterized by low-angle lee-side slopes and a complex shape. *Nat. Geosci.*, **13**, 156–162.

Colombera, L., **Mountney, N.P.**, **Felletti, F.** and **McCaffrey, W.D.** (2014) Models for guiding and ranking well-to-well correlations of channel bodies in fluvial reservoirs. *AAPG Bull.*, **98**, 1943–1965.

Colombera, L., **Reesink, A.J.H.**, **Duller, R.A.**, **Jeavons, V.A.** and **Mountney, N.P.** (2024) The thickness variability of fluvial cross-strata as a record of dune disequilibrium and palaeohydrology proxy: A test against channel deposits. *Sedimentology*, **71**, 590–618.

Conaghan, P.J. and **Jones, J.G.** (1975) The Hawkesbury Sandstone and the Brahmaputra: a depositional model for continental sheet sandstones. *J. Geol. Soc. Aust.*, **22**, 275–283.

Corbett, M.J., **Fielding, C.R.** and **Birgenheier, L.P.** (2011) Stratigraphy of a Cretaceous coastal-plain fluvial succession: the Campanian Masuk Formation, Henry Mountains Syncline, Utah, U.S.A. *J. Sediment. Res.*, **81**, 80–96.

Costa, J.E. and **Jarrett, R.D.** (2008) *An Evaluation of Selected Extraordinary Floods in the United States Reported by the U.S. Geological Survey and Implications for Future Advancement of Flood Science*. U.S. Geological Survey Scientific Investigations Report, 2008-5164, 109–112.

Croke, J., **Jansen, J.D.**, **Amos, K.J.** and **Pietsch, T.J.** (2011) A 100 ka record of fluvial activity in the Fitzroy River Basin, tropical northeastern Australia. *Quat. Sci. Rev.*, **30**, 1681–1695.

Crowley, K.D. (1983) Large-scale bed configurations (macroforms), Platte River Basin, Colorado and Nebraska: primary structures and formative processes. *Geol. Soc. Am. Bull.*, **94**, 117–133.

Cyples, N.N., **Ielpi, A.** and **Dirszowsky, R.W.** (2020) Planform and stratigraphic signature of proximal braided streams: remote-sensing and ground-penetrating radar analysis of the Kicking Horse River, Canadian Rocky Mountains. *J. Sediment. Res.*, **90**, 131–149.

Das, D., **Ganti, V.**, **Bradley, R.**, **Venditti, J.**, **Reesink, A.J.H.** and **Parsons, D.** (2022) The influence of transport stage on preserved fluvial strata. *Geophys. Res. Lett.*, **20**, e2022GL099808.

Davis, R.A. and **Dalrymple, R.W.** (Eds) (2012) *Principles of Tidal Sedimentology*, p. 621. Springer-Verlag, Berlin.

Diessel, C.F.K. (1980) Newcastle and Tomago Coal Measures. In: *A Guide to the Sydney Basin* (Eds Herbert, C. and Helby, R.), *Geol. Surv. NSW Bull.*, **26**, 101–114.

Dillinger, A., **Chanvry, E.**, **Bolat, Y.** and **Fustic, M.** (2024) Architecture and history of uranium-bearing Palaeocene-Eocene strata deposited on the eastern margin of the Peri-Tethys (Chu-Sarysu Basin, south Kazakhstan). *Sed. Geol.*, **468**, 21.

Dinis, P.A., **Garzanti, E.**, **Hahn, A.**, **Vermeesch, P.** and **Cabral-Pinto, M.** (2020) Weathering indices as climate proxies: A step forward based on Congo and SW African river muds. *Earth Sci. Rev.*, **201**, 103039.

Doelling, H. (2003) Geology of Arches National Park, Utah. In: *Geology of Utah's Parks and Monuments*, 2nd edn (Eds Sprinkel, D.A., Chidsey, T.C., Jr. and Anderson, P.B.), *Utah Geol. Assoc. Pub.*, **28**, pp. 11–36.

Duller, R.A., **Mountney, N.P.**, **Russell, A.J.** and **Cassidy, N.C.** (2008) Architectural analysis of a volcaniclastic jökulhlaup deposit, southern Iceland: sedimentary evidence for supercritical flow. *Sedimentology*, **55**, 939–964.

Eaton, G. (1990) Stratigraphic revision of Campanian (Upper Cretaceous) rocks in the Henry Basin, Utah. *Mt. Geol.*, **27**, 27–38.

Ethridge, F.G. (2011) Interpretation of ancient fluvial channel deposits: review and recommendations. In: *From River to Rock Record: The Preservation of Fluvial Sediments and their Subsequent Interpretation* (Eds Davidson, S.K., Leleu, S. and North, C.P.), *SEPM Spec. Publ.*, **97**, 9–35.

Ethridge, F.G., **Skelly, R.L.** and **Bristow, C.S.** (1999) Avulsion and crevassing in the sandy, braided Niobrara River: complex response to base-level rise and aggradation. In: *Fluvial Sedimentology VI* (Eds Smith, N.D. and Rogers, J.), *Int. Assoc. Sedimentol. Spec. Publ.*, **28**, 179–191.

Feldman, H.R., **Franseen, E.K.**, **Joeckel, R.M.** and **Heckel, P.H.** (2005) Impact of longer-term modest climate shifts on architecture of high-frequency sequences (cyclothems), Pennsylvanian of Midcontinent U.S.A. *J. Sediment. Res.*, **75**, 350–368.

Fielding, C.R. (1986) Fluvial channel and overbank deposits from the Westphalian of the Durham coalfield, NE England. *Sedimentology*, **33**, 119–140.

Fielding, C.R. (2006) Upper flow regime sheets, lenses and scour fills: extending the range of architectural elements for alluvial sediment bodies. *Sed. Geol.*, **190**, 227–240.

Fielding, C.R. and **Alexander, J.** (1996) Sedimentology of the upper Burdekin River of north Queensland, Australia – an example of a tropical, variable discharge river. *Terra Nova*, **8**, 447–457.

Fielding, C.R. and **Crane, R.C.** (1987) An application of statistical modelling to the prediction of hydrocarbon recovery factors in fluvial reservoir sequences. In: *Recent Developments in Fluvial Sedimentology* (Eds Ethridge, F.G., Flores, R.M. and Harvey, M.D.), *SEPM Spec. Publ.*, **39**, 321–327.

Fielding, C.R. and **Webb, J.A.** (1996) Facies and cyclicity of the Late Permian Bainmedart Coal Measures in the northern Prince Charles Mountains, MacRobertson Land, Antarctica. *Sedimentology*, **43**, 295–322.

Fielding, C.R., **Alexander, J.** and **Newman-Sutherland, E.** (1997) Preservation of in situ, arborescent vegetation and fluvial bar construction in the Burdekin River of north Queensland, Australia. *Palaeogeogr. Palaeoclimatol. Palaeoecol.*, **135**, 123–144.

Fielding, C.R., **Alexander, J.** and **McDonald, R.** (1999) Sedimentary facies from ground-penetrating radar surveys of the modern, upper Burdekin River of north Queensland, Australia: consequences of extreme discharge fluctuations. In: *Fluvial Sedimentology VI* (Eds Smith, N.D. and Rogers, J.), *Int. Assoc. Sedimentol. Spec. Publ.*, **28**, 347–362.

Fielding, C.R., **Trueman, J.D.** and **Alexander, J.** (2005) Sedimentology of the modern and Holocene Burdekin River Delta of north Queensland, Australia – Controlled by river output, not by waves and tides. In: *River Deltas – Concepts, Models, and Examples* (Eds Giosan, L. and Bhattacharya, J.P.), *SEPM Spec. Publ.*, **83**, 467–496.

Fielding, C.R., **Allen, J.P.**, **Alexander, J.** and **Gibling, M.R.** (2009) Facies model for fluvial systems in the seasonal tropics and subtropics. *Geology*, **37**, 623–626.

Fielding, C.R., **Allen, J.P.**, **Alexander, J.**, **Gibling, M.R.**, **Rygel, M.C.** and **Calder, J.H.** (2011) Fluvial systems and their deposits in hot, seasonal semiarid and subhumid settings: modern and ancient examples. In: *From River to Rock Record: The Preservation of Fluvial Sediments and their Subsequent Interpretation* (Eds Davidson, S.K., Leleu, S. and North, C.P.), *SEPM Spec. Publ.*, **97**, 89–111.

Fielding, C.R., **Alexander, J.** and **Allen, J.P.** (2018) The role of discharge variability in the formation and preservation of alluvial sediment bodies. *Sed. Geol.*, **365**, 1–20.

Fielding, C.R., **Bann, K.L.**, **Martin, M.A.** and **Frank, T.D.** (2019a) Sedimentology and stratigraphy of Permian coastal to shallow-marine successions in the western Bowen Basin, Queensland, Australia: an evaluation of evidence for high-latitude depositional environments. In: *Latitudinal Controls on Stratigraphic Models and Sedimentary Concepts* (Eds Fraticelli, C.M., Markwick, P.J., Martinius, A.W. and Suter, J.R.), *SEPM Spec. Publ.*, **108**, 134–169.

Fielding, C.R., **Frank, T.D.**, **McLoughlin, S.**, **Vajda, V.**, **Mays, C.**, **Tevyaw, A.P.**, **Winguth, A.**, **Winguth, C.**, **Nicoll, R.S.**, **Bocking, M.** and **Crowley, J.L.** (2019b) Age and pattern of the southern high-latitude continental end-Permian extinction constrained by multiproxy analysis. *Nature Comms.*, **10**, 12.

Fielding, C.R., **Nelson, W.J.** and **Elrick, S.D.** (2020) Sequence stratigraphy of the late Desmoinesian to early Missourian (Pennsylvanian) succession of southern Illinois: Insights into controls on stratal architecture in an Icehouse period of Earth history. *J. Sediment. Res.*, **90**, 200–227.

Fielding, C.R., **Frank, T.D.**, **Tevyaw, A.P.**, **Savatic, K.**, **Vajda, V.**, **McLoughlin, S.**, **Mays, C.**, **Nicoll, R.S.**, **Bocking, M.** and **Crowley, J.L.** (2021) Sedimentology of the continental end-Permian extinction event in the Sydney Basin, eastern Australia. *Sedimentology*, **68**, 30–62.

Fielding, C.R., **Frank, T.D.** and **Birgenheier, L.P.** (2023) A revised, late Palaeozoic glacial time-space framework for eastern Australia, and comparisons with other regions and events. *Earth Sci. Rev.*, **236**, 15.

Fischbein, S.A., **Joeckel, R.M.** and **Fielding, C.R.** (2009) Fluvial-estuarine reinterpretation of large, isolated sandstone bodies in epicontinental cyclothems, Upper Pennsylvanian, northern Midcontinent, USA, and their significance for understanding late Paleozoic sea-level fluctuations. *Sed. Geol.*, **216**, 15–28.

Fisk, H.N. (1944) *Geological Investigation of the Alluvial Valley of the Lower Mississippi River*. U.S. Army Corps of Engineers Mississippi River Commission Report, Vicksburg, MS.

Frank, T.D., **Fielding, C.R.**, **Winguth, A.M.E.**, **Savatic, K.**, **Tevyaw, A.P.**, **Winguth, C.**, **McLoughlin, S.**, **Vajda, V.**, **Mays, C.**, **Nicoll, R.**, **Bocking, M.** and **Crowley, J.L.** (2021) Pace, magnitude, and nature of terrestrial climate change through the end-Permian extinction in southeastern Gondwana. *Geology*, **49**, 1089–1095.

Friend, P.F. (1983) Towards the field classification of alluvial architecture or sequence. In: *Modern and Ancient Fluvial Systems* (Eds Collinson, J.D. and Lewin, J.), *Int. Assoc. Sedimentol. Spec. Publ*, **6**, 345–354.

Fryberger, S.G., **Hern, C.Y.** and **Glennie, K.** (2016) Sedimentology of reservoir-scale aeolian-fluvial interactions, Wadi Batha, Northern Wahiba Sand Sea, Oman. *AAPG Search and Discovery article*, **51260**, 18.

Gabel, S.L. (1993) Geometry and kinematics of dunes during steady and unsteady flows in the Calamus River, Nebraska, U.S.A. *Sedimentology*, **40**, 237–269.

Galeazzi, C.P., **Almeida, R.P.**, **Mazoca, C.M.**, **Best, J.L.**, **Freitas, B.T.**, **Ianniruberto, M.**, **Cisneros, J.** and **Tamura, L.N.** (2018) The significance of superimposed dunes in the

Amazon River: Implications for how large rivers are identified in the rock record. *Sedimentology*, **65**, 2388–2403.

Gall, R.D., **Birgenheier, L.P.** and **Vanden Berg, M.D.** (2017) Highly seasonal and perennial fluvial facies: implications for climatic control on the Douglas Creek and Parachute Creek Members, Green River Formation, southeastern Uinta Basin, Utah, U.S.A. *J. Sediment. Res.*, **87**, 1019–1047.

Gawthorpe, R.L., **Collier, R.E.L.**, **Alexander, J.**, **Leeder, M.R.** and **Bridge, J.S.** (1993) Ground penetrating radar: application to sandbody geometry and heterogeneity studies. In: *Characterization of Fluvial and Aeolian Reservoirs* (Eds North, C.P. and Prosser, D.J.), *Geol. Soc. London Spec. Publ.*, **73**, 421–432.

George, G.T. (2000) Characterisation and high resolution sequence stratigraphy of storm-dominated braid delta and shoreface sequences from the Basal Grit Group (Namurian) of the South Wales Variscan peripheral foreland basin. *Mar. Petrol. Geol.*, **17**, 445–475.

Ghienne, J.-F., **Girard, F.**, **Moreau, J.** and **Rubino, J.-L.** (2010) Late Ordovician climbing-dune cross-stratification: a signature of outburst floods in proglacial outwash environments? *Sedimentology*, **57**, 1175–1198.

Ghinassi, M. and **Moody, J.** (2021) Reconstruction of an extreme flood hydrograph and morphodynamics of a meander bend in a high-peak discharge variability river (Powder River, USA). *Sedimentology*, **68**, 3549–3576.

Gibling, M.R. (2006) Width and thickness of fluvial channel bodies and valley fills in the geological record: a literature compilation and classification. *J. Sediment. Res.*, **76**, 731–770.

Gibling, M.R., **Nanson, G.C.** and **Maroulis, J.C.** (1998) Anastomosing river sedimentation in the Channel Country of central Australia. *Sedimentology*, **45**, 595–619.

Gibling, M.R., **Saunders, K.I.**, **Tibert, N.E.** and **White, J.A.** (2004) Sequence sets, high-accomodation events, and the coal window in the Carboniferous Sydney Coalfield, Atlantic Canada. In: *Sequence Stratigraphy, Paleoclimate, and Tectonics of Coal-Bearing Strata* (Eds Pashin, J.C. and Gastaldo, R.A.), *AAPG Stud. Geol.*, **51**, 169–197.

Gibling, M.R., **Bashforth, A.R.**, **Falcon-Lang, H.J.**, **Allen, J.P.** and **Fielding, C.R.** (2010) Log jams and flood sediment buildup caused by channel abandonment and avulsion in the Pennsylvanian of Atlantic Canada. *J. Sediment. Res.*, **80**, 268–287.

Girard, F., **Ghienne, J.-F.** and **Rubino, J.-L.** (2012) Channelized sandstone bodies ("cordons") in the Tassili N'Ajjer (Algeria and Libya): snapshots of a Late Ordovician proglacial outwash plain. In: *Glaciogenic Reservoirs and Hydrocarbon Systems* (Eds Huuse, M., Redfern, J., Le Heron, D.P., Dixon, R.J., Moscariello, A. and Craig, J.), *Geol. Soc. London Spec. Publ.*, **368**, 355–379.

Glover, B.W. and **Powell, J.H.** (1996) Interaction of climate and tectonics upon alluvial architecture: Late Carboniferous-Early Permian sequences at the southern margin of the Pennine Basin, UK. *Palaeogeogr. Palaeoclimatol. Palaeoecol.*, **121**, 13–34.

Gugliotta, M., **Saito, Y.**, **Ben, B.**, **Sieng, S.** and **Oliver, T.S.N.** (2018) Sedimentology of the Late Holocene fluvial levee and point-bar deposits from the Cambodian tract of the Mekong River. *J. Geol. Soc. London*, **175**, 176–186.

Guion, P.D. and **Fielding, C.R.** (1988) Westphalian A and B sedimentation in the Pennine Basin, UK. In: *Sedimentation in a Synorogenic Basin Complex: The Upper Carboniferous of Northwest Europe* (Eds Besly, B.M. and Kelling, G.), pp. 153–177. Blackie, Glasgow.

Guion, P.D., **Banks, N.L.** and **Rippon, J.H.** (1995) The Silkstone Rock (Westphalian A) from the East Pennines, England: Implications for sand body genesis. *J. Geol. Soc. London*, **152**, 819–832.

Gustavson, T.C. (1978) Bed forms and stratification types of modern gravel meander lobes, Nueces River, Texas. *Sedimentology*, **25**, 401–426.

Hampson, G.J. (1998) Evidence for relative sea-level falls during deposition of the Upper Carboniferous Millstone Grit, South Wales. *Geol. J.*, **33**, 243–266.

Hansford, M.R., **Plink-Björklund, P.** and **Jones, E.R.** (2020) Global quantitative analyses of river discharge variability and hydrograph shape with respect to climate types. *Earth Sci. Rev.*, **200**, 102977.

Harbor, D.J. (1998) Dynamics of bedforms in the lower Mississippi River. *J. Sediment. Res.*, **68**, 750–762.

Hartley, A.J. (1993) A depositional model for the Mid-Westphalian A to late Westphalian B Coal Measures of South Wales. *J. Geol. Soc. London*, **150**, 1121–1136.

Haszeldine, R.S. (1983) Fluvial bars reconstructed from a deep, straight channel, Upper Carboniferous coalfield of Northeast England. *J. Sediment. Petrol.*, **53**, 1233–1247.

Heckel, P.H. (2008) Pennsylvanian cyclothems in Midcontinent North America as far-field effects of waxing and waning of Gondwana ice sheets. In: *Resolving the Late Paleozoic Ice Age in Time and Space* (Eds Fielding, C.R., Frank, T.D. and Isbell, J.L.), *Geol. Soc. Am. Spec. Pap.*, **441**, 275–289.

Hess, A.M. and **Fielding, C.R.** (2020) Analysis of coastal-plain fluvial architecture and high-frequency stacking patterns in the Upper Cretaceous Masuk Formation, Utah, U.S.A.: Climate-driven cyclicity? *J. Sediment. Res.*, **90**, 1265–1285.

Hill, P.R., **Lewis, C.P.**, **Desmarais, S.**, **Kauppaymuthoo, V.** and **Rais, H.** (2001) The Mackenzie Delta: sedimentary processes and facies of a high-latitude, fine-grained delta. *Sedimentology*, **48**, 1047–1078.

Holbrook, J.M. and **Allen, S.D.** (2021) The case of the braided river that meandered: Bar assemblages as a mechanism for meandering along the pervasively braided Missouri River, USA. *Geol. Soc. Am. Bull.*, **133**, 1505–1530.

Horn, J.D., **Fielding, C.R.** and **Joeckel, R.M.** (2012a) Revision of Platte River alluvial facies model through observations of extant channels and barforms, and subsurface alluvial valley fills. *J. Sediment. Res.*, **82**, 72–91.

Horn, J.D., **Joeckel, R.M.** and **Fielding, C.R.** (2012b) Progressive abandonment and planform changes of the central Platte River in Nebraska, central USA, over historical timeframes. *Geomorphology*, **139–140**, 372–383.

Ishii, Y., **Tamura, T.** and **Ben, B.** (2021) Holocene sedimentary evolution of the Mekong River floodplain, Cambodia. *Quat. Sci. Rev.*, **253**, 17p.

Jackson, R.G., II (1975) Velocity-bedform-texture patterns of meander bends in the lower Wabash River of Illinois and Indiana. *Geol. Soc. Am. Bull.*, **86**, 1511–1522.

Jackson, R.G., II (1976a) Depositional model of point bars in the lower Wabash River. *J. Sediment. Petrol.*, **46**, 579–594.

Jackson, R.G., II (1976b) Largescale ripples of the lower Wabash River. *Sedimentology*, **23**, 593–623.

Jacob, R.J., **Bluck, B.J.** and **Ward, J.D.** (1999) Tertiary-age diamondiferous fluvial deposits of the Lower Orange

River Valley, Southwestern Africa. *Econ. Geol.*, **94**, 749–758.

Jarrett, R.D. and **Costa, J.E.** (1986) Hydrology, geomorphology, and dam-break modeling of the July 15, 1982 Lawn Lake Dam and Cascade Lake Dam failures, Larrimer County, Colorado. *USGS Prof. Pap.*, **1369**, 85.

Jerolmack, D.J. and **Paola, C.** (2010) Shredding of environmental signals by sediment transport. *Geophys. Res. Lett.*, **37**, L19401.

Joeckel, R.M. (1994) Virgilian (Upper Pennsylvanian) paleosols in the upper Lawrence Formation (Douglas Group) and in the Snyderville Shale Member (Oread Formation, Shawnee Group) of the northern midcontinent USA – pedologic contrasts in a cyclothem sequence. *J. Sediment. Res.*, **A64**, 853–866.

Joeckel, R.M. and **Henebry, G.M.** (2008) Channel and Island change in the lower Platte River, Eastern Nebraska, U.S.A. *Geomorphology*, **102**, 407–418.

Joeckel, R.M., **Tucker, S.T.** and **Fielding, C.R.** (2015) Sedimentological effects and stratigraphic implications of a rare, high-stage flow in an evolving, braided to anabranching stream with riparian woodland. *Sed. Geol.*, **325**, 71–89.

Jordan, D.W. and **Pryor, W.A.** (1992) Hierarchical levels of heterogeneity in a Mississippi River meander belt and application to reservoir systems. *AAPG Bull.*, **76**, 1601–1624.

Kale, V.S., **Singhvi, A.K.**, **Mishra, P.K.** and **Banerjee, D.** (2000) Sedimentary records and luminescence chronology of Late Holocene palaeofloods in the Luni River, That Desert, northwest India. *Catena*, **40**, 337–358.

Karssenberg, D. and **Bridge, J.S.** (2008) A three-dimensional numerical model of sediment transport, erosion and deposition within a network of channel belts, floodplain and hill slope: extrinsic and intrinsic controls on floodplain dynamics and alluvial architecture. *Sedimentology*, **55**, 1717–1745.

Keogh, K.J., **Rippon, J.H.**, **Hodgetts, D.**, **Howell, J.A.** and **Flint, S.S.** (2005) Improved understanding of fluvial architecture using three-dimensional geological models: A case study of the Westphalian A Silkstone Rock, Pennine Basin, UK. In: *Fluvial Sedimentology VII* (Eds Blum, M.D., Marriott, S.B. and Leclair, S.F.), *Int. Assoc. Sedimentol. Spec. Publ.*, **35**, 481–491.

Kimbrough, R.A. and **Holmes, R.R., Jr.** (2015) *Flooding in the South Platte River and Fountain Creek Basins in eastern Colorado, September 9-18, 2013*. USGS Scientific Investigations Report 2015-5119, 26 pp.

Kocurek, G., **Westerman, R.**, **Hern, C.**, **Tatum, D.**, **Rajapara, H.M.** and **Singhvi, A.K.** (2020) Aeolian dune accommodation space for Holocene Wadi Channel Avulsion Strata, Wahiba Dune Field, Oman. *Sed. Geol.*, **399**, 13.

Krapf, C.B.E., **Stollhofen, H.** and **Stanistreet, I.G.** (2003) Contrasting styles of ephemeral river systems and their interaction with dunes of the Skeleton Coast erg (Namibia). *Quat. Int.*, **104**, 41–52.

Lang, J., **Le Heron, D.P.**, **van den Berg, J.H.** and **Winsemann, J.** (2021) Bedforms and sedimentary structures related to supercritical flows in glacigenic settings. *Sedimentology*, **68**, 1539–1579.

Lawton, T.F. (1982) Lithofacies correlations within the Upper Cretaceous Indianola Group, central Utah. In: *Overthrust Belt of Utah* (Ed. Nielsen, D.L.), *Utah Geol. Assoc. Publ.*, **10**, 199–213.

Leary, K.C. and **Ganti, V.** (2020) Preserved fluvial cross strata record bedform disequilibrium dynamics. *Geophys. Res. Lett.*, **47**, e2019GL085910.

Leckie, D.A. (2003) Modern environments of the Canterbury Plains and adjacent offshore areas, New Zealand – an analog for ancient conglomeratic depositional systems in nonmarine and coastal zone settings. *Bull. Can. Petrol. Geol.*, **51**, 389–425.

Levey, R.A. (1978) Bed-form distribution and internal stratification of coarse-grained point bars, upper Congaree River, S.C. In: *Fluvial Sedimentology* (Ed. Miall, A.D.), *Can. Soc. Petrol. Geol. Mem.*, **5**, 105–127.

Levey, R.A., **Kjerfve, B.** and **Getzen, R.T.** (1980) Comparison of bed form variance spectra within a meander bend during flood and average discharge. *J. Sediment. Petrol.*, **50**, 149–155.

Long, D.G.F. (2021) Trickling down the paleoslope: an empirical approach to paleohydrology. *Earth Sci. Rev.*, **220**, 25.

Lunt, I.A. and **Bridge, J.S.** (2004) Evolution and deposits of a gravelly braid bar, Saganvanirktok River, Alaska. *Sedimentology*, **51**, 415–432.

Lunt, I.A., **Bridge, J.S.** and **Tye, R.S.** (2004) A quantitative, three-dimensional depositional model of gravelly braided rivers. *Sedimentology*, **51**, 377–414.

Lyster, S.J., **Whittaker, A.C.** and **Hajek, E.A.** (2022a) The problem of paleo-planforms. *Geology*, **50**, 822–826.

Lyster, S., **Whittaker, A.C.**, **Hajek, E.A.** and **Ganti, V.** (2022b) Field evidence for disequilibrium dynamics in preserved fluvial cross-strata: A record of discharge variability or morphodynmaic hierarchy? *Earth Planet. Sci. Lett.*, **579**, 117355.

Mackey, S.D. and **Bridge, J.S.** (1995) Three-dimensional model of alluvial stratigraphy: theory and application. *J. Sediment. Res.*, **65**, 7–31.

Maitan, R., **Finotello, A.**, **Tognin, D.**, **D'Alpaos, A.**, **Fielding, C.R.**, **Ielpi, A.** and **Ghinassi, M.** (2024) Hydrologically driven modulation of cutoff regime in meandering rivers. *Geology*, **52**, 336–340.

Maizels, J.K. (1989) Sedimentology, palaeoflow dynamics and flood history of jokulhlaup deposits: palaeohydrology of sediment sequences in southern Iceland sandur deposits. *J. Sediment. Petrol.*, **59**, 204–223.

Manna, M.O., **Scherer, C.M.d.S.**, **Bállico, M.B.**, **dos Reis, A.D.**, **Moraes, L.V.**, **Ferrari, L.A.B.**, **Roisenberg, H.B.** and **de Oliveira, V.G.** (2021) Changes in fluvial architecture induced by discharge variability, Jaicós Formation (Silurian-Devonian), Parnaíba Basin, Brazil. *Sediment. Geol.*, **420**, 105924.

Maroulis, J.C. (2000) *Stratigraphy and Mid-to-Late Quaternary Chronology of the Cooper Creek Floodplain, Southwest Queensland, Australia*. PhD thesis, p. 214. University of Wollongong, Wollongong.

Marren, P.M., **Russell, A.J.** and **Rushmer, E.L.** (2009) Sedimentology of a sandur formed by multiple jökulhlaups, Kverkfjöll, Iceland. *Sed. Geol.*, **213**, 77–88.

Mason, J., **Cardenas, B.T.**, **Day, M.D.**, **Daniller-Verghese, M.**, **Brothers, S.C.**, **Kocurek, G.** and **Mohrig, D.** (2020) Pattern evolution and interactions in subaqueous dune fields: North Loup River, Nebraska, U.S.A. *J. Sediment. Res.*, **90**, 1734–1746.

McGowen, J.H. and **Garner, L.E.** (1970) Physiographic features and stratification types of coarse-grained point bars: modern and ancient examples. *Sedimentology*, **14**, 77–111.

McKee, E.D., **Crosby, E.J.** and **Berryhill, H.L., Jr.** (1967) Flood deposits, Bijou Creek, Colorado, June 1965. *J. Sediment. Petrol.*, **37**, 829–851.

McLeod, J.S., **Wood, J.**, **Lyster, S.J.**, **Valenza, J.M.**, **Spencer, A.R.** and **Whittaker, A.C.** (2023) Quantitative constraints on flood variability in the rock record. *Nat. Commun.*, **14**, 3362.

McLoughlin, S. and **Drinnan, A.N.** (1997) Revised stratigraphy of the Permian Bainmedart Coal Measures, northern Prince Charles Mountains, East Antarctica. *Geol. Mag.*, **134**, 335–353.

Meade, R.H., **Bobrovitskaya, N.N.** and **Babkin, V.I.** (2000) Suspended-sediment and fresh-water discharges in the Ob and Yenisey rivers, 1960–1988. *Int. J. Earth Sci.*, **89**, 461–469.

Miall, A.D. (1977) A review of the braided river depositional environment. *Earth Sci. Rev.*, **13**, 1–62.

Miall, A.D. (1978) Fluvial sedimentology: an historical review. In: *Fluvial Sedimentology* (Ed. Miall, A.D.), *Can. Soc. Petrol. Geol. Mem.*, **5**, 1–47.

Miall, A.D. (1985) Architectural-element analysis: A new method of facies analysis applied to fluvial deposits. *Earth Sci. Rev.*, **22**, 261–308.

Miall, A.D. (2010) Alluvial deposits. In: *Facies Models 4* (Eds James, N.P. and Dalrymple, R.W.), *Geoscience Association of Canada GEOtext*, **6**, 105–139.

Miall, A.D. and **Jones, B.G.** (2003) Fluvial architecture of the Hawkesbury Sandstone (Triassic), near Sydney, Australia. *J. Sediment. Res.*, **73**, 531–545.

Moody, J.A. and **Meade, R.H.** (2014) Ontogeny of point bars in a cold semi-arid climate. *Geol. Soc. Am. Bull.*, **126**, 1301–1316.

Moore, A.E., **Cotterill, F.P.D.**, **Main, M.P.L.** and **Williams, H.B.** (2022) The Zambezi: origins and legacies of Earth's oldest river system. In: *Large Rivers: Geomorphology and Management* (Ed. Gupta, A.), pp. 457–487. Wiley-Blackwell, Oxford.

Moreton, D.J., **Ashworth, P.J.** and **Best, J.L.** (2002) The physical scale modelling of alluvial architecture and estimation of subsurface permeability. *Basin Res.*, **14**, 265–285.

Muhs, D.R., **Bettis, E.A., III**, **Aleinikoff, J.N.**, **McGeehin, J.P.**, **Beann, J.**, **Skipp, G.**, **Marshall, B.D.**, **Roberts, H.M.**, **Johnson, W.C.** and **Benton, R.** (2008) Origin and paleoclimatic significance of late Quaternary loess in Nebraska: Evidence from stratigraphy, chronology, sedimentology, and geochemistry. *Geol. Soc. Am. Bull.*, **120**, 1378–1407.

Mumpy, A.J., **Jol, H.M.**, **Kean, W.F.** and **Isbell, J.L.** (2007) Architecture and sedimentology of an active braid bar in the Wisconsin River based on 3-D ground penetrating radar. In: *Stratigraphic Analyses Using GPR* (Eds Baker, G.S. and Jol, H.M.), *Geol. Soc. Am., Spec. Pap.*, **432**, 111–131.

Nanson, G.C., **Rust, B.R.** and **Taylor, G.** (1986) Coexistent mud braids and anastomosing channels in an arid-zone river: Cooper Creek, central Australia. *Geology*, **14**, 175–178.

National Oceanographic and Atmospheric Administration (NOAA). (1976) *Big Thompson Canyon flash flood of July 31st – August 1st, 1976 – a report to the administrator*. US Department of Commerce, Natural Disaster Survey Report 76-1, 48.

Nittouer, J.A., **Mohrig, D.**, **Allison, M.A.** and **Peyret, A.-P.B.** (2011) The lowermost Mississippi River: a mixed bedrock-alluvial channel. *Sedimentology*, **58**, 1914–1934.

Nittrouer, J.A., **Allison, M.A.** and **Campanella, R.** (2008) Bedform transport rates for the lowermost Mississippi River. *J. Geophys. Res.*, **113**, 16.

Nittrouer, J.A., **Shaw, J.**, **Lamb, M.P.** and **Mohrig, D.** (2012) Spatial and temporal trends for water-flow velocity and bed-material sediment transport in the lower Mississippi River. *Geol. Soc. Am. Bull.*, **124**, 400–414.

Parker, N.O., **Sambrook Smith, G.H.**, **Ashworth, P.J.**, **Best, J.L.**, **Lane, S.N.**, **Lunt, I.A.**, **Simpson, C.J.** and **Thomas, R.E.** (2013) Quantification of the relation between surface morphodynamics and subsurface sedimentological product in sandy braided rivers. *Sedimentology*, **60**, 839.

Parsons, D.R., **Best, J.L.**, **Orfeo, O.**, **Hardy, R.J.**, **Kostaschuk, R.** and **Lane, S.N.** (2005) Morphology and flow fields of three-dimensional dunes, Rio Paraná, Argentina: Results from simultaneous multibeam echo sounding and acoustic Doppler current profiling. *J. Geophys. Res.*, **110**, 9.

Plink-Björklund, P. (2015) Morphodynamics of rivers strongly affected by monsoon precipitation: review of depositional style and forcing factors. *Sediment. Geol.*, **323**, 110–147.

Plink-Björklund, P. (2019) Latitudinal controls on river systems: implications of precipitation variability. In: *Latitudinal Controls on Stratigraphic Models and Sedimentary Concepts* (Eds Fraticelli, C.M., Markwick, P.J., Martinius, A.W. and Suter, J.R.), *SEPM Spec. Publ.*, **108**, 59–81.

Rahman, M.M. (2016) *Modeling Flood Inundation of the Jamuna River*. PhD thesis. Bangladesh University of Engineering and Technology, Dhaka.

Reesink, A.J.H., **Ashworth, P.J.**, **Sambrook smith, G.H.**, **Best, J.L.**, **Parsons, D.R.**, **Amsler, M.L.**, **Hardy, R.J.**, **Lane, S.N.**, **Nicholas, A.P.**, **Orfeo, O.**, **Sandbach, S.D.**, **Simpson, C.J.** and **Szupiany, R.N.** (2014) Scales and causes of heterogeneity in bars in a large multi-channel river: Rio Paraná, Argentina. *Sedimentology*, **61**, 1055–1085.

Rennie, C.D. and **Church, M.** (2010) Mapping spatial distributions and uncertainty of water and sediment flux in a large gravel bed river reach using an acoustic Doppler current profiler. *J. Geophys. Res.*, **115**, 27.

Rice, S.P., **Church, M.**, **Wooldridge, C.L.** and **Hickin, E.J.** (2009) Morphology and evolution of bars in a wandering gravel-bed river; lower Fraser river, British Columbia, Canada. *Sedimentology*, **56**, 709–736.

Romans, B.W., **Castelltort, S.**, **Covault, J.A.**, **Fildani, A.** and **Walsh, J.P.** (2016) Environmental signal propagation in sedimentary systems across timescales. *Earth Sci. Rev.*, **153**, 7–29.

Rosenau, N.A., **Tabor, N.J.**, **Elrick, S.D.** and **Nelson, W.J.** (2013a) Polygenetic history of paleosols in Middle-Upper Pennsylvanian cyclothems of the Illinois Basin, USA: Part I. Characterization of paleosol types and interpretation of pedogenic processes. *J. Sediment. Res.*, **83**, 606–636.

Rosenau, N.A., **Tabor, N.J.**, **Elrick, S.D.** and **Nelson, W.J.** (2013b) Polygenetic history of paleosols in Middle-Upper Pennsylvanian cyclothems of the Illinois Basin, USA: Part II. Integrating geomorphology, climate, and glacioeustasy. *J. Sediment. Res.*, **83**, 637–668.

Roy, M., **Clark, P.U.**, **Barendregt, R.W.**, **Glasmann, J.R.** and **Enkin, R.J.** (2004) Glacial stratigraphy and paleomagnetism of late Cenozoic deposits of the north-central United States. *Geol. Soc. Am. Bull.*, **116**, 30–41.

Russell, A.J. and **Knudsen, Ó.** (2002) The effects of glacier-outburst flood flow dynamics on ice-contact deposits:

November 1996 jökulhlaup, Skeiðarársandur, Iceland. In: *Flood and Megaflood Processes and Deposits: Recent and Ancient Examples* (Eds Martini, I.P., Baker, V.R. and Garzón, G.), *Int. Assoc. Sedimentol. Spec. Publ.*, **32**, 67–84.

Rust, B.R. and **Gibling, M.R.** (1990) Braidplain evolution in the Pennsylvanian South Bar Formation, Sydney Basin, Nova Scotia, Canada. *J. Sediment. Petrol.*, **60**, 59–72.

Rust, B.R. and **Jones, B.G.** (1987) The Hawkesbury Sandstone south of Sydney, Australia: Triassic analogue for the deposit of a large braided river. *J. Sediment. Petrol.*, **57**, 222–233.

Rygel, M.C., **Lally, C.**, **Gibling, M.R.**, **Ielpi, A.**, **Calder, J.H.** and **Bashforth, A.R.** (2015) Sedimentology and stratigraphy of the type section of the Pennsylvanian Boss Point formation, Joggins Fossil Cliffs, Nova Scotia, Canada. *Atlantic Geol.*, **51**, 1–43.

Sambrook Smith, G.H., **Ashworth, P.J.**, **Best, J.L.**, **Woodward, J.** and **Simpson, C.J.** (2006) The sedimentology and alluvial architecture of the sandy braided South Saskatchewan River, Canada. *Sedimentology*, **53**, 413–434.

Sambrook Smith, G.H., **Ashworth, P.J.**, **Best, J.L.**, **Lunt, I.A.**, **Orfeo, O.** and **Parsons, D.R.** (2009) The sedimentology and alluvial architecture of a large braid bar, Rio Paraná, Argentina. *J. Sediment. Res.*, **79**, 629–642.

Sambrook Smith, G.H., **Best, J.L.**, **Ashworth, P.J.**, **Lane, S.N.**, **Parker, N.O.**, **Lunt, I.A.**, **Thomas, R.E.** and **Simpson, C.J.** (2010) Can we distinguish flood frequency and magnitude in the sedimentological record of rivers? *Geology*, **38**, 579–582.

Schopf, J.M. (1973) Coal, climate, and global tectonics. In: *Implications of Continental Drift to the Earth Sciences* (Eds Tarling, D.H. and Runcorn, S.K.), pp. 609–622. Academic Press, London.

Schöpfer, K., **Nadaskay, R.** and **Martinek, K.** (2022) Evaluation of climatic and tectonic imprints in fluvial successions of an early Permian depositional system (Asselian Vrchlabí Formation, Krkonoše Piedmont Basin, Czech Republic). *J. Sediment. Res.*, **92**, 275–303.

Schwartz, D.E. (1978a) Hydrology and current orientation analysis of as braided-to-meandering transition: the Red River in Oklahoma and Texas, U.S.A. In: *Fluvial Sedimentology* (Ed. Miall, A.D.), *Can. Soc. Petrol. Geol. Mem.*, **5**, 231–255.

Schwartz, D.E. (1978b) Sedimentary facies, structures, and grain-size distribution: the Red River in Oklahoma and Texas. *Trans. Gulf Coast Assoc. Geol. Socs.*, **28**, 473–492.

Schwartz, T.M., **Dechesne, M.** and **Zellman, K.L.** (2021) Evidence for variable precipitation and discharge from Upper Cretaceous-Paleogene fluvial deposits of the Raton Basin, Colorado-New Mexico, U.S.A. *J. Sediment. Res.*, **91**, 571–594.

Shan, X., **Shi, X.F.**, **Clift, P.D.**, **Seddique, A.A.**, **Liu, S.F.**, **Tan, C.P.**, **Liu, J.G.**, **Hasan, R.**, **Li, J.R.** and **Song, Z.J.** (2020) Sedimentology of the modern seasonal lower Ganges River with low inter-annual peak discharge variance, Bangladesh. *J. Geol. Soc. London*, **178**, jgs2020-094.

Shao, L.Y., **Fielding, C.R.**, **Mu, G.Y.**, **Lu, J.**, **Zhang, P.X.**, **Li, Y.N.**, **Wang, Y.**, **Shao, Y.W.** and **Wen, H.** (2024) Coal accumulation patterns and paleoclimates in a Carboniferous-Permian cratonic basin, North China. In: *Field Trip Guidebook on Chinese Sedimentary Geology* (Ed. Hu, X.M.), pp. 231–357. Science Press/Springer, Beijing.

Sharma, N., **Whittaker, A.C.**, **Adatte, T.** and **Castelltort, S.** (2024) Water discharge and sediment flux intermittency in the fluvial Escanilla Formation, Spain: Implications for changes in stratigraphic architecture. *Deposit. Rec.*, **10**, 245–259.

Skelly, R.L., **Bristow, C.S.** and **Ethridge, F.G.** (2003) Architecture of channel-belt deposits in an aggrading shallow sandbed braided river: the lower Niobrara river, northeast Nebraska. *Sed. Geol.*, **158**, 249–270.

Sloan, J., **Miller, J.R.** and **Lancaster, N.** (2001) Response and recovery of the Eel River, California, and its tributaries to floods in 1955, 1964, and 1997. *Geomorphology*, **36**, 129–154.

Smith, N.D. (1970) The braided stream depositional environment: comparison of the Platte River with some Silurian clastic rocks, North-Central Appalachians. *Geol. Soc. Am. Bull.*, **81**, 2993–3014.

Smith, N.D. (1971a) Transverse bars and braiding in the lower Platte River, Nebraska. *Geol. Soc. Am. Bull.*, **82**, 3407–3420.

Smith, N.D. (1971b) Pseudo-planar stratification produced by very low amplitude sand waves. *J. Sediment. Petrol.*, **41**, 624–634.

Smith, R.M.H., **Mason, T.R.** and **Ward, J.D.** (1993) Flash-flood sediments and ichnofacies of the Late Pleistocene Homeb Silts, Kuiseb River, Namibia. *Sediment. Geol.*, **85**, 579–599.

Snorrason, Á., **Jónsson, P.**, **Sigurðsson, O.**, **Pálsson, S.**, **Árnason, S.**, **Vikingsson, S.** and **Kaldal, I.** (2002) November 1996 jökulhlaup on Skeiðarársandur outwash plain, Iceland. In: *Flood and Megaflood Processes and Deposits: Recent and Ancient Examples* (Eds Martini, I.P., Baker, V.R. and Garzón, G.), *Int. Assoc. Sedimentol. Spec. Publ.*, **32**, 55–65.

Sobczak, K., **Bryan, S.E.**, **Fielding, C.R.** and **Corkeron, M.** (2019) From intrabasinal volcanism to far-field tectonics: Causes of abrupt shifts in sediment provenance in the Devonian-Carboniferous Drummond Basin, Queensland. *Aust. J. Earth Sci.*, **66**, 497–518.

Stanistreet, I.G. and **Stollhofen, H.** (2002) Hoanib River flood deposits of Namib Desert interdunes as analogues for thin permeability barrier mudstone layers in aeolianite reservoirs. *Sedimentology*, **49**, 719–736.

Stanley, K.O. and **Wayne, W.J.** (1972) Epeirogenic and climatic controls of Early Pleistocene fluvial sediment dispersal in Nebraska. *Geol. Soc. Am. Bull.*, **83**, 36753690.

Tamura, L.N., **Almeida, R.P.**, **Galeazzi, C.P.**, **Freitas, B.T.**, **Ianniruberto, M.** and **Prado, A.H.** (2019) Upper-bar deposits in large Amazon rivers: Occurrence, morphology and internal structure. *Sediment. Geol.*, **387**, 1–17.

Thorne, C.R., **Russell, A.P.G.** and **Alam, M.K.** (1993) Planform pattern and channel evolution of the Brahmaputra River, Bangladesh. In: *Braided Rivers* (Eds Best, J.L. and Bristow, C.S.), *Geol. Soc. London Spec Publ.*, **75**, 257–276.

Tooth, S. and **McCarthy, T.S.** (2004) Anabranching in mixed bedrock-alluvial rivers: the example of the Orange River above Augrabies Falls, Northern Cape Province, South Africa. *Geomorphology*, **57**, 235–262.

Tye, R.S. (2004) Geomorphology: An approach to determining subsurface reservoir dimensions. *AAPG Bull.*, **88**, 1123–1147.

Vesakoski, J.-M., **Nylén, T.**, **Arheimer, B.**, **Gustafsson, D.**, **Isberg, K.**, **Holopainen, M.**, **Hyyppä, J.** and **Alho, P.** (2017)

Arctic Mackenzie Delta channel planform evolution during 1983-2013 utilising Landsat data and hydrological time series. *Hydrol. Process.*, **31**, 3979–3995.

Waldron, J.W.F. and **Rygel, M.C.** (2005) Role of evaporite withdrawal in the preservation of a unique coal-bearing succession: Pennsylvanian Joggins Formation, Nova Scotia. *Geology*, **33**, 337–340.

Walker, R.G. (1979) General Introduction. In: *Facies Models* (Ed. Walker, R.G.), pp. 1–7. Geoscience Canada Reprint Series 1, Geological Association of Canada, St John's.

Walker, S. and **Holbrook, J.** (2023) Structures, architecture, vertical profiles, palaeohydrology and taphonomy of an upper-flow-regime-dominated fluvial system. The Triassic Dockum Group of the Palo Duro Canyon, Texas. *Sedimentology*, **70**, 645–684.

Wang, J.Q. and **Plink-Björklund, P.** (2019) Stratigraphic complexity in fluvial fans: Lower Eocene Green River Formation, Uinta Basin, USA. *Basin Res.*, **31**, 892–919.

Wang, J.Q. and **Plink-Björklund, P.** (2020) Variable-discharge-river macroforms in the Sunnyside Delta Interval of the Eocene Green River Formation, Uinta Basin, USA. *Sedimentology*, **67**, 1914–1950.

Wanless, H.R. and **Shepard, F.P.** (1936) Sea level and climate changes related to late Paleozoic cycles. *Geol. Soc. Am. Bull.*, **47**, 1177–1206.

Wolfe, J.A. and **Upchurch, G.R.** (1987) North American nonmarine climates and vegetation during the Late Cretaceous. *Palaeogeogr. Palaeoclimatol. Palaeoecol.*, **61**, 33–77.

Wooldridge, C.L. and **Hickin, E.J.** (2005) Radar architecture and evolution of channel bars in wandering, gravel-bed rivers: Fraser and Squamish Rivers, British Columbia, Canada. *J. Sediment. Res.*, **75**, 844–860.

Wu, Y.Y., **Chu, D.L.**, **Tong, J.N.**, **Song, H.J.**, **Dal Corso, J.**, **Wignall, P.B.**, **song, H.Y.**, **Du, Y.** and **Cui, Y.** (2021) Six-fold increase of atmospheric pCO_2 during the Permian-Triassic mass extinction. *Nature Comms.*, **12**, 8p.

Yang, D.Q., **Ye, B.S.** and **Shiklomanov, A.** (2004) Discharge characteristics and changes over the Ob River watershed in Siberia. *J. Hydrometeorol.*, **5**, 595–610.

Zellman, K.L., **Plink-Björklund, P.** and **Fricke, H.C.** (2020) Testing hypotheses on signatures of precipitation variability in the river and floodplain deposits of the Paleogene San Juan Basin, New Mexico, U.S.A. *J. Sediment. Res.*, **90**, 1770–1801.

Zhu, Z.C., **Liu, Y.Q.**, **Kuang, H.W.**, **Benton, M.J.**, **Newell, A.J.**, **Xu, H.**, **An, W.**, **Ji, S.A.**, **Xu, S.C.**, **Peng, N.** and **Zhai, Q.G.** (2019) Altered fluvial patterns in North China indicate rapid climate change linked to the Permian-Triassic mass extinction. *Sci. Rep.*, **9**, 11p.

Zhu, Z.C., **Kuang, H.W.**, **Liu, Y.Q.**, **Benton, M.J.**, **Newell, A.J.**, **Xu, H.**, **An, W.**, **Ji, S.A.**, **Xu, S.C.**, **Peng, N.** and **Zhai, Q.G.** (2020) Intensifying aeolian activity following the end-Permian mass extinction: Evidence from the Late Permian-Early Triassic terrestrial record of the Ordos Basin, North China. *Sedimentology*, **67**, 2691–2720.

Zinger, J.A., **Rhoads, B.L.** and **Best, J.L.** (2011) Extreme sediment pulses generated by bend cutoffs along a large meandering river. *Nat. Geosci.*, **4**, 675–678.

Manuscript received 16 April 2024; revision accepted 2 September 2024

Supporting Information

Additional information may be found in the online version of this article:

Table S1. Summary of hydrographic data used to calculate the discharge statistics used in this study.